Reduced aryl hydrocarbon receptor (AhR) expression drives the pathogenesis of cigarette smoke-induced emphysema.

Department of Pathology

McGill University, Montreal

December 2018

A thesis submitted to McGill University in partial fulfillment of the requirements of the degree Doctor of Philosophy (PhD).

Table of Contents

Acknowledgements

I would like to begin by thanking my supervisor Dr. Carolyn Baglole for her mentorship throughout my PhD. Moreover, I would also like to acknowledge and thank Dr. David Eidelman and Dr. Inga Murawski for their support and assistance with the editing of my thesis. Additionally, I would also like to thank Dr. Edith Zorychta for her involvement and support during my time at McGill. A big thank-you also goes out the all of the Baglole lab members who I have had the pleasure of getting to know over the past several years. Last, but most certainly not least, I would like to thank my wonderful husband, mother and father for their love and support throughout life and throughout this degree.

Contribution of Authors

This doctoral thesis is based on my original work and was formatted in accordance with the manuscript-based style outlined by the McGill University Graduate and Postdoctoral studies thesis preparation guidelines. Although I wrote this thesis, as well as designed/conducted the majority of experiments presented here within, important contributions were made by the co-authors. These contributions include:

1. **Assessment of airspace enlargement *in vivo* (Chapter 2):** Dr. Thomas H. Thatcher (University of Rochester) conducted one of the *in vivo* 4-month CS-exposures and analyzed airspace enlargement in the mouse lungs.
2. **Assessment of lung function *in vivo* (Chapter 2):** Leora Simon (McGill University) assisted with the technical manipulation of mice and equipment during acquisition of lung function parameters using the FlexiVent. Dr. Annette Robichaud (SCIREQ) provided us with the FlexiVent software and conducted the raw data analysis of the lung function data acquired from the FlexiVent.
3. **Smoke exposures and sacrifice days (Chapter 2):** Dr. Hussein Traboulsi, Swati Pareek and Dr. Angela Rico de Souza (McGill University) assisted me with smoke exposures and mouse sacrifice days. Angela Rico de Souza also conducted the differential cell counts of BAL fluid from the 8-week smoke-exposed mice.
4. **Human lung eQTL data (Chapter 2):** Dr. Yohan Bossé (University of Laval) provided us with human COPD AhR/AhRR lung mRNA expression and AhR/AhRR SNP data for subjects participating in the eQTL cohort. Yohan's student, Maxime Lamontagne (University of Laval), conducted the analysis of this data.

5. **Human lung St Joseph's Healthcare Hamilton data (Chapter 2):** Dr. Parameswaran Nair (McMaster University) provided human lung tissue samples that we used for mIHC.
6. **Human blood CanCOLD data (Chapter 2):** Dr. Jean Bourbeau (Research Institute of the McGill University Health Centre) provided whole blood RNA samples from subjects participating in the CanCOLD study. Dr. Michela Zago (Klox Technologies) conducted RNA extractions and cDNA synthesis of these samples. Pei Z. Li (Research Institute of the McGill University Health Centre) assisted with statistical analysis of protected information pertaining to subjects.
7. **Gene expression data:** Caitlin Mehorata and Luca Cuccia (McGill University) were undergraduate students who worked under my supervision/mentorship. Caitlin performed the RNA extractions and Luca performed qRT-PCR and corresponding analysis, to assess *Mmp9* and *Timp1* mRNA expression in the mouse lungs **(Chapter 2).** Kashmira Prasade (McGill University) was a MSc. intern who worked under my supervision/mentorship and performed the RNA extractions and qRT-PCR and corresponding analysis to assess mRNA expression of autophagy genes **(Chapter 3).**
8. **A549-AhR^{KO} cells (Chapter 3):** Dr. Jason Matthews (University of Toronto, University of Oslo) created and provided A549-AhR^{KO} cells used for cell culture experiments.
9. **Intellectual contributions and editing:** Dr. James Martin, Dr. Qutayba Hamid, Dr. David Eidelman, Dr. Benjamin Smith, and Dr. Carolyn Baglole (McGill University) all provided intellectual contributions for this work. Additionally, Dr. David Eidelman, Dr. Benjamin Smith, Dr. Jason Matthews and Dr. Carolyn Baglole also assisted with thesis editing.

List of Figures

List of Tables

Abbreviations Used

A549: human alveolar epithelial cell line
AAT: Alpha-1 antitrypsin
ActD: Actinomycin D
AIP: Aryl hydrocarbon receptor interacting protein
AhR: Aryl hydrocarbon receptor
AhRE: Aryl hydrocarbon receptor response element
AhRR: Aryl hydrocarbon receptor repressor
ALDH: Aldehyde dehydrogenase
ANOVA: Analysis of variance
ARNT: AhR nuclear translocator
ATF: Activating transcription factor
ATG: Autophagy related gene
BAL: Bronchoalveolar lavage
Becn1: Beclin-1
bHLH: basic helix loop helix
BCA: Bicinchoninic acid
BMDM: Bone marrow derived macrophages
BSA: Bovine serum albumin
C: Cleaved
CanCOLD: Canadian chronic obstructive lung disease
CAT: Catalase
CH-223191: 2-methyl-2H-pyrazole-3-carboxylic acid methyl-4-o-tolylazo-phenyl)-amide
CHOP: C/EBP homologous protein
CHX: Cyclohexamide
COPD: Chronic obstructive pulmonary disease
COX-2: Cyclo-oxygenase 2
CS: Cigarette smoke
CSE: Cigarette smoke extract
CT: Computed tomography
CYP: Cytochrome P450
DAB: 3,3'- diaminobenzidine
ddPCR: Digital droplet polymerase chain reaction
DMEM: Dulbecco's Modified Eagle Medium
DNA: Deoxyribonucleic acid
DRE: Dioxin response element
e-cigarette: Electronic cigarettes
eIF2α: eukaryotic translation initiation factor 2α
ECL- Enhanced chemiluminescence
ER: Endoplasmic reticulum
ERAD: Endoplasmic reticulum associated degradation
eQTL: Expression quantitative trait loci
FBS: Fetal bovine serum
FEV_1: Forced expiratory volume in 1 second
FDA: Food and drug administration
FICZ: 6-formylindolo (3,2-b) carbazole
FRC: Functional residual capacity
FVC: Forced vital capacity
GABARAPL1: Guinea pig gamma-aminobutyric acid receptor-associated protein-like 1
GADD34: Growth arrest and DNA-damage inducible protein 34
GC: Guanine-cytosine
GNF351: N-(2-(1H-indol-3-yl) ethyl)-9-isopropyl-2-(5-methylpyridin-3-yl)-9H-purin-6-amine
GOLD: Global Initiative for Obstructive Lung Disease
GRP78: Glucose regulated protein 78
GSH: Glutathione
GST: Glutathione s-transferase
HAH: Halogenated aromatic hydrocarbon
HRCT: High resolution computed tomography
HSP: Heat shock protein
HU: Hounsfield Unit
HuR: Human antigen R
HRP: Horse radish peroxidase
ICS: Inhaled corticosteroid
IC/TLC: Inspiratory capacity/ Total lung capacity
IDO: Indoleamine 2,3- dioxygenase

IL: Interleukin
IRE1α: Inositol-requiring enzyme 1
ITE- 2: (1′H-indole-3′-carbonyl)-thiazole-4-carboxylic acid methyl ester
LABA: Long acting β_2-adrenergic agonists
LAMA: Long acting muscarinic antagonists
LC3: Microtubule associated protein 1 light chain 3
Lm: Mean linear intercept
lncRNA: Long noncoding RNA
MEM: Minimum essential medium
miRNA: micro RNA
mIHC: Multiplex immunohistochemistry
MLE12: Mouse lung epithelial cell line
MLF: Mouse lung fibroblast
MMP: Matrix metalloproteinase
MNGC: Multinucleated giant cell
mTOR: Mammalian target of rapamycin
ncRNA: Non-coding RNA
NES: Nuclear export signal
NLS: Nuclear localization signal
NF-κB: Nuclear Factor Kappa B
NQO1: NAD(P)H quinone oxidoreductase 1
PAH: Polycyclic aromatic hydrocarbon
PAS: PER-ARNT SIM
PCB: Polychlorinated biphenyl
PCDD: Polychlorinated dibenzodioxins
PCDF: Polychlorinated dibenzofuran
PCR: Polymerase chain reaction
p-EIF2α: phosphorylated (at serine 51) eukaryotic translation initiation factor 2α
PERK: Protein kinase RNA-like endoplasmic reticulum kinase
PFA: Paraformaldehyde
PV: Pressure volume
PVDF: Polyvinylidene difluoride
qPCR: Quantitative polymerase chain reaction
RI-MUHC: Research Institute of the McGill University Health Center
RIPA: Radio-immunoprecipitation assay
RNA: Ribonucleic acid
ROS: Reactive oxygen species
SABA: Short acting β_2-adrenergic agonists
SAMA: Short acting muscarinic antagonists
SAhRM: Selective AhR modulator
SDS-PAGE: Sodium dodecyl sulfate polyacrylamide gel electrophoresis
siRNA: Small- interfering RNA
SNP: Single nucleotide polymorphism
SOD: Superoxide dismutase
SP: Specificity protein
sXBP-1: spliced X-box binding protein 1
TCDD: 2,3,7,8- Tetrachlorodibenzo-p-dioxin
TEM: Transmission electron microscopy
Th: Helper T lymphocytes
THC: Tetrahydrocannabinol
TIMP: Tissue inhibitor of metalloproteinase
TiPARP: TCDD-inducible Poly ADP-Ribose Polymerase
Treg: Regulatory T lymphocytes
UGT: UDP-glucuronosyltransferase
ULK1: Uncoordinated 51-like kinase 1
UPR: Unfolded protein response
UV: Ultraviolet
WHO: World Health Organization
XAP2: Immunophilin-like X-associated protein 2
XBP-1: X box binding protein 1
XME: Xenobiotic metabolizing enzymes
XRE: Xenobiotic response element
ZFN: Zinc finger nuclease

Abstract

Chronic Obstructive Pulmonary Disease (COPD) is a prevalent and complex respiratory disorder primarily caused by inhalational exposure to cigarette smoke (CS). However, only approximately 15% of cigarette smokers develop COPD, suggesting that genetic or epigenetic factors may contribute to disease susceptibility. One feature of COPD is emphysema, which is characterized by permanent alveolar wall destruction leading to airspace enlargement. The alveolar wall destruction in emphysema is a consequence of multiple pathogenic mechanisms including chronic inflammation, a protease: anti-protease imbalance and the upregulation of cell death programs such as apoptosis, autophagy and endoplasmic reticulum (ER) stress. However, molecular mechanism(s) that regulate these pathogenic events, and thus the development of emphysema, are poorly understood. This regulation may involve the aryl hydrocarbon receptor (AhR), which is a ligand-activated transcription factor whose involvement in COPD pathogenesis is unknown. Our lab has previously published that AhR-deficiency exacerbates CS-induced cell death and inflammation in lung structural cells. Thus, we hypothesized that AhR-deficiency would promote the development of CS-induced emphysema and COPD pathogenesis.

Using a preclinical model of CS-exposure, we demonstrate that AhR deficiency worsens the development of a CS-induced emphysema-like phenotype in the murine lung. AhR ablation promoted the CS-induced: (1) upregulation of pathogenic mechanisms underlying emphysema development (*i.e.* inflammation, an antiprotease imbalance, and the activation of cell death machinery), (2) lung parenchymal destruction, and (3) declines in lung function. In COPD subjects, there was less pulmonary and systemic AHR expression. In humans, systemic *AHR* mRNA levels also positively correlated with lung function. There was no alteration in the frequency of *AHR* single nucleotide polymorphisms (SNPs) that could explain this decrease in

AHR in COPD subjects. However, elevated expression of the AhR Repressor (*AHRR*), which is a negative regulator of the AHR, in the COPD lung may contribute to reduced AHR expression in these subjects.

We also utilized an *in vitro* model of CS exposure to evaluate if the AhR attenuation of CS-induced cell death in lung structural cells involves its regulation of cell death modalities such as autophagy and/or ER stress. We show that the expression of the autophagy and ER stress protein LC3II was significantly elevated in cigarette smoke extract (CSE)-exposed AhR-deficient lung structural cells; these cells were primary mouse lung fibroblasts (MLFs), mouse lung epithelial cells (MLE12) and alveolar epithelial cells (A549). Heightened LC3II expression could not be explained by the transcriptional upregulation of key autophagy genes (*Gabarapl1*, *Beclin1*, *Lc3b*), upregulation of upstream autophagic machinery (ATG5-12, ATG3) or impaired autophagic flux. This suggested that elevated LC3II in CSE-treated AhR-deficient cells is likely mediated by an autophagy-independent mechanism. This was further supported by the absence of autophagosomes in transmission electron micrographs. However, CSE-treated $Ahr^{-/-}$ MLFs showed significantly reduced viability, widespread ER-dilation, elevated expression of ER stress markers (*i.e.* CHOP and GADD34) and the accumulation of ubiquitinated proteins. Thus, the AhR attenuates an ER stress response that is autophagy-independent yet associated with elevated LC3 expression and processing.

Collectively, our data position the AhR as a central player in the homeostatic maintenance of lung health by demonstrating that loss of the AhR promotes the development of CS-induced emphysema. Given that no effective therapeutic options currently exist to stop or slow COPD progression, these findings could provide the basis for the development of new therapeutic agents or biomarkers for COPD.

Résumé

La Maladie Pulmonaire Obstructive Chronique (MPOC) est une maladie respiratoire complexe à prévalence élevée, dont le principal facteur de risque est l'exposition à la fumée de cigarette. Cependant, seuls 15% des fumeurs développent une MPOC, suggérant l'implication de facteurs génétiques ou épigénétiques dans la susceptibilité à la maladie. Une des composantes de la MPOC est l'emphysème, défini par une destruction irréversible des parois alvéolaires aboutissant à un élargissement permanent des espaces aériens distaux. La destruction alvéolaire est la conséquence de multiples mécanismes physiopathologiques incluant l'inflammation chronique, le déséquilibre de la balance protéases : anti-protéases et l'activation de divers programmes de mort cellulaire tels que l'apoptose, l'autophagie ou le stress du réticulum endoplasmique (ER stress). Toutefois, les mécanismes moléculaires régulant ces événements, et par suite le développement de l'emphysème, sont encore imparfaitement connus. Cette régulation pourra impliquer l'aryl hydrocarbon receptor (AhR), qui est un facteur de transcription activé par un ligand et dont son implication dans le développement de MPOC est inconnue. Notre laboratoire a précédemment montré que le déficit en AhR dans les cellules pulmonaires exacerbe la mort cellulaire et l'inflammation induites par la fumée de cigarettes. C'est pour cela, nous avons émis l'hypothèse que la déficiance en AhR favoriserait le développement de l'emphysème et de la pathogenèse de la MPOC induits par la fumée de cigarettes.

Dans notre modèle murin, nous démontrons que le déficit en AhR aggrave le développement d'un phénotype semblable à un emphysème induit par l'exposition à la fumée de cigarettes. L'ablation AhR a promu: 1) des mécanismes pathogéniques aboutissant au développement d'emphysème (ex : inflammation, déséquilibre protéases-antiprotéases au niveau pulmonaire et activation de programmes de mort cellulaire), (2) destruction de parenchyme

pulmonaire, et (3) le déclin de la fonction respiratoire. L'expression pulmonaire et systémique de l'AHR était diminuée chez les patients atteints de MPOC. De plus, les niveaux d'ARN messagers systémiques de l'*AHR* étaient positivement corrélés à la fonction respiratoire. Enfin, on ne retrouvait pas d'altération dans la fréquence des polymorphismes nucléotidiques (SNP ; single nucleotide polymorphism) permettant d'expliquer la diminution de l'expression de l'*AHR* dans la MPOC. Cependant, nous avons observé que l'expression du répresseur d'AHR (*AHRR*), qui est un régulateur négatif d'AHR, est élevée dans les poumons de MPOC. Ceci pourra expliquer la diminution d'AHR observée chez ces sujets.

De plus, nous avons utilisé un modèle *in vitro* d'exposition à la fumée de cigarette afin d'évaluer si AhR réduit le mort des cellules structurales en régulant les programmes de mort cellulaire, comme autophagie et/ou ER. Nous montrons que l'expression du marqueur d'autophagie et d'ER la protéine LC3II était significativement augmentée dans les cellules pulmonaires de structure déficientes pour l'AhR, exposées à de l'extrait de fumée de cigarette (CSE), ces cellules étant des fibroblastes pulmonaires primaires de souris (MLFs ; mouse lung fibroblasts), des cellules épithéliales pulmonaires murines (MLE12) et des cellules épithéliales alvéolaires humaines (A549). L'augmentation de l'expression de LC3II n'était pas relative à une surexpression transcriptionnelle des gènes clés mis en jeu dans l'autophagie (*Gabarapl1*, *Beclin1*, *Lc3b*), une régulation positive de la machinerie autophagique d'amont (ATG5-12, ATG3), ou une altération du flux autophagique. Ces résultats suggèrent que l'élévation de LC3II dans les cellules déficientes pour l'AhR exposées à la fumée de cigarette est potentiellement médiée par un mécanisme indépendant de l'autophagie. L'absence d'autophagosome en microscopie électronique en transmission soutient cette hypothèse. Cependant, les MLFs $Ahr^{-/-}$ présentaient une viabilité significativement réduite, une dilatation diffuse du réticulum endoplasmique, une

élévation de l'expression du marqueur d'ER-stress, CHOP, et l'accumulation de protéines ubiquitinylées. Ainsi, l'AhR semble atténuer une réponse de type ER stress de manière indépendante de l'autophagie, mais en association avec une augmentation de l'expression et de l'activité de LC3II.

L'ensemble de ces données positionne l'AhR comme un facteur central dans la préservation de l'homéostasie pulmonaire en démontrant que la perte de l'AhR favorise le développement de l'emphysème induit par la fumée de cigarettes. Étant donnée l'absence actuelle de traitements efficaces pour arrêter ou ralentir la progression de la MPOC, ces résultats pourraient constituer une base de travail pour le développement de nouveaux traitements.

1 Literature Review

1.1 Chronic Obstructive Pulmonary Disease (COPD)

1.1.1 Clinical Presentation

1.1.1.1 Phenotypes

COPD is a respiratory illness characterized by progressive and irreversible air flow obstruction. Although often referred to as a "disease", COPD encompasses a spectrum of disorders with two predominant phenotypes: chronic bronchitis and emphysema. Chronic bronchitis is characterized by the presence of a sputum-producing cough for at least three consecutive months per year during a two-year period (1). Chronic bronchitis predominantly affects the airways and is the consequence of goblet cell hyperplasia and subsequent mucus hypersecretion, which functionally leads to airway obstruction (2). In addition to mucus production, chronic bronchitis is also typified by other structural changes in the airways referred to as remodeling. Airway remodeling in COPD is characterized by thickening of the airway wall due largely to increased extracellular matrix deposition, which contributes to the development of fibrosis in the small airways (3, 4). This mucus production and airway remodeling collectively results in airway narrowing and obstruction.

Emphysema is an anatomical condition characterized by the permanent destruction of the alveolar walls distal to the terminal bronchioles; this results in airspace enlargement and consequently impaired gas exchange (1, 5). Lung parenchymal destruction also results in impaired elastic recoil capabilities of the lung, causing further airflow limitation. Clinically, emphysema is diagnosed using high resolution computed tomography (HRCT) scans, where airspace enlargement is identified as low density (*i.e.* low attenuation) regions in the lung (6). Although the cutoffs for defining emphysema can vary as a consequence of HRCT slice thickness or the reconstruction algorithm used, it is generally accepted that a diagnosis of emphysema is made

when more than 10% of the pixels on a HRCT scan of the lung are less than -910 Hounsfield Units (HU) (6).

The two most commonly-observed pathological subtypes of emphysema are centrilobular and panlobular. Although both types can be present, cigarette smoking is most commonly associated with centrilobular emphysema and predominately affects the respiratory bronchioles in the upper lobes of the lungs. In contrast, panlobular emphysema is typically associated with alpha-1 antitrypsin deficiency (further discussed in *1.1.2.1* "*Risk Factors*") and this type of destruction affects both the respiratory bronchioles and alveolar sacs (5, 7).

Although both chronic bronchitis and emphysema are phenotypes under the larger umbrella of COPD, patients often have evidence of either phenotype before they reach the threshold of airflow obstruction used for the diagnosis of COPD (see *1.1.1.2 "Diagnosis and Staging"*). This is likely because significant mucus production/airway remodeling (8) and/or emphysematous lung destruction (upwards of 50%) occurs before symptoms associated with lung function decline become evident (https://my.clevelandclinic.org/health/diseases/9370-emphysema). Despite the fact that chronic bronchitis and emphysema can present independently of one another, it is now widely accepted that most cases of COPD typically fall somewhere in the middle of a "COPD-spectrum" and individuals with COPD often exhibit characteristics of both chronic bronchitis and emphysema to varying extents (2).

1.1.1.2 Diagnosis and Staging

Given that COPD is a heterogenous condition, it lacks rigorous diagnostic criteria, which introduces subjectivity into the diagnostic process. This subjectivity likely accounts for the high rates of under-diagnosis of COPD subjects (see *1.1.2.2* "*Prevalence and Incidence*"). Despite this subjectivity, several benchmarks are used for the diagnosis of COPD. One benchmark is that individuals with COPD classically present with symptoms such as dyspnea (breathlessness) and

cough, which is often accompanied by sputum production. A cough is typically the first symptom to develop, whereas excessive dyspnea while participating in day-to-day activities is often why individuals seek medical consultation (9). These symptoms, coupled with the presence of chronic bronchitis (*i.e.* sputum-producing cough for at least three consecutive months per year during a two-year period) and/or emphysema (*i.e.* anatomical evidence of lung parenchymal destruction) is suggestive of a diagnosis of COPD. Furthermore, evaluating the patient's life-history to determine the presence of COPD-associated risk factors (see *1.1.2.1* "*Risk Factors*") is also used for the diagnosis of COPD. Spirometric determination of the forced expiratory volume in 1 second (FEV_1) to the forced vital capacity (FVC) ratio is used to confirm airflow obstruction, and is another benchmark used for the diagnosis of COPD. Since COPD is largely insensitive to the effects of bronchodilators, airflow obstruction in COPD is diagnosed in individuals with an $FEV_1/FVC \leq 0.7$ following bronchodilation (10).

COPD severity is staged using the Global Initiative for Chronic Obstructive Lung Disease (GOLD) classification system. Here, staging is accomplished using the FEV_1 % predicted, which compares FEV_1 to the FEV_1 that one would expect or "predict" in an individual without obstructive lung disease. This predicted value is based on the individual's age, height and sex (9). Subjects at risk for the development of COPD (GOLD 0) are not considered to have COPD as they do not reach the threshold used by GOLD for defining airflow obstruction (*i.e.* $FEV_1/FVC < 0.7$), but they do exhibit COPD-associated symptoms (*e.g.* cough with sputum). Mild COPD (GOLD I) is defined by a $FEV_1 \geq 80\%$ predicted; moderate COPD (GOLD II) is defined by a FEV_1 of 50-80% predicted; severe COPD (GOLD III) is defined by a FEV_1 of 30-50% predicted; and very severe COPD (GOLD IV) is defined by a $FEV_1 \leq 30\%$ predicted (11).

1.1.1.3 Exacerbations

In addition to these classic features of COPD, patients can also have exacerbations, which are bouts of worsened symptoms that have significant negative impacts on a patient's quality of life (12). COPD exacerbations are a consequence of exposure to environmental pollutants or lung infections in 10% and 50-70% of cases, respectively (13). The cause of COPD exacerbations is unknown in approximately 30% of cases (13). Exacerbations due to lung infections include both viral or bacterial pathogens. These lung infections account for 11% of deaths among COPD patients (14). The most commonly-occurring viral infection associated with COPD exacerbations is rhinovirus (23%), although influenzae is also commonly reported following an exacerbation (5-28%) (13). The most commonly-isolated bacteria associated with COPD exacerbations are *Haemophilus influenzae* (20-30%), *Streptococcus pneumoniae* (10-15%), *Moraxella catarrhalis* (10-15%) and *Pseudomonas aeruginosa* (5-10%) (15).

1.1.1.4 Extra-Pulmonary Manifestations

COPD is also typically characterized by extra-pulmonary manifestations. Two of the most commonly observed extra-pulmonary manifestations in COPD are weight loss and skeletal muscle dysfunction (1). Weight loss in COPD subjects is proposed to be attributable to several factors including cigarette smoking, decreased appetite and undernutrition due to depression, and ingestion of medications such as glucocorticoids (16). However, significant weight loss is only reported in 25-40% of COPD patients (16, 17). In particular, more severe COPD (*i.e.* GOLD III and IV) shows the strongest association with being underweight (18).

Skeletal muscle weakness is also commonly observed among COPD subjects, although its prevalence ranges considerably between reports. For example, a study conducted in the United Kingdom reported that 33% of COPD subjects experience quadricep femoris (hereafter referred to

as quadricep) weakness (19), whereas an independent study conducted in India observed quadricep weakness in 92% of COPD subjects (20). Despite differences in the prevalence of quadricep weakness among COPD subjects, both these studies observed that this weakness was increasingly prevalent as COPD severity worsened (19, 20). Quadricep weakness is an important consideration in COPD patients because it is associated with fatigue and reduced exercise capacity. Additionally, COPD-associated skeletal muscle weakness also manifests as weakness of the diaphragm. In support of this, muscle fibers from the diaphragm of COPD patients have reduced ability to generate force, reduced calcium sensitivity and impaired contractile properties (21). Diaphragm weakness in COPD results in respiratory failure, which is the leading cause of death among COPD patients (14). In addition to weight loss and skeletal muscle dysfunction, COPD patients often present with pathologies affecting a variety of different organ systems referred to as co-morbidities.

1.1.1.5 Co-morbidities

It is estimated that upwards of 80% of COPD patients present with at least one co-morbid condition (22). Several co-morbidities, such as lung cancer (4-8% of COPD patients) and cardiovascular disease (29-70% of COPD patients), are likely a consequence of exposure to cigarette smoke (CS) (22, 23). Lung cancer and heart failure are the cause of death in 7% and 13% of COPD patients, respectively (14). Other common co-morbidities such as osteoporosis (21-66% of COPD patients), cognitive impairment (2-20% of COPD patients) and diabetes (21-57% of COPD patients) may be a consequence of the older age of COPD patients (22, 23).

1.1.2 Epidemiology

1.1.2.1 Risk Factors

1.1.2.1.1 Age and Sex

Age is a risk factor for the development of COPD (24, 25). In Ontario, the highest prevalence

of COPD occurs in older (65+ yrs) men at a rate of 249.1 per 1000 (26). Although COPD is most commonly-observed among older males, in younger individuals (aged 50-59 yrs), COPD is more frequent in females (27). It is generally accepted that women are more susceptible to CS-induced pulmonary damage (28, 29). In support of this, a comparison of FEV_1-matched male and female COPD patients revealed that females were both younger than males (average age of 57 yrs in females compared to an average age of 65 yrs in males) and had less of a smoking history (average of 48 pack-years in females compared to 69 pack-years in males) (30). Interestingly, the COPD phenotype may also be influenced by sex, as men exhibit more emphysematous lung destruction than women at all stages of COPD severity (31). Women on the other hand exhibit more of a chronic bronchitis phenotype (28, 29).

1.1.2.1.2 Genetics

Currently, the only established genetic risk factor for COPD is alpha-1 antitrypsin (AAT) deficiency (32). AAT deficiency is present in 3-10% of individuals with COPD (33, 34). AAT, a glycoprotein encoded by the *SERPINA1* gene, is a serine proteinase inhibitor. Thus, individuals with AAT deficiency exhibit widespread lung damage as a result of excessive serine proteinase activity (35). Approximately 15% of AAT-deficient individuals also develop liver damage in the form of cirrhosis, and in rare cases an inflammatory condition of the skin called panniculitis (36).

There are four variants of AAT: F, M, S and Z (32). The most common variant associated with AAT deficiency is the Z mutation in the *SERPINA1* gene, which results in the loss of one (heterozygosity) or both (homozygosity) of the Z alleles; these are referred to as the MZ or SZ phenotype, respectively (35, 37). The Z mutation causes impaired AAT folding at the endoplasmic reticulum (ER) during synthesis in the liver. This misfolding results in insufficient AAT secretion and as a consequence, reduced serum and extra-hepatic AAT levels (37). AAT deficiency increases the risk of emphysema, especially in individuals exposed to inhalational toxicants such as CS or

air pollution (35, 38, 39). Experimentally, AAT-deficient mice develop CS-induced lung parenchymal destruction and a decline in lung function more rapidly than AAT-expressing mice (40).

1.1.2.1.3 Inhalation of Toxicants

The single most important risk factor for COPD is inhalational exposure of environmental contaminants, particularly mainstream CS (2017). CS is a complex mixture of more than 5,000 chemicals, including metals (iron, nickel), gases (ozone), biological agents (plant pollen, endotoxins, bacteria), minerals (quartz, asbestos) and organic chemicals such as nicotine, polychlorinated dibenzodioxins [PCDDs] and polycyclic aromatic hydrocarbons [PAH] (41-44). Furthermore, CS is a major source of oxygen free radicals such as superoxide and hydroxyl.

Cigarette smoking is associated with the development of approximately 75% of COPD cases (45). The role of cigarette smoking as a causative factor in the development of COPD is supported by experimental models. Mice exposed to a chronic CS regime exhibit a COPD-like phenotype characterized by reduced lung function, airspace enlargement, mucus hypersecretion and heightened pulmonary inflammation that is glucocorticoid-resistant (46). Interestingly, although only about 15% of human cigarette smokers develop COPD (*i.e.* as defined by airflow obstruction), approximately 40% of smokers exhibit significant emphysematous lung destruction (47). For example, one group reported that among 59 individuals with a history of cigarette smoking who exhibited normal lung function, 43% of them were diagnosed with emphysema using HRCT (48). This highlights that CS exposure is a driver of emphysematous airspace enlargement.

Exposure to side-stream smoke, a component of second-hand smoke, may also be a risk factor for the development of COPD. Non-smokers exposed to one hour of second-hand smoke exhibit a transient reduction in lung function and increased inflammatory cytokine production (49). Additionally, animal studies have also demonstrated that exposure to second-hand smoke induces

lung structural damage (50). Similarly, electronic cigarette (e-cigarette) usage may be another risk factor for the development of COPD. E-cigarettes are battery-powered nicotine delivery systems that were invented in 2003. Today, 8.5% of all Canadians (aged 15 years and older) have reported using e-cigarettes, and 1.8% of Canadians are likely regular users having reported using an e-cigarette within the past month (51). Although e-cigarettes are marketed as safe alternatives to traditional cigarettes, many of the same compounds present in CS are also present in e-cigarette re-fill solutions and vapors (*e.g.* PAHs, pesticides, metals).

Although COPD is predominantly caused by exposure to CS, approximately 25-30% of all COPD patients are never-smokers, suggesting that factors other than CS contribute to COPD (45, 52). One of these factors may be air pollution. COPD incidence is positively associated with increased long-term exposure to air traffic pollution (53). Additionally, short-term exposure to air pollution is associated with an increased risk of exacerbations (54). Exposure to biomass pollution is another important risk factor in the overall COPD prevalence (55). It is estimated that one third of the world's population use biomass (*i.e.* wood and dung) and coal for heating and cooking (WHO). Thus, exposure to biomass fuels are postulated to account for the high rates of COPD among never-smoking women in developing countries (56).

Finally, occupational exposures may account for approximately 15% of all COPD cases (57). Exposure to coal dust is an important risk factor for COPD, as both lung function decline and other COPD-like symptoms are present in individuals following two years of work in coal mines (58). Employees in pulp and paper manufacturing companies also have an increased risk of developing COPD due to inhalational exposure of soft paper dust (59). COPD may also be a consequence of exposure to silica dust and fumes encountered in furnace and boiler installation industries (60).

Taken together, inhalational exposure of toxicants such as CS and air pollution (ambient,

biomass and occupational) are the primary risk factors for the development of COPD. As of 2016, the WHO reports that 92% of the world's population resides in locations with air pollution in excess of the "WHO's ambient air quality guidelines". These guidelines state that the annual exposure to particulate matter with a diameter less than 2.5 μm should not exceed 10 $\mu g/m^3$ (http://www.who.int/mediacentre/news/releases/2016/air-pollution-estimates/en/). Given the expansive nature of these environmental risk factors, COPD is likely to remain a major health care issue for many decades (61).

1.1.2.2 Prevalence and Incidence

Worldwide, COPD affects an estimated 380 million people (62). COPD is also the third leading cause of death worldwide, claiming the lives of approximately 3 million people in 2015 (63). The global prevalence of COPD ranges from 10.2-20.9%, depending on whether airflow obstruction is defined using a fixed FEV_1/FVC ratio of less than 0.7, or a FEV_1/FVC below the lower limit of normal; this latter definition yields lower estimates (64).

The prevalence of COPD in Canada is 12-17% among Canadians between the age of 35-79 yrs (65). However, these prevalence estimates are likely conservative given that there is significant under-diagnosis of COPD worldwide. In Spain, 73% of subjects with COPD-compatible airflow obstruction had not been diagnosed (66). Additionally, in Ontario, 67% of subjects exhibiting airflow obstruction compatible with COPD had never been diagnosed with the disease (67). These values reported in Ontario are similar across Canada, with a recent study reporting that 70% of Canadians with COPD are undiagnosed (68). The burden of undiagnosed COPD in Canada is particularly evident in respect to health care use. This is supported by findings that more than half of all COPD-associated exacerbation events, which typically require hospitalization or medical consultation, were reported among subjects that had never been previously diagnosed with COPD

(68).

In Ontario, the incidence of COPD among adults 35 years and older was 8.2 per 1,000 individuals between 2002 and 2011 (26). The mortality rate from COPD was 4.5 per 1,000 individuals (26). Statistics Canada (69) reports that in 2011, COPD accounted for 4.4% of deaths among Canadians.

1.1.3 Disease Management

Despite the significant disease burden of COPD, there are no known disease modifying therapeutic options that can interfere with the natural history of this disease. Therefore, current COPD therapy is aimed at minimizing the impact of the disease and maximizing the patient's functional status. The first step of COPD management is smoking cessation and/or minimizing exposure to environmental contaminants such as air pollution. Those with COPD typically manage their symptoms via the use of inhaled bronchodilators to alleviate breathlessness and to mitigate exacerbations (10).

In addition to GOLD staging, COPD patients are further categorized into one of four groups (A-D) based on exacerbation frequency and the number of symptoms that they experience. These groups influence the type of bronchodilator that is prescribed (70). Patients in group A are classified as GOLD stage I-II, present with few symptoms and exhibit minimal exacerbations (0-1) annually. Short acting muscarinic antagonists (SAMA) or β_2-adrenergic agonists (SABA) are used for patients in group A. Group B differs from group A in that patients belonging to group B present with more symptoms than those in group A (70). In contrast, individuals who are classified as GOLD stage III-IV and exhibit more frequent exacerbations (≥ 2) are categorized into groups C or D. Patients in group C present with fewer symptoms than those belonging to group D. Long acting muscarinic antagonists (LAMA) or β_2-adrenergic agonists (LABA) are used (individually or in combination) to treat patients belonging to groups B-D. Individuals belonging to either group

C or D may also be prescribed inhaled corticosteroids (ICS) (70). Although the effectiveness of ICS is controversial throughout the literature (71), ICS have been reported in some instances to reduce exacerbation frequency and improve the quality of life in COPD patients belonging to group C or D (71).

1.2 Pathogenesis of Cigarette Smoke-induced Emphysema

The fact that no therapeutic options are currently available to stop or slow the progression of COPD is likely due to the complexity of its pathogenesis, particularly the emphysema component. Emphysema is proposed to be mediated by several inter-dependent mechanisms including chronic inflammation, oxidative stress, a protease: anti-protease imbalance and accelerated cell death in the lung (72).

1.2.1 Inflammation

COPD is widely recognized as being associated with chronic inflammation. Under physiological conditions, alveolar macrophages are the predominant immune cell in the lung, representing upwards of 95% of pulmonary leukocytes (73). This balance in immune cells in the lung shifts in response to CS. For example, human cigarette smokers have heightened levels of pulmonary neutrophils, macrophages and $CD8^+$ T-lymphocytes (74). These cell types are also increased in mice exposed to CS (75).

In COPD subjects, the quantity and predominance of these cell types (particularly macrophages and $CD8^+$ T-lymphocytes) are further increased compared to smokers without COPD (76). Similarly, heightened numbers of macrophages and $CD8^+$ T-lymphocytes are also observed in murine models of a CS-induced COPD-like phenotype (46). Of these immune cells, macrophages and T-lymphocytes are thought to play a dominant role in emphysema development. One supporting line of evidence comes from human studies whereby the Cosio laboratory reported that the quantity of alveolar macrophages and T-lymphocytes per mm^3 of lung tissue is

significantly and positively correlated with the extent of emphysematous destruction in the lung (77). A role for macrophages in emphysema development is further supported by evidence from animal models that clodronate-induced macrophage depletion in the murine lung attenuates the development of CS-induced airspace enlargement (Beckett et al. 2013). Data from these animal models also suggest that macrophages are not the only immune cell involved in disease induction, as T-lymphocyte depletion also attenuates the development of CS-induced airspace enlargement in the murine lung (78).

Although macrophages and $CD8^+$ T-lymphocytes are the predominant inflammatory cell types in the lungs of humans with COPD, neutrophilia is also common (79). Elevated neutrophil numbers are also seen in the bronchoalveolar lavage (BAL) of CS-exposed mice (46). While neutrophilia likely contributes to COPD pathogenesis, neutrophilia alone does not appear to drive emphysema progression. This is supported by findings from human studies demonstrating that there is no difference in neutrophil numbers between smokers with and without emphysema (80). Moreover, elevated neutrophil numbers are also significantly correlated with areas of the lung exhibiting no emphysematous destruction (77). This finding led these authors to speculate that neutrophils do not likely drive emphysematous lung destruction (77). Additionally, animal models have demonstrated that neutrophil depletion does not suppress the development of a CS-induced emphysema-like phenotype in the murine lung (46).

The collective infiltration of neutrophils, macrophages and CD8+ T-lymphocytes to the lung leads to the production of reactive oxygen species (ROS) and the release of proteases and perforins, respectively. Collectively, this excessive production of ROS and destructive proteases in the lung may contribute to lung parenchymal destruction and emphysema pathogenesis (81).

1.2.2 Protease : Anti-Protease Imbalance

Given the importance of AAT deficiency as a cause of genetically determined emphysema, a potential explanation for the development of CS-induced airspace enlargement could be an imbalance between proteases and antiproteases. There are now several lines of evidence to support this. In the healthy lung, there is a higher concentration of anti-proteases than proteases, which creates a protective "anti-protease screen". In emphysema, the concentration of proteases is greater than that of the anti-proteases, which renders the "anti-protease screen" insufficient to counterbalance the destructive effects of the proteases on the lung parenchyma (82).

One class of proteases believed to contribute to emphysema is matrix metalloproteinases (MMPs). MMPs are extracellular matrix-degrading enzymes secreted by immune cells such as neutrophils and macrophages (83). MMPs are inhibited by endogenous tissue inhibitors of metalloproteinases (TIMPs) (84). In particular, MMP9 is responsible for the degradation of gelatins and basement membrane collagens, such as collagen IV (85). Human studies have demonstrated that alveolar macrophages from smokers with COPD secrete higher levels of enzymatically-active MMP9, and significantly less TIMP1, compared to alveolar macrophages from smoking or non-smoking subjects without COPD (86). Similar findings have been reported in animal models, demonstrating that an increased MMP9:TIMP1 ratio is associated with the development of pulmonary emphysema in a mouse model of aging (87). However, although elevated MMP9 may contribute to COPD pathogenesis, it may not be the sole causal factor in emphysema development, as MMP9-deficient mice develop CS-induced airspace enlargement to the same extent as MMP9-expressing mice (88). Thus, additional pathogenic mechanisms are likely needed for the clinical manifestation of COPD. Given that another consequence of elevated

protease activity in the lung is an increased production of ROS (89), oxidative stress may be another pathogenic mechanism contributing to the development of COPD.

1.2.3 Oxidative Stress

Oxidative stress is the consequence of an imbalance between ROS- including superoxide anions, hydroxyl radicals and hydrogen peroxide- and antioxidants. In the healthy lung, ROS are counterbalanced by the production of endogenous antioxidants, including superoxide dismutase (SOD), catalase (CAT) and the glutathione (GSH)/glutathione peroxidase system (90). When ROS production exceeds the capabilities of these antioxidant defenses, oxidative stress ensues. Oxidative stress is proposed be another mechanism that contributes to COPD pathogenesis (72).

Inhalational exposure to CS results in heightened ROS production in the lungs- as approximately 10^{17} oxidant molecules are produced with each puff of a cigarette (91). Additionally, ROS production by recruited immune cells- such as neutrophils and macrophages- represent another major oxidant source (90). Cigarette smokers exhibit oxidative stress-induced lipid peroxidation (*i.e.* increased systemic malonyldialdehyde expression) (92) and reduced antioxidant capacities (*i.e.* reduced SOD and CAT activity) (93). However, factors other than strictly CS likely contribute to the oxidative stress observed in COPD. This is supported by several lines of evidence, including the fact that systemic malonyldialdehyde levels are significantly elevated in individuals with COPD that have never smoked relative to subjects without COPD (94). Furthermore, COPD subjects have significantly reduced antioxidant activity (*i.e.* SOD, GSH) and elevated lipid peroxidation relative to smokers without COPD (95). This unopposed oxidative stress burden in the COPD lung yields numerous pathogenic consequences including lipid peroxidation, deoxyribonucleic acid (DNA) damage, inflammation, impaired phagocytic functions of inflammatory cells and ultimately cell death (96).

1.2.4 Cell Death

Of particular importance to the pathogenesis of the emphysema component of COPD is the loss of lung structural cells (72, 97). This includes loss of alveolar epithelial cells that are responsible for gas exchange and fibroblasts that synthesize the extracellular matrix necessary for lung structure and elasticity. Thus, loss/absence of these cell types may drive parenchymal destruction in emphysema (98-100). There are several cell death programs, including apoptosis, autophagy, and ER stress, that may be initiated by CS and/or drive emphysematous lung tissue destruction. These are further described below.

1.2.4.1 Apoptosis

Apoptosis, or type 1 programmed cell death, is mediated by a signaling cascade that involves the activating cleavage of cysteine proteases called caspases. These caspases function to cleave molecular components involved in DNA repair and cytoskeletal integrity (101). Activation of this cascade is typified by morphological features such as DNA fragmentation, chromatin condensation and membrane blebbing. This is followed by the "budding" of cellular constituents into apoptotic bodies, which are cleared via macrophage-mediated phagocytosis (101). Caspase activation and the morphological hallmarks of apoptosis can be induced via either the intrinsic or extrinsic apoptotic signaling pathway, which is characterized by mitochondrial permeability or activation of transmembrane receptors, respectively (101).

CS induces apoptosis in all major lung structural cell types, including bronchial and alveolar epithelial cells, fibroblasts, endothelial cells and airway smooth muscle cells (97, 102-105). Furthermore, humans with emphysema exhibit heightened levels of pulmonary apoptotic cell death (106). A causal role for apoptosis in the pathogenesis of emphysema is supported by the finding

that an intra-tracheal injection of cleaved caspase-3 induces epithelial cell apoptosis and airspace enlargement in the murine lung (98).

1.2.4.2 Autophagy

In response to a common stimulus, different cell death mechanisms are executed in different cells within the same organ (107). Moreover, different cell death mechanisms can also be initiated within a single cell (108). Therefore, it is likely that CS-induced emphysema is not solely the result of apoptosis but of other mechanisms including autophagy (109, 110). In contrast to apoptosis, which is characterized by caspase activation and cell death, activation of autophagy may or may not result in cell death. This is because autophagy is the process of protein and organelle recycling, and although critical for the maintenance of cellular homeostasis, excessive or chronic induction of autophagy results in autophagic, or type 2 programmed, cell death.

Autophagy and the ubiquitin-proteasome system together represent the two major degradative pathways in the cell. The ubiquitin-proteasome system is involved in the targeted breakdown of ubiquitin-tagged proteins, whereas autophagy involves the bulk sequestration and degradation of both proteins and organelles (111). Thus, autophagy is an intracellular lysosomal-degradative pathway, and it can be divided into three subtypes: microautophagy, chaperone-mediated autophagy and macroautophagy (112). Microautophagy involves the direct lysosomal engulfment of cytoplasmic constituents. In contrast, chaperone-mediated autophagy involves the heat shock chaperone 70-dependent delivery of targeted cytoplasmic substrates that contain the consensus sequence KFERQ to the lysosome. The physiological and/or pathological contributions of these two autophagy subtypes are relatively unexplored in the literature. However, the third autophagy subtype macroautophagy (hereafter referred to simply as autophagy), has been much more extensively characterized in health and disease. This subtype involves the cytoplasmic uptake

of damaged proteins, substrates and organelles by double-membraned vesicles (autophagosomes) and their subsequent lysosomal degradation (113).

Mechanistically, autophagy is defined by a coordinated initiation and progression through several sequential steps (extensively reviewed in: (114, 115)). The first step is vesicle nucleation, which involves the *de novo* formation of the early autophagosomal membrane, also known as the isolation membrane or phagophore. In mammals, vesicle nucleation is mediated by the activating phosphorylation of the autophagy initiation uncoordinated 51-like kinase (ULK1) complex. ULK1 activation is critical for the recruitment of proteins encoded by autophagy-related genes (ATGs) to the phagophore assembly site (116). Next, the autophagosomal membrane undergoes elongation via the actions of the ubiquitin-like conjugation system ATG12-5-16. This conjugate subsequently facilitates the processing of ATG8, also known as microtubule-associated protein 1 light chain 3 (LC3), from the unconjugated isoform (LC3I) to the autophagosomal membrane-bound and phosphatidylethanolamine conjugated isoform (LC3II) (117). LC3II is important for both the maturation and closure of the autophagosomal membrane. Before fully closing, the developing autophagosome engulfs its cytoplasmic cargo in a process dependent on p62 (118). The autophagosome next fuses with a lysosome to form an autolysosome, which leads to the degradation and recycling of both the autophagic cargo and the autophagosome (**Figure 1.1**).

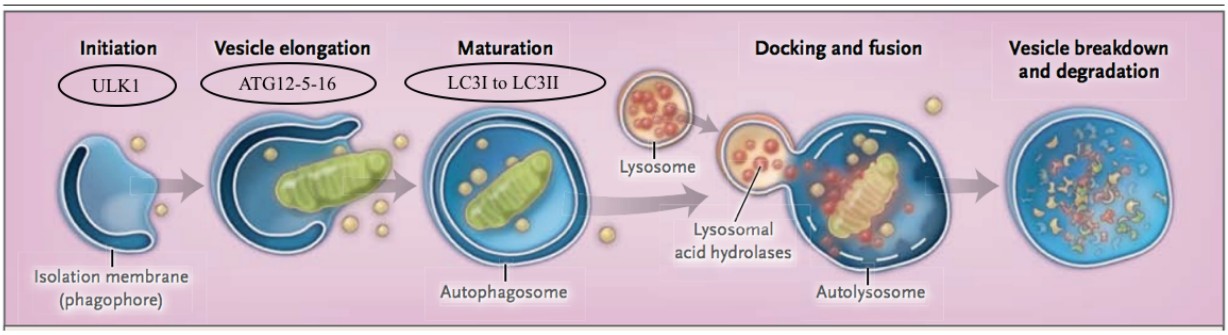

Figure 1.1. Sequential steps of macroautophagy. The "initiation" of autophagy begins with the *de novo* formation of the phagophore, which is mediated in part by ULK1. The "elongation" of the

phagophore (involving ATG12-5-16) is followed by the engulfment of cytoplasmic cargo into the autophagosome. The "maturation" (*i.e.* closure) of the autophagosome requires post-translational processing of LC3I to LC3II. The mature autophagosome next undergoes "fusion" with a lysosome to become an autolysosome. The cargo and autophagosome then undergo "breakdown and degradation", which is mediated by lysosomal acid hydrolases.
Reproduced (and slightly modified) with permission from (119), Copyright Massachusetts Medical Society.

Autophagy serves several important physiologic functions. Basal autophagy is important for intracellular quality control via the continual recycling of long-lived or damaged proteins/organelles. Additionally, autophagy can be induced by nutrient deprivation; the subsequent inhibition of the mammalian target of rapamycin (mTOR) initiates autophagy and restores the amino acid pool within the cell (120). Finally, autophagy plays essential roles during embryological development and regulates the immune response, including the mediation of T-lymphocyte self-tolerance (121).

In contrast to the homeostatic roles for autophagy, aberrant or chronic induction of autophagy is associated with disease. Increased autophagy has been consistently reported in cancers, including breast and lung cancer (122). Elevated autophagy typically promotes tumor growth, likely via the replenishment of amino acid pools, which facilitates cancer cell growth and resistance to chemotherapy. As such, clinical trials are ongoing to therapeutically target and impair the autophagic pathway to induce autophagic cell death in cancer cells. In combination with traditional chemotherapy, these clinical trials also administer hydrochloroquine, which inhibits formation of the autolysosome, resulting in an intracellular accumulation of autophagosomes and consequent cell death (122). Early phase clinical trials have demonstrated that the combination of chemotherapy and hydrochloroquine induces cancer cell death better than chemotherapy alone (122).

Similar to hydrochloroquine, CS can also impair the formation of the autolysosome (*i.e*. impair autophagic flux), resulting in autophagic cell death (123). Even alveolar macrophages from the lungs of human cigarette smokers exhibit defects in autophagy, which may impair pathogen clearance (124). Heightened autophagy may also drive the ability of CS to cause apoptosis. This is supported by observations that morphological features of autophagy (*i.e.* presence of autophagosomes) precede signs of apoptosis (*i.e*. nuclear fragmentation) (125). Additionally, *in vitro* studies have demonstrated that lung structural cells incapable of undergoing autophagy are protected against CS-induced apoptosis (126, 127). This notion, that autophagy may drive the ability of CS to cause apoptosis, is further supported by experiments conducted in LC3-deficient mice, which lack fully mature autophagosomes and are therefore unable to undergo autophagy. Findings from this mouse model demonstrate that CS-exposed LC3-deficient mice exhibit reduced levels of both pulmonary apoptosis and airspace enlargement relative to CS-exposed LC3-expressing mice (109). This suggests that autophagy may be an upstream regulator of both CS-induced apoptosis and airspace enlargement, as mice incapable of undergoing autophagy (*i.e.* LC3-deficient mice) exhibit attenuation in both of these CS-induced processes.

The idea that CS-induced autophagy precedes apoptosis is further supported by human studies, which report that heightened levels of autophagy markers are observed in the lungs of human COPD subjects as early as GOLD 0 and persist until GOLD IV (127). In contrast to this, an elevated expression of apoptotic markers is not detected in the human COPD lung until GOLD III-IV (127). Taken together, these data illustrate cross-talk between autophagy and apoptosis-which could have important consequences for lung tissue destruction.

1.2.4.3 Endoplasmic Reticulum Stress

Endoplasmic reticulum (ER) stress is another pathway with implications for COPD pathogenesis, which intersects with apoptosis and autophagy. In eukaryotic cells, the ER can be divided into two primary sub-compartments: the smooth ER and rough ER. The smooth ER is primarily responsible for the production of lipids and steroid hormones and the detoxification of endogenous and exogenous compounds. In contrast, the rough ER is studded with ribosomes and is the site of protein synthesis and folding. The rough ER is also critically involved in the regulation of cellular quality control via the unfolded protein response (UPR) (**Figure 1.2**)- reviewed in (128-131).

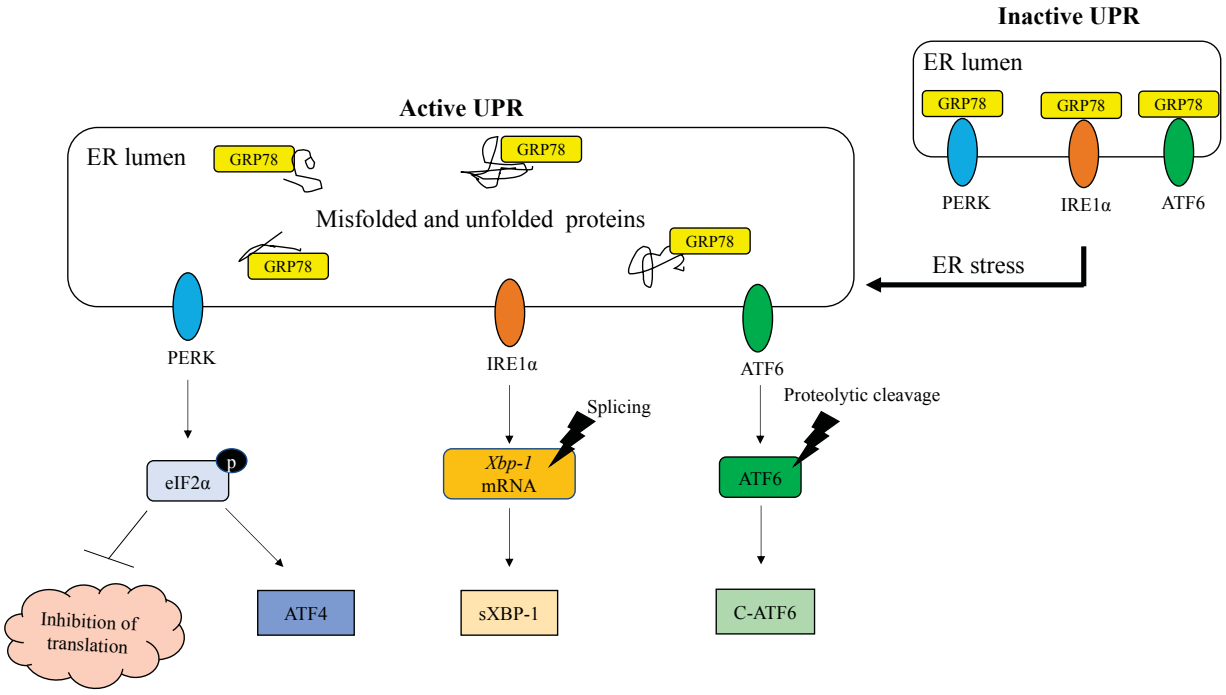

Figure 1.2. Cellular machinery involved in the unfolded protein response (UPR). Under physiologic conditions, GRP78 is anchored to each of the three ER-transmembrane proteins: PERK, IRE1α and ATF6, resulting in an inactive UPR (small diagram-top right). Activation of the UPR (large diagram) results in the dissociation of GRP78 from PERK, IRE1α and ATF6, leading to their activation. PERK activation induces the phosphorylation (p) of eIF2α, resulting in the general inhibition of translation while favoring the translation of ATF4. IRE1α activation triggers the splicing of *Xbp-1* mRNA, which is then translated into spliced (s)XBP-1. ATF6 activation induces the proteolytic cleavage (C) of ATF6, producing a 50 kDa ATF6 subunit (C-ATF6). ATF4,

sXBP-1 and C-ATF6 translocate to the nucleus where they function as transcription factors, upregulating genes involved in a variety of processes including protein folding and the clearance of protein aggregates. Figure based on (131).

Under physiologic conditions, the ER-resident molecular chaperone glucose-regulated protein 78-KDa (GRP78) is anchored to each of the three ER-transmembrane proteins: protein kinase RNA-like endoplasmic reticulum kinase (PERK), inositol-requiring enzyme 1 (IRE1α) and activating transcription factor 6 (ATF6), which renders them inactive. When misfolded protein aggregates accumulate in the ER lumen, it initiates the unfolded protein response (UPR). The UPR is a three branched signaling cascade that becomes activated by a calcium-mediated dissociation of GRP78 from any combination of the three ER-transmembrane proteins (PERK, IRE1α and ATF6). This dissociation of GRP78 from PERK, IRE1α and/or ATF6 leads to the activation of the respective UPR branch.

In the first UPR branch, PERK activation induces the phosphorylation of eIF2α at serine 51 (p-eIF2α), which results in the general inhibition of translation by sequestration of mRNA into stress granules (132). Although eIF2α phosphorylation inhibits the translation of most proteins, it favors the translation of the activating transcription factor 4 (ATF4) due to the presence of two upstream open reading frames in the 5' region of ATF4 mRNA (133). In the second UPR branch, IRE1α activation triggers the splicing of X-box binding 1 (*Xbp-1*) mRNA, with the spliced and translated XBP-1 (sXBP-1) functioning as a transcription factor. In the third UPR branch, dissociation of GRP78 from ATF6 induces the proteolytic cleavage of ATF6 in the golgi apparatus, which produces a 50 kDa ATF6 subunit (*i.e.* cleaved (C)-ATF6) that subsequently functions as a transcription factor. The purpose of UPR activation is to remove improperly folded protein aggregates. The transcription factors that are activated downstream of the three UPR branches (*i.e.* ATF4, sXBP-1 and C-ATF6) accomplish this by: 1) transcriptionally-upregulating the expression

of ER-associated molecular chaperones to increase protein folding capacity; 2) halting translation and thus protein synthesis; and 3) facilitating the proteasomal degradation of misfolded proteins via upregulation of ER-associated degradation (ERAD) genes (128). The UPR can be activated in response to physiologic stressors such as increased cholesterol or hyper/hypoglycemia (134) as well as viral or bacterial infections (135).

When activation of the UPR cannot restore homeostasis, the 'pro-death' arm of the ER stress response dominates (131). This pro-death arm is dependent on the upregulation of the transcription factor C/EBP homologous protein (CHOP) (136-138). CHOP mediates ER stress-induced cell death largely via the transcriptional upregulation of growth arrest and DNA damage-inducible gene 34 (GADD34), which functions to dephosphorylate p-eIF2α and thus resume protein synthesis (131). ATF4 and CHOP also upregulate genes involved in protein synthesis, which further contributes to ATP depletion, oxidative stress and ultimately cell death (139). Thus, chronic or aberrant ER stress may contribute to lung parenchymal destruction.

In further support of this notion, CS also induces the UPR in the lung (140, 141). Additionally, exposure to CS *in vitro* induces the UPR in lung structural cells and macrophages (142, 143). Activation of the UPR triggers CS-induced apoptotic cell death (141). Furthermore, subjects with severe emphysema have significantly higher expression of p-eIF2α and CHOP in their lungs relative to mild emphysema or control subjects (144). A causal role for ER stress in emphysema pathogenesis is supported by the finding that pharmacological alleviation of ER stress prevents CS-induced airspace enlargement, inflammation and apoptosis in the murine lung (110). Taken together, these findings provide a basis to postulate that ER stress may be a factor in emphysema pathogenesis (145).

1.2.4.4 Intersecting Cross-Roads: ER Stress and Autophagy

There has been much debate surrounding the source(s) of the autophagosomal membrane, but there is growing evidence to support that the ER is critically required for the earliest steps of autophagosome formation. Integral membrane proteins found on ribosome-free regions of the rough ER are present on both the inner and outer membranes of newly-formed autophagosomes (146). Additionally, the earliest step of autophagosome formation *(i.e.* the establishment of the ULK1 complex) is dependent on functional ER-to-golgi protein trafficking (147). The ULK1 complex also physically associates with phosphatidylinositol synthase-enriched subdomains of the ER before interacting with other autophagosome precursor proteins (148, 149). Not only is the ER critically important in the *de novo* formation of the autophagosome, but ULK1 is also required to maintain ER-to-golgi protein trafficking (150). This illustrates that cross-signaling between ER stress and autophagy is important for cellular homeostasis.

There is also ample evidence to support the notion that ER stress leads to the induction of autophagy. ER stress can trigger autophagosome formation and nucleation via several pathways. First, nucleation can be induced via the transcriptional upregulation of BECLIN-1 in an IRE1α-XBP-1 dependent manner. Alternatively, ER stress-induced calcium release from the ER lumen inhibits mTOR activity, which subsequently leads to ULK1 activation (151). Second, PERK-mediated phosphorylation of eIF2α represses mTORC activity, which is associated with increased autophagy and heightened susceptibility to oxidative stress-induced cell death (152). In line with this, tetrahydrocannabinol (THC)-induced cell death in human glioma cells is driven by ER stress-mediated phosphorylation of eIF2α, leading to autophagic cell death (153). ER stress-induced autophagy is also observed in CS-exposed umbilical vein endothelial cells (154). ER stress also

initiates the elongation of the autophagosomal membrane via the upregulation of ATF4, resulting in elevated ATG12 and ATG5 expression (151).

ER stress and autophagy also intersect at recently-described cell death mechanisms referred to as cytoplasmic vacuolation death and paraptosis. Although relatively little is known about these two mechanisms, both are generally characterized by ER dilation, heightened expression of ER stress proteins such as CHOP, the absence of autophagosomes, accumulation of ubiquitinated proteins and the elevated expression of LC3II (155, 156). Thus, although cytoplasmic vacuolation death and paraptosis are autophagy-independent cell death mechanisms (*i.e.* absence of autophagosomes), they are characterized by the heightened expression of LC3II- but without changes in other autophagy-related proteins (157).

1.3 The Aryl Hydrocarbon Receptor (AhR)

How these pathogenic processes are regulated at the molecular level in COPD is unknown. However, the observation that only 15-20% of all individuals who smoke develop COPD, suggests that disease development is not solely the consequence of CS exposure but instead, that unknown genetic or epigenetic factors may contribute to COPD pathogenesis (158, 159). One potential contributor to such gene-environment interactions may involve alterations in the expression of the aryl hydrocarbon receptor (AhR). This speculation is based on reports from the Baglole lab demonstrating that the AhR attenuates several of the mechanisms involved in emphysema pathogenesis including acute CS-induced inflammation *in vivo*, as well as oxidative stress and apoptosis *in vitro* (160-162).

1.3.1 Overview of the AhR

The AhR is a ligand-activated transcription factor that is evolutionarily-conserved among multicellular organisms (163). Although present in all tissues, the highest expression of the AhR occurs in first-line defense organs such as the skin, liver, gut and lungs (164). The AhR belongs to

the basic helix loop helix (bHLH) superfamily due to the presence of a basic domain and a helix loop helix (HLH) domain (**Fig. 1.3**).

Figure 1.3. Diagrammatic representation of the AhR protein. The protein structure of the AhR. The basic helix loop helix (bHLH) domain harbors both the nuclear localization signal (NLS) and nuclear export signal (NES). The PER-ARNT-SIM (PAS) domain harbors the ligand binding domain. Figure based on (165).

The basic domain enables binding of the AhR to the DNA, whereas the HLH domain enables protein dimerization (166). This superfamily has been further subdivided into six classes (A-F) based on a phylogenetic classification system. The AhR belongs to the bHLH class C because it both recognizes and binds ACGTG or GCGTG DNA sequences and contains a PER-ARNT-SIM (PAS) domain (166). Although the bHLH and PAS domains are located on the amino-terminus of the AhR protein, the transactivation domain can be found on the carboxy-terminus and influences the influences the nucleo-cytoplasmic shuttling functions of the amino-terminus (167). Thus, the AhR belongs to the bHLH/PER-ARNT-SIM family whose members are involved in the sensing of exogenous and endogenous stimuli (168).

1.3.2 AhR Ligands

The conventional way through which the AhR responds to stimuli is via ligand activation. Therefore, recognizing the diverse range of substances that are capable of acting as ligands to induce AhR activation is necessary to understand the biological functions of the AhR. Furthermore, understanding the breadth of substances that can act as AhR ligands is also important

given that different AhR ligands can elicit differential outcomes depending on the context (*i.e.* organ-specific differences, physiological vs. disease state etc.).

AhR ligands are typically hydrophobic in nature and thus enter the cell via simple diffusion through the plasma membrane (169). AhR ligands are also classically small (i.e. estimated to be between 1.2 and 1.4 nm in length) and planar substances (170), although structurally diverse AhR ligands that deviate from these properties have also been recently identified (171). Upon entering the cytoplasm, AhR ligands bind to the ligand-binding domain located on the amino terminus of the cytoplasmic AhR. The ligand binding affinity influences the specific residues within the AhR ligand binding pocket to which the ligands will interact with and bind (172). The AhR is activated by a wide variety of agonists of either exogenous or endogenous origin.

1.3.2.1 Exogenous AhR Agonists

The most well-characterized class of AhR ligands are exogenous environmental toxicants including polycyclic aromatic hydrocarbons (PAHs) and halogenated aromatic hydrocarbons (HAHs) (170). Both PAHs and HAHs are produced from the incomplete combustion of organic compounds, which can occur naturally (*e.g.* forest fires and volcanic eruptions) or from anthropogenic sources (*e.g.* burning of fossil fuels, pulp and paper manufacturing, air pollution, cigarette smoke) (171). Exposure to PAHs and HAHs typically induce the expression of xenobiotic metabolizing enzymes (XMEs), which are target genes of the AhR (see *1.3.4.1 "Xenobiotic Metabolism"*). Although these XMEs are important in the metabolism and clearance of most PAHs (171), they are often ineffective in metabolizing many HAHs- particularly chlorinated HAHs. Chlorinated HAHs are also known as dioxin-like compounds, which can be sub-divided into three classes: polychlorinated biphenyls (PCBs), polychlorinated dibenzofurans (PCDFs) and

polychlorinated dibenzodioxins (PCDDs). The most well-characterized AhR ligand belongs to the PCDD class, and is the toxicant 2,3,7,8-tetrachlorodibenzo-p-dioxin (TCDD; dioxin).

TCDD is a colorless and odorless solid whose chemical structure is characterized by the presence of a central oxygenated ring surrounded by two benzene rings. TCDD toxicity is a consequence of its chlorine substituents being located in the lateral positions (on carbons 2, 3, 7 and 8), resulting in impaired metabolism and clearance. Although the exact duration of TCDD persistence will vary as a consequence of dose, exposure duration and body composition (173), the half-life of TCDD in humans ranges from approximately 7-12 years (174, 175). Furthermore, TCDD is a high affinity AhR ligand exhibiting binding affinity to the AhR in the pM to nM range (164).

What is known about the effects of TCDD comes from both human exposures and animal models. There have been a number of reported human exposures to TCDD, including occupational exposures (*e.g.* chemical and pesticide production employees) and accidental environmental contaminations (*e.g.* oil spills and industrial waste) (176). Several of the most well-characterized examples of human exposures to TCDD come from individuals subjected to the herbicide Agent Orange during the US-Vietnam war (177), the 1976 explosion of a chemical manufacturing plant in Seveso, Italy (178, 179), and the poisoning of the former Ukrainian President Viktor Yushenko (180). Based on data from these human cohorts, hallmark clinical manifestations of TCDD-induced toxicity are hepatotoxicity, epidermal manifestations including chloracne and hyperpigmentation, cancers of the breast, lung and liver as well as immunosuppression (181). Data from animal models have confirmed that these deleterious health effects of TCDD are mediated by the AhR (182-184).

In addition to PAHs and HAHs, several classes of naturally occurring exogenous AhR ligands have been recently described, including bacterial products and dietary compounds. One of the ways through which the AhR contributes to the defense against bacterial infection (see *1.3.4.3* "*Immunity*") is by sensing bacterial products (185). More specifically, these authors demonstrated that virulence factors from *Pseudomonas aeruginosa* [*P. aeruginosa*] and *Mycobacterium tuberculosis* [*M. tuberculosis*] act as AhR agonists (185). Furthermore, this virulence factor-induced AhR activation promoted the survival of the infected mice via an AhR-mediated recruitment of neutrophils, resulting in a reduced bacterial burden (185).

In addition to bacterial products, food is another important source of naturally occurring exogenous AhR ligands. Food-derived AhR ligands typically have low affinity for the AhR, with a binding affinity in the μM to mM range (164). Several classes of dietary AhR agonists include indole-3-carbinol derivatives found in leafy greens such as broccoli and Brussels sprouts, as well as flavonoids found in fruits and vegetables (170).

1.3.2.2 Endogenous AhR Agonists

In addition to exogenous AhR agonists, several classes of endogenous AhR agonists have also been characterized. Two of these classes are heme-derivatives (*e.g.* bilirubin and biliverdin) and arachidonic acid metabolites (*e.g.* prostaglandins and leukotrienes). Although several prostaglandins have been reported to induce AhR activation (*i.e.* prostaglandin B_2, D_2, $F_{3\alpha}$, G_2, H_1 and H_2), both prostaglandins and heme-derivatives are considered low-affinity ligands because they require μM concentrations to induce AhR activation (164, 170). In contrast, the arachidonic acid metabolite Lipoxin A_4 has emerged as a high-affinity AhR ligand, as it binds to the AhR and induces significant AhR activation in nM concentrations (186).

Another class of endogenous AhR agonists are tryptophan metabolites. Two of the most well-characterized members of this class are kynurenine and 6-formylindolo (3,2-b) carbazole (FICZ). Kynurenine is produced during the first step of tryptophan metabolism, which is mediated by the enzyme indoleamine 2,3- dioxygenase (IDO) (187), whereas FICZ is a tryptophan-derived ultraviolet (UV)-photoproduct (170). Although not a tryptophan metabolite, another widely studied endogenous AhR ligand that was first described in the pig lung is 2-(1′H-indole-3′-carbonyl)-thiazole-4-carboxylic acid methyl ester (ITE) (170). Kyurenine (and its metabolites), FICZ and ITE are all high affinity AhR agonists, inducing significant AhR activation in pM to nM concentrations (164, 170, 188).

1.3.2.3 AhR Antagonists

In addition to AhR agonists, there also exist AhR antagonists that inhibit agonist-induced AhR activation. Most AhR antagonists that have been identified are low-affinity ligands (*i.e.* binding affinity in the μM to mM range (164)). However, high-affinity AhR antagonists have also been identified, such as N-(2-(1H-indol-3-yl) ethyl)-9-isopropyl-2-(5-methylpyridin-3-yl)-9H-purin-6-amine (GNF351), which inhibits AhR activity at concentrations in the nM range (189).

Like AhR agonists, AhR antagonists can be naturally-occurring or synthetic in origin. Many naturally occurring AhR antagonists are flavonoids found in fruits, vegetables and flowers, including resveratrol (190), kaempferol (191), and alpha napthoflavone (192), respectively. An example of a well-characterized synthetic AhR antagonist is 2-methyl-2H-pyrazole-3-carboxylic acid methyl-4-o-tolylazo-phenyl)-amide (CH-223191). CH-223191 prevents TCDD from binding to the AhR, thereby inhibiting TCDD-induced AhR activation (193). Furthermore, CH-223191 exhibits ligand-specific antagonism. This is supported by findings that although CH-223191 prevents the binding of TCDD and PAHs such as benzo[a]pyrene and CS (*i.e.* complex mixture

containing PAHs) to the AhR (194), it is ineffective in preventing AhR activation by PAHs such as benzo[a]anthracene and benzo[k]fluoranthene (195). This ligand-specific antagonism by CH-223191 demonstrates that AhR ligands are not homogenous, which likely contributes to the broad spectrum of AhR-regulated processes.

1.3.3 How the AhR Exerts its Effects: AhR Signaling

1.3.3.1 Canonical AhR Signaling

The canonical (*i.e.* classical) way by which the AhR exerts its effects is through a signaling cascade beginning with the inactive cytosolic AhR undergoing ligand-induced AhR activation. The ligand-activated AhR translocates to the nucleus, resulting in the AhR-mediated transcriptional upregulation of AhR target genes. The sequential steps required for canonical AhR signaling are further discussed below.

1.3.3.1.1 Inactivated Cytosolic AhR Complex

In the absence of ligands, the AhR is inactive and located in the cytoplasm complexed to a heat shock protein 90 (HSP90) homodimer, immunophilin-like X-associated protein 2 (XAP2) and the co-chaperone p23 (170, 196). In this core complex, HSP90 ensures proper folding of newly-synthesized AhR protein (197). XAP2 (also known as ARA9 or AhR-interacting protein [AIP]) stabilizes unligated AhR, resulting in heightened AhR expression and transcriptional activity (197). The role of p23 is to prevent degradation of the unligated AhR, as supported by findings that a down-regulation of p23 results in increased ubiquitination and proteasomal degradation of the AhR protein (198). Thus, the cumulative effect of the AhR complex is to stabilize the inactive and unligated cytoplasmic AhR protein.

1.3.3.1.2 Ligand-induced AhR Activation and Nuclear Translocation

Upon ligand binding, the AhR core complex translocates from the cytoplasm to the nucleus. In the nucleus, the AhR dissociates from its chaperone proteins (199, 200) prior to its heterodimerization with the constitutively expressed aryl hydrocarbon receptor nuclear translocator (ARNT). This AhR-ARNT complex binds to the dioxin response element (DRE), also known as the xenobiotic response element (XRE) or the aromatic hydrocarbon response element (AhRE) (**Figure 1.4**).

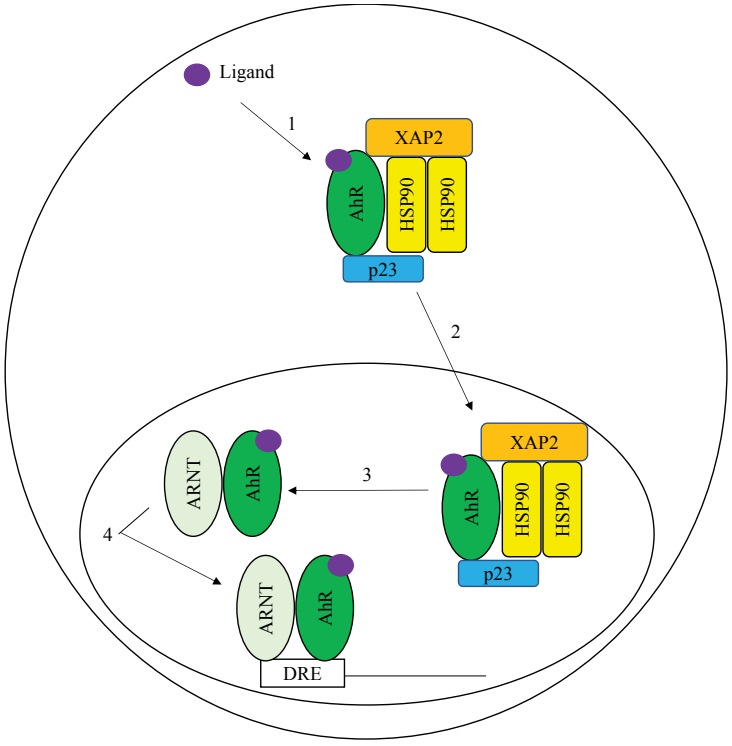

Figure 1.4. Diagrammatic representation of the canonical AhR signaling pathway. Inactivated AhR is found in the cytoplasm complexed to a HSP90 homodimer, XAP2 and p23. Ligand binding (1) to the AhR induces the translocation (2) of the AhR complex from the cytoplasm to the nucleus, where it dissociates from its chaperone proteins and subsequently forms a heterodimer with ARNT (3). The AhR-ARNT complex binds to DRE sequence (4) located in the promoter of AhR target genes to induce transcription into mRNA. Based on (201).

1.3.3.1.3 Transcriptional Upregulation of AhR Target Genes

The DRE has a core sequence of 5'-TNGCGTG-3' and is located in the promoter region of AhR target genes, the prototypical of which is cytochrome P450 (CYP) CYP1A1 (202). There are eight DREs located within the murine CYP1A1 promoter (202). The DRE transcriptional activity is affected by several factors including the position of the DRE within the promoter, the DRE orientation, neighboring sequences and nucleotide variation, such that transcriptional activity is greatest when 'N' is thymine or cytosine (203). Once the AhR-ARNT complex is bound to the DRE, transcriptional coactivators facilitate the recruitment of RNA polymerase II to this complex, resulting in the initiation of transcription (204). Activation of the AhR also initiates the transcription of the AhR repressor (AhRR). The AhRR is an AhR target gene that functions as a negative regulator of the AhR (see *1.3.5 "Mechanisms Regulating AhR Expression").*

Following the transcriptional induction of AhR target genes, the AhR dissociates from ARNT and is shuttled back to the cytoplasm via unmasking of its nuclear export signal (NES) (205). Following nucleocytoplasmic shuttling, the AhR protein is degraded by the 26S ubiquitin-proteasome system (206).

1.3.3.2 Non-canonical AhR Signaling

The toxic effects of the high-affinity AhR ligand TCDD are widely understood to be mediated through the canonical AhR pathway described above (183, 184). The canonical AhR signaling pathway is characterized by 1) ligand binding, 2) AhR nuclear translocation, 3) AhR-ARNT heterodimerization and 4) AhR binding to the DRE in target genes to induce transcription of mRNA. However, activation of the AhR by the high-affinity AhR ligands FICZ and ITE yield non-toxic effects. One proposed reason why these (and other) ligands may induce differential AhR-mediated outcomes is through activation of alternative AhR signaling mechanisms, known

as non-canonical *(i.e.* non-classical) AhR signaling pathways. A number of non-canonical signaling mechanisms exist, and include ligand-independent AhR signaling, interactions with different proteins, and regulation of non-coding (nc)RNAs, which are further described below.

1.3.3.2.1 Ligand-independent AhR signaling

AhR-regulated signaling can be ligand-independent. One example involves the AhR-mediated regulation of fibroblast proliferation. AhR-expressing cells have higher proliferation rates than AhR-deficient cells (207). The AhR-mediated regulation of fibroblast proliferation is postulated to be ligand-independent because these differences in proliferation rates are unaffected by either 1) exposure to AhR ligands, or 2) deletion of the AhR ligand-binding domain (207). In support of ligand-independent activation of the AhR, despite the absence of a functional ligand binding domain (*i.e.* ligand binding to the AhR cannot occur) the AhR can still both dimerize with ARNT and induce transcription of AhR target genes (208). These examples illustrate that the AhR is capable of regulating cellular processes independent of ligand-induced activation.

1.3.3.2.2 Protein Interactions

Non-canonical AhR signaling can also occur through direct physical interactions with proteins not required for canonical AhR signaling. The AhR can form dimers with a variety of proteins that are involved in the cell cycle, apoptosis and the immune response (209). For example, the AhR physically interacts with the estrogen receptor (210, 211) and non-canonically functions as an E3-ligase and mediates estrogen receptor degradation (212, 213). Such AhR-dependent ER degradation demonstrates how exposure to TCDD can modulate sex hormone expression. In breast cancer cells, the AhR interacts with the NFκB-transcription factor RelA, resulting in cellular proliferation and tumorigenesis (214). In lung cancer cells, AhR-RelA dimers bind to a DRE-independent NFκB response element in the promoter of the pro-inflammatory cytokine interleukin-

6 (IL6), resulting in increased IL6 expression and inflammation (215).

1.3.3.2.3 Non-coding RNA (ncRNA)

The AhR can also non-canonically influence cellular processes through the regulation of non-coding RNA (ncRNA). One type of ncRNA is microRNA (miRNA), which targets mRNA for degradation. Many miRNA, including miR-196a, miR-96, miR-137 and miR-133b are significantly reduced in the lungs of AhR-knockout (*Ahr*$^{-/-}$) mice (216), illustrating that the AhR regulates miRNA expression in the lung. The attenuation of CS-induced apoptosis in lung structural cells is mediated by the AhR dependent regulation of miR-196a (217). Additionally, the ability of the AhR to regulate cellular reprogramming and pluripotency induced by the anti-allergy drug Tranilast is mediated by an AhR-dependent regulation of miR-302 (218). Finally, an anti-metastatic signaling pathway in breast cancer cells is regulated via AhR agonist-induced transcriptional upregulation of miR-212/132 (219). Long non-coding RNA (lncRNA) are another type of ncRNA that may be regulated by the AhR. One example is that the AhR target gene TCDD-inducible poly ADP-ribose polymerase (TiPARP) and its lncRNA TIPARP-AS1 have both been reported to negatively regulate AhR activity (220).

1.3.4 Outcomes of AhR Signaling: Physiologic Functions of the AhR

Initiation of an AhR signaling pathway(s) results in AhR activation and thus the regulation of diverse downstream physiological processes. Several of these physiological processes include xenobiotic metabolism, organ development, immunity and the regulation of cellular processes.

1.3.4.1 Xenobiotic Metabolism

The first-identified members of the AhR gene battery (*i.e.* AhR target genes containing DRE sequences) were XMEs including CYP1A1, CYP1A2, NAD(P)H quinone oxidoreductase 1 (NQO1), aldehyde dehydrogenase (ALDH) ALDH3a1, UDP-glucuronosyltransferase (UGT)

UGT1a6 and glutathione s-transferase (GST) GSTa1 (221). It is important to note that contrary to what their name implies, XMEs do not solely mediate the metabolism of xenobiotics (*i.e.* environmental toxicants, drugs, dietary products etc.), but are also involved in the metabolism of endogenous substances such as eicosanoids including prostaglandins and leukotrienes (222).

XMEs function to render hydrophobic substances water soluble to facilitate their elimination from the body. The CYP enzymes are Phase I XMEs that catalyze the addition, or the unmasking, of a polar functional group (*e.g.* -OH, -SH, $-NH_2$), resulting in the formation of an active metabolite. Induction of CYP enzymes, especially CYP1A1, is classically used as evidence of AhR activation (223, 224). In eukaryotic cells, the primary site of induced CYP enzymes is the ER (225, 226). In contrast, NQO1, ALDH3a1, UGT1a6 and GSTa1 are Phase II XMEs (227). Phase II reactions increase water solubility of the xenobiotic via the conjugation of polar subgroups, leading to the formation of an inactive metabolite that is subsequently excreted (228). Small lipophobic metabolites are typically excreted via the kidney into the urine, whereas larger and more lipophilic metabolites are preferentially excreted by the liver into the bile and subsequently into fecal matter (229). Although not the predominant route of excretion, many xenobiotics (particularly gases, vapors and highly lipophilic xenobiotics) are eliminated via the lungs (230). Thus, the AhR is an important regulator of many XMEs that are required for the metabolism of both exogenous and endogenous compounds.

1.3.4.2 Organ Development

The AhR is also necessary for the proper development of a variety of organs including the liver and cardiovascular system. Studies utilizing *Ahr*$^{-/-}$ mice show that these mice exhibit reduced liver weight and have hepatic ductal fibrosis (231). Moreover, mice with an AhR incapable of nuclear localization or DRE binding also exhibit abnormal liver development (183, 184). This illustrates that normal liver development requires canonical AhR signaling.

With respect to the cardiovascular system, AhR activity in both endothelial and hematopoietic cells is crucial for vascular development and the closure of the ductus venosus (232). The ductus venosus is a fetal structure that typically closes after birth and serves to redirect oxygenated blood coming from the placenta away from the fetal liver and towards the inferior vena cava of the fetal heart. Persistence of a patent ductus venosus after birth is associated with liver disease in adults (233). Additionally, both *Ahr*$^{-/-}$ mice and TCDD-exposed AhR-expressing (*Ahr*$^{+/+}$) mice exhibit defects in cardiac development and function (234), suggesting that homeostatic regulation of AhR expression and/or activity is necessary for proper cardiac development.

Although incompletely understood, evidence supports that the AhR may also contribute to the development of the central nervous system. In support of this, the AhR regulates neuronal differentiation in developing *Caenorhabditis elegans* (*C. elegans*) (235). More specifically, AhR-deficient *C. elegans* exhibit impairments in neuronal migration, differentiation and axonal branching (235). These neuronal changes observed as a consequence of AhR deficiency result in cognitive defects in the hippocampus, which is important for functions such as memory (236). This is supported by evidence of reduced fear memory in *Ahr*$^{-/-}$ mice (236). Interestingly, models utilizing constitutively active AhR demonstrate that over-activation of the AhR elicits similar outcomes to AhR deficiency, as constitutive AhR activation impairs neuronal migration in both the hippocampus and olfactory bulb (237, 238). These studies highlight that homeostatic levels of AhR expression/activity are likely critical for central nervous system development. Consistent with this notion, the AhR exhibits distinct spatio-temporal expression patterns throughout the central nervous system during murine development (239). During early embryonic development, *Ahr* mRNA is expressed in the cerebral cortex, whereas after birth it can be detected in the hippocampus, cerebellum, cerebral cortex and olfactory bulb. Furthermore, in particular regions

of the hippocampus, *Ahr* expression continues to increase into adulthood (*i.e.* significantly higher *Ahr* levels in adults (12 wk old) relative to juveniles (7 days old)) (239).

Additionally, AhR ablation also results in abnormal ocular movements (240). Visual impairments observed in $Ahr^{-/-}$ mice may be a consequence of optic nerve demyelination and thus defective signal transduction. This is supported by the observation that AhR ablation causes altered myelin composition (*i.e.* lipid content) and an increased proportion of demyelinated axons in the optic nerve (241). Collectively, these studies illustrate a physiological role for the AhR in proper neural development.

1.3.4.3 Immunity

Complementary to its role in organ development, the AhR also plays an important physiological role in protecting organs from foreign invaders via its influence in both the innate and adaptive branches of the immune system. In the context of the innate immune system, $Ahr^{-/-}$ mice exhibit increased susceptibility to bacterial infections (*i.e. P. aeruginosa* and *M. tuberculosis*), resulting in elevated pulmonary bacterial loads and reduced survival following pathogen challenge (185). The AhR contributes to the coordination of an appropriate immune response through direct binding to bacterial virulence factors, which results in AhR activation (185). Thus, the AhR represents one of the mechanisms by which the immune system detects the presence of infection. Additionally, the AhR promotes endotoxin tolerance, thereby dampening the pathologic effects of infection on the host (242).

The AhR is also critical for the regulation of different branches of adaptive immunity. In the humoral arm of the adaptive immune system, the AhR is critical for optimal levels of B-cell proliferation (243) and B-cell differentiation decisions (*i.e.* differentiation into antibody-secreting plasma B-cells vs. memory B-cells) (244). In regard to T-cell mediated immunity, the AhR influences the differentiation of both helper T lymphocytes (Th)17 and regulatory T lymphocytes

(Tregs) through several different signaling mechanisms (245). The AhR may influence T-lymphocyte differentiation through both direct and indirect mechanisms. One direct mechanism is via methylation changes. This is supported by reports demonstrating that an AhR-activation by TCDD promotes Treg differentiation and inhibits Th17 differentiation, which is mechanistically mediated by demethylation of CpG islands in the *Foxp3* promoter and hypermethylation of CpG islands in the IL17 promoter, respectively (246). However, these authors note that the exact mechanism by which TCDD-induced AhR-activation regulates these methylation changes remains unclear (246). These methylation changes may involve an AhR-mediated transcriptional regulation of DNA methyltransferase expression, as supported by findings demonstrating that AhR activation by various chlorinated HAHs causes a significant reduction in DNA methyltransferase-1 mRNA expression across different organ systems in a rat model (247). Additionally, an indirect mechanism through which the AhR may influence Th17 levels is via the regulation of the gut microbiome. For example, *Ahr*$^{-/-}$ mice have an increased abundance of *Verrucomicrobiota* and segmented filamentous bacteria in the gut, which is directly linked to elevated intestinal inflammation and heightened IL17a expression suggesting increased Th17 differentiation (248). The outcome of Treg vs. Th17 cell differentiation is also differentially influenced by different AhR ligands. This is supported by findings that kynurenine activates the AhR, resulting in an AhR-dependent production of Tregs, whereas AhR activation by FICZ leads to the production of Th17 cells (187).

1.3.4.4 Cellular Processes

One of the most important physiological roles for the AhR is its regulation of cellular processes. These include an AhR-dependent promotion of cellular differentiation (249), proliferation (243, 250), cell-cycle progression and cell migration (251); and an AhR-dependent attenuation of apoptotic cell death (252). These studies not only serve to illustrate that the AhR is an important global regulator of diverse cellular processes, but also that the collective effect of the AhR under physiological conditions is the promotion of cellular expansion and survival. Although critical for the maintenance of homeostasis, dysregulation in these processes underlie pathology.

1.3.5 Mechanisms Regulating AhR Expression

Changes in AhR expression leads to alterations in AhR activity, which has important implications on downstream AhR-regulated processes. Despite the extensive body of research regarding the signaling mechanisms through which the AhR exerts its effects, and the subsequent physiological roles of the AhR, relatively little is known about the mechanisms regulating AhR expression.

1.3.5.1 Transcriptional Regulation of the AhR

Despite evidence that the AhR can physically interact, and forms dimers, with a diverse number of proteins (209), relatively few reports have demonstrated direct evidence of proteins binding to, and transcriptionally regulating, the AhR. One exception is the NF-*κB* family member RelB, which has been demonstrated to bind to the AhR promoter (253). RelB-mediated transcriptional regulation of the AhR is further supported by findings that RelB ablation results in reduced AhR mRNA and protein expression (253). Another example is the transcription factor specificity protein (SP)-1, which is known for its high affinity binding to guanine and cytosine (GC)-rich elements in the promoters of a diverse array of genes (254). SP-1 has been reported to

transcriptionally regulate basal *Ahr* mRNA expression via the binding to any combination of the four SP-1 binding sites in the mouse *Ahr* promoter (255). Furthermore, SP-1 likely regulates AhR expression and/or activity via non-transcriptional mechanisms as well, as it has been observed to immunoprecipitate with the AhR-ARNT protein complex (256).

1.3.5.2 Single Nucleotide Polymorphisms (SNPs)

Although variants in the human *AHR* gene are infrequent (257), single nucleotide polymorphisms (SNPs) may influence AhR expression via several independent mechanisms. Two *AHR* SNPs identified in a Japanese cohort (K401R and N487D) are associated with approximately 50% reduction of AhR protein expression (258). However, these authors demonstrated that the reduced AhR protein expression was not a consequence of alterations in its mRNA expression, as it could be reversed by proteasomal inhibition. This suggests that reduced AhR protein expression caused by K401R and N487D is a direct consequence of enhanced AhR degradation via the proteasome (258).

Another *AHR* single nucleotide polymorphism (SNP), Arg554Lys, is implicated in the pathogenesis of diseases related to smoking and air pollution. The Arg554Lys SNP is located in exon 10 and is associated with increased DNA damage in peripheral blood lymphocytes of coke-oven workers, as well as with an increased risk of both lung and breast cancer (259-262). The Arg554Lys SNP is associated with significantly reduced systemic *AHR* mRNA expression (263), suggesting that a predicted consequence of this SNP is to reduce transcription or mRNA stability of the AHR. Furthermore, Arg554Lys was also associated with reduced AhR activity, as evidenced by reduced *CYP1B1* expression (263). Although Arg554Lys is associated with reduced *AHR* expression and AHR activity, this SNP does not interfere with TCDD-induced binding of the AHR to the DRE or the induction of CYP1A1 (264). This latter finding suggests that reduced *CYP1B1*

expression observed in Arg554Lys is a downstream consequence of reduced *AHR* expression as opposed to impaired AHR-mediated transcriptional activities.

1.3.5.3 Epigenetic Modifications

An epigenetic modification is defined as a heritable trait that is independent of changes in DNA sequence. Several epigenetic regulatory mechanisms have been demonstrated to influence AhR expression. For example, increased AHR expression in estrogen-exposed human breast cancer cells is a consequence of a histone modification on the *AHR* promoter, specifically decreased trimethylation of histone 3 at lysine 27 (265). This particular histone modification is associated with a poor clinical outcome in patients with breast cancer (266). Additionally, AHR expression is reduced in human acute lymphoblastic leukemia, which is a consequence of *AHR* promoter hypermethylation (267). Additional evidence that AhR expression can be influenced by changes in promoter methylation status was observed in contaminant-exposed Atlantic killifish, where low hepatic expression of the AhR1 isoform was associated with *Ahr1* promoter hypermethylation, and high hepatic expression of the AhR2 isoform was associated with *Ahr2* promoter hypomethylation (268).

Interestingly, although the AhR-mediated regulation of ncRNAs represents an avenue of non-canonical AhR signaling (see *1.3.3.2.3 "Noncoding RNA (ncRNA)"*), ncRNA can also regulate expression of the AhR. For example, a miRNA-mediated regulation of AhR expression is supported by findings that miR-203 binds to the 3'-untranslated region (UTR) of the AhR promoter resulting in the repression of AhR expression following TCDD-exposure (269). Additionally, lncRNA may also regulate AhR expression. For example, knock-down of the lncRNA AK170409 in immortalized murine bone marrow derived macrophages resulted in a 100-fold reduction in AhR expression, although the mechanism of action remains unknown (270).

1.3.5.4 Negative Regulators of the AhR

1.3.5.4.1 The AhR Repressor (AhRR)

The AhRR is an AhR target gene that functions to negatively regulate AhR activity. One mechanism through which the AhRR may suppress AhR activity is via competition with ARNT. Wood-smoke (WS) suppresses CS-induced AhR activation (271) by increasing AhRR expression, which is followed by competitive removal of the AhR from the CS-induced AhR-ARNT complex (271). This was also associated with reduced nuclear AhR, leading to the speculation that once the AhR was displaced by the AhRR, AhR was subsequently degraded (271). This finding illustrates that the AhRR can directly interfere with AhR-ARNT interactions, thereby reducing AhR activity and facilitating AhR protein degradation. Additionally, AhRR-overexpressing mice exhibit dampened levels of TCDD-induced CYP1A1 expression in the kidneys, spleen and adipose tissue. This finding is also likely a consequence of an AhRR-mediated disruption of AhR-ARNT interactions and thus impaired CYP1A1 induction (272).

Alternatively, the AhRR can also negatively regulate AhR activity in an ARNT-independent manner. This is supported by findings that the AhRR-mediated transcriptional repression of the AhR is unaffected by overexpression of ARNT (273). Additionally, AhRR-overexpressing mice exhibit reduced TCDD-induced DNA-binding of C/EBP and NFκB, which are two transcription factors known to interact with the AhR (272). These authors postulate that dampened TCDD-induced C/EBP and NFκB DNA-binding in AhRR-overexpressing mice may be the result of a trans-repression mechanism, whereby the AhRR interferes with AhR-protein interactions (272).

1.3.5.4.2 TCDD-inducible Poly ADP-Ribose Polymerase (TiPARP)

An alternative mechanism by which AhR expression can be regulated is via the AhR target gene TiPARP, also a negative regulator of the AhR (274). TiPARP likely modulates AhR expression via the regulation of AhR protein degradation. This is supported by evidence that TiPARP overexpression results in heightened proteolytic degradation and thus reduced protein expression of the AhR, whereas TiPARP knock-down leads to elevated AhR protein expression (274). It is important to note that TiPARP and the AhRR are not the only regulators that can induce AhR proteosomal degradation. As previously discussed, one well-established feature of the AhR signaling cascade is proteosomal degradation of the AhR protein following its ligand-induced activation and nuclear translocation (206). Thus, AhR protein expression typically exhibits a transient reduction following ligand-induced activation.

Understanding the mechanisms that regulate AhR expression is important because homeostatic expression and activity of the AhR is required for the physiological functions of the AhR and thus the maintenance of health. However, deviations from these homeostatic levels of AhR expression is associated with a number of pathological conditions.

1.3.6 AhR in Disease

Changes in the expression of AhR is observed in many diseases. However, whether alterations in AhR expression is a cause or consequence of the disease-state has not been elucidated. Over-expression of the AhR has been reported in many types of human cancers including lung, breast and gastric cancers (214, 215, 251, 275, 276). In contrast, reduced AhR expression has been reported in several chronic inflammatory diseases affecting barrier organs including Crohn's disease (277), ocular Behçet's disease (278), and chronic rhinosinusitis (279).

AhR activation by endogenous ligands elicits protective effects in a variety of diseases whose pathogenesis involves chronic inflammation. One such ligand is FICZ, a tryptophan-derived UV-photoproduct. FICZ has been demonstrated to attenuate psoriasis-like skin inflammation *in vivo* (280), pulmonary inflammation in a mouse model of asthma (281, 282), and gastrointestinal inflammation in a murine model of colitis (283, 284). In addition to FICZ, exposure to TCDD alleviates inflammation in experimental colitis in AhR expressing mice (246). Another example of an AhR ligand that elicits AhR-mediated anti-inflammatory effects is ITE, which alleviates Th17 mediated inflammatory responses in patients with allergic rhinitis (285) and attenuates inflammation associated with a murine model of colitis via the induction of Tregs (286).

These studies collectively illustrate that reduced AhR expression is associated with a number of chronic inflammatory conditions affecting barrier organs. Despite low levels of AhR expression in many of these chronic inflammatory conditions, experimental intervention using AhR agonists to increase AhR activity has proved effective in attenuating disease pathogenesis. One such disease that has yet to be assessed in relation to the AhR is COPD. Although COPD is a condition associated with chronic inflammation of the lung, which is predominantly caused by the inhalational exposure to compounds comprised of AhR ligands (*i.e.* air pollution and cigarette smoke), whether reduced AhR expression is observed in subjects with COPD, or contributes to COPD pathogenesis, is currently unknown.

1.4 Project Introduction

Rationale: The only established relationship between the AhR and COPD is that cultured COPD-derived lung fibroblasts exhibit significantly reduced AhR protein expression relative to fibroblasts derived from subjects without COPD (287). Additionally, it has been previously reported that the AhR attenuates pathogenic mechanisms associated with COPD development, including acute cigarette smoke (CS)-induced inflammation *in vivo*, oxidative stress and apoptosis *in vitro* (160-162). Taken together, this raises the possibility that reduced levels of the AhR contributes to the pathogenesis of emphysema, and that low AHR levels may predispose some smokers to developing COPD.

Hypothesis: AhR deficiency promotes the development of a CS-induced emphysema-like phenotype *in vivo*, and that human COPD subjects exhibit reduced AHR expression relative to subjects without COPD.

Objectives: This work aimed to address the following objectives:

1) Assess if AHR expression differs between human subjects with and without COPD.
2) Experimentally test if AhR deficiency promotes the development of a CS-induced emphysema-like phenotype *in vivo*.
3) Determine if the AhR deficiency promotes novel cell death modalities that have been postulated to contribute to emphysema pathogenesis, including CS-induced autophagy and ER stress.

2 Deficiency of the aryl hydrocarbon receptor (AhR) underlies chronic obstructive pulmonary disease (COPD) pathogenesis

Necola Guerrina[1,3], Yohan Bossé[13], Maxime Lamontagne[13], Thomas H. Thatcher[9], Annette Robichaud[14], Angela Rico de Souza[1], Luca Cuccia[4], Caitlin Mehorata[4], Pei Z. Li[8], Leora Simon[2], Hussein Traboulsi[1], Swati Pareek[1,3], Jean Bourbeau[1,2,8], Wan C. Tan[16,] Andrea Benedetti[1,2,5,6,7,8], Richard P. Phipps[9], Patricia J. Sime[9], Parameswaran Nair[12], Michela Zago[15], James Martin[1,2], David H. Eidelman[1,2], Qutayba Hamid[1,2,17], Benjamin M. Smith[1,2,8] and Carolyn J. Baglole[1,2,3,4]

[1]Research Institute of the McGill University Health Centre, Departments of [2]Medicine, [3]Pathology, [4]Pharmacology and Therapeutics, [5]Epidemiology, [6]Biostatistics, [7]Occupational Health, McGill University, Montreal, Quebec, Canada; Department of [8]Respiratory Epidemiology and Clinical Research Unit, McGill University Health Centre, Montreal, Quebec, Canada; Department of [9]Environmental Medicine, University of Rochester School of Medicine and Dentistry, 601 Elmwood Avenue, Rochester, NY; [12]Department of Medicine, McMaster University & St Joseph's Healthcare, Hamilton, Ontario, Canada; [13]Institut universitaire de cardiologie et de pneumologie de Québec, Department of Molecular Medicine, Laval University, Quebec City, Quebec, Canada; [14]SCIREQ Scientific Respiratory Equipment Inc., Montreal, Quebec, Canada; [15]Klox Technologies, Laval, Quebec, Canada. [16]The UBC James Hogg Research Centre, University of British Columbia, Vancouver, BC, Canada. [17]University of Sharjah College of Medicine, University of Sharjah, United Arab Emirates.

Correspondence and requests for materials should be addressed to:
Carolyn J. Baglole
1001 Decarie Blvd (EM22248)
Montreal, Quebec H4A3J1
Telephone: (514) 934-1934 ext. 76109
E-mail: Carolyn.baglole@mcgill.ca

ACKNOWLEDGEMENTS

This work was supported by the Canada Foundation for Innovation (CFI), Natural Sciences and Engineering Research Council of Canada (NSERC), and the Canadian Institutes for Health Research (CIHR). Y.B. holds a Canada Research Chair in Genomics of Heart and Lung Diseases. B.M.S and C.J.B. were supported by a salary award from the Fonds de recherche du Quebec-Sante (FRQ-S). This work was supported in part by National Institutes of Health grants HL075432 and HL120908 to R.P.P. and P.J.S. Grant support for R.P.P and P.J.S was also provided by P30ES001247, RO1HL120908 and T32HL066988. A.R is employed by SCIREQ Inc., a commercial entity involved in a subject area related to the content of this article. SCIREQ is an emka Technologies company. P.N is supported by a Frederick E. Hargreave Teva Innovation Chair in Airway Diseases. The authors would like to thank the staff at the Respiratory Health Network Tissue Bank of the FRQS for their valuable assistance with the lung eQTL dataset at Laval University. We also acknowledge the assistance of Katherine Radford and the Division of Thoracic Surgeon and the Department of Pathology of McMaster University and St Joseph's Healthcare Hamilton. The mIHC images were acquired through the Histopathology Platform of the RI-MUHC.

The authors declare no conflicts of interest.

2.1 ABSTRACT

Background: Chronic obstructive pulmonary disease (COPD) is primarily caused by the inhalational exposure to environmental contaminants such as cigarette smoke (CS). Emphysema, a component of COPD, is characterized by irreversible alveolar destruction that results in a progressive decline in pulmonary function. This alveolar destruction is mediated by inter-related pathogenic mechanisms including inflammation, a protease : anti-protease imbalance, oxidative stress and cell death. How these inter-related mechanisms, and thus the pathogenesis of emphysema, are regulated at the molecular level remains poorly understood. Our lab has previously published that loss of the aryl hydrocarbon receptor (AhR) promotes CS-induced oxidative stress, cell death and inflammation in lung structural cells. This led us to hypothesize that reduced AhR expression may contribute to the development of CS-induced emphysema and COPD pathogenesis. **Objective**: To evaluate the contribution of the AhR pathway to the development of COPD. **Methods**: *Ahr*$^{-/-}$ and *Ahr*$^{+/-}$ mice were exposed to chronic CS and alveolar destruction, lung function, inflammation, cell death mechanisms and protease expression evaluated. Human tissue from COPD and control subjects were evaluated to assess AHR mRNA and protein expression. **Results**: Using our preclinical model of CS exposure, we report that the AhR protects against emphysema and prevents declines in lung function. The AhR also attenuated chronic pulmonary inflammation, an anti-protease imbalance and the activation of cell death machinery in the lung. In humans with COPD, including those with emphysema, there was less pulmonary and systemic AHR expression. *AHR* mRNA expression levels positively correlated with lung function in humans. Although there was no alteration in the frequency of *AHR* single nucleotide polymorphisms (SNPs), reduced AHR in COPD subjects may be, in part, attributable to the elevated expression of the AhR repressor (*AHRR*). **Discussion**: This study identifies the AhR

as a regulator of the homeostatic maintenance of lung health by attenuating COPD pathogenesis.

2.2 INTRODUCTION

Chronic obstructive pulmonary disease (COPD), characterized by progressive and irreversible air flow obstruction, is associated with significant morbidity and mortality. Worldwide, COPD affects an estimated 380 million people (62) and is the third leading cause of death. Although COPD is predominantly caused by cigarette smoke (CS), approximately 25% of all COPD patients are never-smokers (45). Inhalation of air pollution (ambient or biomass) and occupational exposures are also associated with COPD (57, 288, 289). The pervasive nature of these environmental toxicants is illustrated by the fact that 92% of the world's population currently live in areas where air pollution levels exceed the World Health Organization (WHO) ambient air quality guidelines. Thus, COPD is likely to remain a major health care issue for many decades. Despite the significant disease burden of COPD, no therapeutic options exist to stop or slow disease progression (96), in part because the mechanistic basis of this disease remains incompletely understood.

COPD is an umbrella term that encompasses chronic bronchitis and emphysema (alveolar airspace enlargement). The pathogenesis of emphysema is mediated by several inter-dependent mechanisms including chronic inflammation, oxidative stress, an anti-protease imbalance and accelerated cell death in the lung (72). Oxidants and proteases released by recruited immune cells such as neutrophils and macrophages, along with oxidants in smoke, induce cell death by mechanisms that include apoptosis and autophagy (98, 109, 290). Apoptosis is mediated by the executioner caspase, caspase-3, resulting in chromatin condensation and DNA fragmentation (291). Autophagy involves the cytoplasmic uptake of damaged proteins, substrate and organelles for degradation (113). CS exposure causes an accumulation of autophagosomes, cellular hallmarks of the autophagy, which leads to autophagic cell death and the development of emphysema (109,

124, 127). How these pathogenic processes are controlled is unknown but is an important consideration, given that only 15-20% of CS-exposed individuals develop COPD. This suggests that unknown genetic or epigenetic factors contribute to overall disease pathogenesis (158, 159).

We postulate that the aryl hydrocarbon receptor (AhR) pathway protects against the development of COPD. The AhR is best-known for its ability to mediate the deleterious effects of the man-made toxicant 2,3,7,8-tetrachlorodibenzo-p-dioxin (TCDD; dioxin) (182, 292, 293). In the absence of ligand, the AhR is found in the cytoplasm complexed with chaperone proteins (170, 196, 294). After binding dioxin, the AhR translocates to the nucleus and forms a heterodimer with the AhR nuclear transporter (ARNT). This AhR-ARNT complex binds to DNA sequences termed the dioxin response element (DRE), initiating the transcription of genes. These include genes such as cytochrome P450 (CYP) CYP1A1 and the AhR repressor (AhRR), the latter of which is a negative regulator of the AhR (295). Persistent activation of the AhR by dioxin is associated with toxic responses (*e.g.* hepatomegaly) (183). However, a broad range of biochemical and genetic studies have shown that the AhR is important for many biological functions, including liver development, induction of endotoxin tolerance and the suppression of inflammation (231, 242, 280, 296). Not only have we published that CS activates the AhR (162, 194), but we have also shown the importance of the AhR pathway in attenuating acute CS-induced inflammation *in vivo* and oxidative stress and apoptosis *in vitro* (160-162, 194, 297). We have also published that there is less AhR protein in COPD-derived lung structural cells (298), raising the possibility that low AHR levels predispose some individuals to develop COPD. Why AHR may be lower in COPD is not known but may be due to single nucleotide polymorphisms (SNPs). SNPs may influence transcription and/or render the protein unstable and susceptible to proteolytic degradation (258, 263, 264, 299). The *AHR* SNP Arg554Lys is implicated in the pathogenesis of diseases related to

smoking and air pollution (259-262) and is associated with reduced *AHR* expression and activity (263). Cigarette smoking is also associated with hypomethylation of the *AHRR* (cg05575921), leading to increased *AHRR* expression (300). Theoretically, increased AhRR would inhibit the protective AhR pathway.

Despite compelling evidence that the AhR prevents pathological events linked to the development of COPD (*e.g.* inflammation, oxidative stress, apoptosis), there is currently no information on whether the AhR pathway contributes to this disease. Using our preclinical CS model, together with analysis of AHR expression in COPD we illustrate that reduced AhR expression drives the pathogenesis of COPD, which is a finding that may provide a basis for the development of new therapeutic agents or biomarkers for subjects at risk for this disease.

2.3 METHODS

Chemicals

All chemicals were purchased from Sigma-Aldrich (St. Louis, MO) unless otherwise indicated.

Preclinical Cigarette Smoke (CS) Model

AhR-knockout (*Ahr*$^{-/-}$; B6.129-Ahr^{tm1}/J) C57BL/6 mice were bred in house and maintained on an *ad libitum* diet. The *Ahr*$^{-/-}$ mouse strain carries a targeted deletion of exon 2 of the AhR gene and has been backcrossed for 12 generations onto C57BL/6 (231, 301). A breeding scheme of heterozygous *Ahr*$^{+/-}$ to *Ahr*$^{-/-}$ was used, rendering mice of the *Ahr*$^{+/-}$ genotype as littermate controls. *Ahr*$^{+/-}$ mice are phenotypically indistinguishable from wild-type (*Ahr*$^{+/+}$) mice and are often used as controls when examining the physiological, pathophysiological and toxicological parameters of the AhR (231, 302-305). Thus, *Ahr*$^{+/-}$ mice serve as suitable controls for this study because they enable us to reduce the number/cages of mice required for the breedings to conduct the various experiments. Age and gender-matched male and female *Ahr*$^{-/-}$ and *Ahr*$^{+/-}$ mice were exposed to CS using a whole-body exposure system (InExpose; SCIREQ Inc., Montreal, Canada) for up to 4 months as previously described (162, 194, 301). All mice were at least 8-weeks of age before commencing CS-exposures to ensure complete development of the lung. Briefly, mice were exposed to research cigarettes (3R4F; University of Kentucky, Lexington, KY) for two, 1-hr CS-exposures/day for 5 days/week. All animal procedures were approved by the McGill University Animal Care Committee (Protocol Number: 5933) and were carried out in accordance with the Canadian Council on Animal Care.

Tissue Harvest and Bronchoalveolar Lavage (BAL) Collection

Following the last CS exposure, mice were anesthetized with Avertin (2,2,2-tribromoethanol, 250 mg/kg ip; Sigma-Aldrich, St Louis, MO) and sacrificed by exsanguination. The lungs were removed and lavaged three times with 0.5 ml of PBS. The bronchoalveolar lavage (BAL) fluid was then centrifuged at 5000 RPM at 4^0C for 5 min. Following centrifugation, the supernatant was removed, and the BAL cell pellets were resuspended in PBS. BAL cells were used for the quantification of differential cell counts after cytospin slide preparation (Thermo Shandon, Pittsburgh, PA) following staining with Hema-Gurr Stain (Merck, Darmstadt, Germany). Lung tissue was collected and either frozen immediately in liquid nitrogen and stored at −80°C for protein/gene expression analysis, or fixed intratracheally with 5% formalin at 20 cm H_2O for at least 24 hr for lung morphometry analysis.

Lung Morphometry- Mean Linear Intercept (Lm)

Following formalin fixation, the left lung was embedded in paraffin, sectioned and stained with hematoxylin-eosin (306). Airspace enlargement was assessed by calculating the mean linear intercept (Lm) (307).

Lung Function Assessment

Respiratory mechanics were assessed using a FlexiVent FX system equipped with a FX2 module (SCIREQ Inc., Montreal, QC, Canada) 18 hr after the last CS exposure of the 4-month session. Each mouse was administered xylazine ip (10 mg/Kg) 5 min before being anaesthetized with 50 mg/Kg of sodium pentobarbital ip. As previously described, mice were cannulated and mechanically ventilated for measurements of respiratory mechanics (308) and assessment of lung volume and capacities (309). Mechanical ventilation was set at a frequency of 150 breaths/min, a

tidal volume of 10 mL/kg, a 2:3 inspiratory : expiratory ratio and a 3 cm H_2O positive end expiratory ratio. Rocuronium (0.2 mg/Kg) was then administered, followed by a deep lung inflation maneuver to 30 cm H_2O and a 2-3 min equilibration period. Next, deep lung inflation and a stepwise pressure-volume (PV)-curve, both set to a final pressure of 35 cm H_2O, were run and the mechanical ventilation was switched from room air to 100% oxygen for 5 min to degas the lungs by oxygen absorption prior to the construction of a full-range PV curve (Robichaud et al., 2017). That procedure was used for the determination of various lung volumes and capacities over the entire lung volume range.

Analysis of Gene Expression

Total ribonucleic acid (RNA) was isolated from mouse lung tissue using a Qiagen miRNeasy kit (Qiagen Inc., Hilden, Germany). Reverse transcription of total RNA was carried out in a 25-µl reaction mixture by iScript II^{TM} Reverse Transcription Supermix (Bio- Rad Laboratories, Mississauga, ON, Canada) at 25°C for 5 min, at 42°C for 30 min and at 85°C for 5 min. Quantitative PCR (qPCR) was performed with 1 µl cDNA, and 0.5 µM primers added in Ssofast^{TM} Eva Green® Super-mix (Bio-Rad). PCR amplification was performed using a CFX96 Real-Time PCR Detection System (Bio-Rad) as described (194). Primer sequences utilized for qPCR are: TIMP1: CCATGCACTGGGCTTAGATCAT(f) and CAGATACTGGATGCCGTCTATGTC(r); MMP9: CCAGAGCCGTCACTTTGCTT(f) and AGGAAAAGTAGACAGTGTTCAGGCTT(r); and β-actin: CTACCATGAGCTGCGTGTG(f) and TGGGGTGTTGAAGGTCTC(r). Gene expression was analyzed using the $^{\Delta\Delta}$Ct method following normalization to the housekeeping gene β-actin.

Western Blot

Total protein from whole lung homogenate was prepared using radioimmunoprecipitation assay (RIPA) lysis buffer supplemented with protease inhibitor cocktail (Roche Diagnostics, Germany) and protein quantification performed with the bicinchoninic acid (BCA) method (Pierce, Rockford, IL). Twenty to forty μg of cellular proteins were fractionated using sodium dodecyl sulfate polyacrylamide gel electrophoresis (SDS-PAGE) and electroblotted onto immunoblot polyvinylidene difluoride (PVDF) membrane (Bio-Rad Laboratories, St. Laurent, QC, Canada). Incubation with a primary antibody followed by the horse radish peroxidase (HRP)-conjugated secondary antibody was used to assess changes in protein levels. Primary antibodies used were: MMP9 (Abcam: #Ab38898; 1:1000), TIMP1 (Abcam: #Ab86482; 1:1000), Tubulin (Sigma-Aldrich: #T7816; 1:10000), SOD2 (R&D Systems: #MAB3419), LC3B (Cell Signaling: #3868; 1:1000), Cleaved Caspase-3 (Cell Signaling: #9664; 1:1000) and Actin (Millipore: #MAB1501; 1:50000). Protein levels were visualized by enhanced chemiluminescence (ECL) and detected using a gel documentation system (Bio-Rad). Densitometry was performed using ImageJ and target protein expression was normalized to tubulin or actin.

Genetic Analysis of Human Lung Tissue

Expression of *AHR* mRNA was assessed in human lung tissue collected from patients undergoing lung cancer surgery at the *Institut universitaire de cardiologie et de pneumologie de Québec* (Table 2.1). Non-tumor lung tissues were harvested from a site distant from the tumor, snap-frozen in liquid nitrogen and stored at -80^{o}C until further processing. Gene expression profiling was performed using an Affymetrix custom array (GEO platform GPL10379). SNPs located 10 kb up and down-stream of both the *AHR* and *AHRR* genes were evaluated for expression quantitative

trait loci (eQTL) as previously described (310). Briefly, eQTL are regions of the genome containing a DNA mutation that is significantly associated with the expression of one (or several) genes. A region is considered an eQTL when a particular allelic variant exhibits a strong association with increased mRNA expression of a given gene. The frequency of these eQTL, for both *AHR* and *AHRR,* were then evaluated between subjects with and without COPD using chi-square tests in PLINK.

Multiplex Immunohistochemistry (mIHC)

Expression of the AHR protein was assessed by mIHC in human lung tissue collected from non-smoking, smoking and COPD subjects undergoing lung resection at St Joseph's Healthcare Hamilton (Table 2.2). Human subjects were approved by the Research Ethics Board of St Joseph's Healthcare Hamilton (00-1839). Lung tissue was fixed in 10% formalin and embedded in paraffin. Five-µm thick sections were first incubated in primary AhR antibody (Abcam #2770; 1:100) for 16 min at 37^0C, followed by incubation in secondary antibody OMap anti-Ms HRP (Roche #760-4310) for 16 min at 37^0C. Sections were next incubated in primary vimentin antibody (Cell Signaling #3932; 1:50) for 16 min at 37°C, followed by incubation in secondary antibody UltraMap Anti Rb Alk Phos (Roche #760-431) for 16 min at 37°C. Lastly, sections were incubated in pre-diluted primary cytokeratin-19 antibody (Roche #760-4281) for 16 min at 37°C, followed by incubation in secondary antibody OMap anti-Ms HRP (Roche #760-4310) for 16 min at 37°C. Sections were counter-stained using hematoxylin. Detection was accomplished using a 3,3'-diaminobenzidine (DAB) detection kit.

Canadian Cohort of Obstructive Lung Disease (CanCOLD)

Expression of *AHR* mRNA was assessed in the whole blood of non-smoking, smoking and COPD subjects participating in CanCOLD (Table 2.3). CanCOLD is a prospective longitudinal cohort of approximately 1,500 subjects and comprises two COPD subsets (GOLD ≥2 and GOLD 1) and two subsets of non-COPD peers, *i.e.*, normal post bronchodilator spirometry (ever-smoker for those at-risk and never-smoker for the healthy controls), matched for sex and age. CanCOLD has been described in detail (311). Peripheral blood was collected using PAXgene blood RNA tubes (PreAnalytiX GmbH, Hombrechtikon, Germany) at initial visit and frozen at −80°C until analysis as previously described (312). Total RNA was isolated using a PAXgene blood RNA kit (PreAnalytiX GmbH) according to the supplier protocol. RNA was reverse transcribed to cDNA, diluted (313) and primers added in QX200 ddPCR Eva Green® Super-mix (Bio-Rad). Samples were then partitioned into 20,000 droplets and PCR amplification was performed using the QX100 Droplet Digital™ PCR (ddPCR) System (Bio-Rad). Primer sequences for human AHR are AGAGGCTCAGGTTATCAGTTT(f) and AGTCCATCGGTTGTTTTTT(r). Primer sequences for β-actin are CTACCATGAGCTGCGTGTG(f) and TGGGGTGTTGAAGGTCTC(r). Gene expression data was normalized to the housekeeping gene (β-actin).

Statistical Analyses

Statistical analysis was performed using Prism 6-1 (La Jolla, CA) unless otherwise indicated. A two-way analysis of variance (ANOVA) followed by a Bonferroni correction was used unless otherwise indicated. Systemic *AHR* mRNA expression in CanCOLD subjects were analyzed using a Kruskal-Wallis non-parametric one-way ANOVA (two+ comparison groups) or a Komologrov-Smirnov non-parametric t-test (two comparison groups). Statistical analysis was conducted for

CanCOLD subjects (Table 2.3) using SAS v9.4 (SAS Institute Inc., Cary, NC). These subject data were analyzed either using a one-way ANOVA (for a normal distribution) or a Kruskal-Wallis non-parametric one-way ANOVA test, and a chi-squared test for category variables. Statistical analysis was conducted for St Joseph's Healthcare Hamilton subjects (Table 2.2) using a Kruskal-Wallis non-parametric one-way ANOVA. Genetic associations in the eQTL study were evaluated using chi-square tests in PLINK. In all cases, a p value < 0.05 is considered statistically significant.

2.4 RESULTS

AhR deficiency worsens the development of CS-induced emphysema

To address the potential role for the AhR in the development of emphysema, we first quantified airspace enlargement (mean linear intercept [Lm]) in *Ahr*$^{-/-}$ and *Ahr*$^{+/-}$ mice exposed to CS for 4 months. CS-exposed *Ahr*$^{-/-}$ mice have a significant increase in Lm compared CS-exposed *Ahr*$^{+/-}$ mice (Fig. 2.1A and Fig 2.1B). This change in structure corresponded with alterations in lung function, which we assessed using a full-range pressure-volume (PV) curve maneuver. Representative PV curves are virtually super-imposable between the air-exposed *Ahr*$^{+/-}$ and *Ahr*$^{-/-}$ mice (Fig. 2.1C). In *Ahr*$^{-/-}$ mice exposed to CS for 4-months, there is an upward/leftward shift of the PV curve compared to CS-exposed *Ahr*$^{+/-}$ mice (Fig. 2.1D). This shift in the PV curve of the CS-exposed *Ahr*$^{-/-}$ mice is consistent with the PV curve shift in patients with emphysema due to the loss of elastic tissue and parenchymal destruction (314). From these curves, we calculated the functional residual capacity (FRC). FRC is a parameter of lung function that increases in emphysema as the result of elastic destruction, leading to air trapping due to the relatively unopposed outward recoil of the lung (314). The FRC was significantly increased in the CS-exposed *Ahr*$^{-/-}$ mice (Fig. 2.1E). The ratio of the inspiratory capacity to the total lung capacity (IC/TLC) is also reduced in emphysema (315) and was significantly reduced in the CS-exposed *Ahr*$^{-/-}$ mice (Fig. 2.1F).

AhR deficiency worsens pathogenic mechanisms of emphysema development

To assess if the absence of the AhR was also associated with an increase in the mechanisms believed to contribute to emphysema pathogenesis, we chose an 8-week CS exposure, a time-frame that precedes the development of lung structural and functional alterations. We first assessed if

there was heightened inflammation. There were significantly more cells in the BAL of CS-exposed *Ahr*$^{-/-}$ mice compared to *Ahr*$^{+/-}$ mice (Fig. 2.2A and 2.2B). We also observed that CS-exposed *Ahr*$^{-/-}$ mice have significantly more macrophages and multi-nucleated giant cells (MNGCs) in the BAL (Fig. 2.2C and 2.2D). Although neutrophil numbers were significantly elevated as a consequence of an 8-week CS-exposure, there was no significant difference in BAL neutrophils between the CS-exposed *Ahr*$^{-/-}$ and *Ahr*$^{+/-}$ mice (Fig 2.2E). There was also no significant difference in lymphocytes (Fig. 2.2F). T-lymphocytes are proposed to be critical to emphysema pathogenesis, as supported by evidence that T-lymphocyte depletion attenuates the development of CS-induced airspace enlargement in the murine lung (78). Although we did not observe an AhR-dependent regulation in overall lymphocyte counts, because lymphocyte subpopulations were not characterized in this study, we cannot rule out the possibility that the AhR may differentially regulate certain lymphocyte populations (*e.g.* T-lymphocytes) and not others (*e.g.* B-lymphocytes) in response to a chronic CS regime. However, because macrophages were the predominant cell type that increased in the CS exposed *Ahr*$^{-/-}$ mice, we next evaluated the expression of MMP9, which degrades gelatins and basement membrane collagens such as collagen IV. MMP9 activity is inhibited by the endogenous tissue inhibitor of metalloproteinases TIMP1 (84). Along these lines, there was a significant elevation in the MMP9:TIMP1 ratio in the lungs of *Ahr*$^{-/-}$ mice (Fig. 2.3). Individually, MMP9 protein expression was significantly higher in both the air and CS-exposed *Ahr*$^{-/-}$ mice relative to the *Ahr*$^{+/-}$ mice (data not shown). However, because TIMP1 protein expression was significantly upregulated only in the CS-exposed *Ahr*$^{-/-}$ mice (data not shown), the MMP9:TIMP1 ratio was reduced in the CS-exposed *Ahr*$^{-/-}$ mice relative to that observed in these mice at baseline. This increased TIMP1 expression in the CS-exposed *Ahr*$^{-/-}$ mice may be a compensatory response to an elevated protease burden, not unlike similar findings reported in

COPD subjects, where TIMP1 upregulation often co-occurs with increased MMP9 expression (316). Taken together, these findings suggest that there is regulation of proteases by the AhR.

CS, together with recruited and activated immune cells, creates a significant oxidative burden in the lung (287). Enzymes such as superoxide dismutase (SOD) are potent antioxidants that scavenge superoxide radicals. Of the three SOD isoforms in mammals (SOD1, SOD2 or SOD3), SOD2 is responsible for approximately 90% of all SOD activity (116). SOD2 upregulation by smoke exposure is one mechanism through which oxidative stress is dampened in the lung. Consistently, there was an increase in SOD2 expression in response to CS in both $Ahr^{-/-}$ and $Ahr^{+/-}$ mice (Fig. 2.4A). However, this increase in CS-induced SOD2 was significantly less in $Ahr^{-/-}$ mice relative to the CS-exposed $Ahr^{+/-}$ mice (Fig. 2.4A and 2.4B).

Lower anti-oxidant defenses, including SOD2, can lead to increased cell death (98, 110, 127). We therefore analyzed the expression of the activated form of caspase-3 (cleaved (C) caspase-3) as an established marker of apoptosis. C-Caspase-3 expression was upregulated in the lungs of the $Ahr^{-/-}$ mice in response to CS; however, there was no significant change in C-Caspase 3 expression following CS-exposure in the $Ahr^{+/-}$ mice (Fig. 2.4C, 2.4D). In addition to apoptosis, autophagy initiated by CS may also drive emphysematous lung destruction (109). Post-translational processing of microtubule-associated protein 1 light chain 3 (LC3) from the unconjugated LC3I to the phosphatidylethanolamine (PE) conjugated LC3II is critical for autophagy (117). Therefore, we assessed LC3II expression and observed that it was significantly elevated in the lungs of the CS-exposed $Ahr^{-/-}$ mice compared to CS-exposed $Ahr^{+/-}$ mice (Fig. 2.4E and 2.4F). These findings illustrate that AhR deficiency is associated with an upregulation of cell death machinery in the lung in response to CS. Collectively, our data position the AhR as a protector against lung injury, as evidenced by our findings that loss of AhR promotes the

development of an emphysema-like phenotype and worsens pathogenic mechanisms that underlie disease development (*i.e.* chronic inflammation, an anti-protease imbalance, SOD2, activation of cell death machinery).

AHR expression is reduced in the lungs and blood of COPD subjects

Results from our preclinical model led us to wonder about the AHR pathway in people with COPD. Therefore, we evaluated AHR expression in COPD subjects from three separate cohorts. In our first cohort (Table 2.1), there was significantly less *AHR* mRNA in the lungs of COPD subjects compared to subjects without COPD (Fig. 2.5A). We next analyzed AHR protein expression in Cohort 2 (Table 2.2), using multiplex immunohistochemistry (mIHC) (AHR is indicated in purple color in Figure 2.5B). AHR was present in all lung samples analyzed. AHR was particularly high in the epithelium of the parenchyma (Fig. 2.5B) of Non-smokers as well as those classified as At Risk. It was evident that AHR expression was greatest in the lungs of Non-smokers/At Risk subjects and lowest in the lungs of those with COPD (Fig. 2.5B). Finally, we assessed systemic *AHR* mRNA expression in whole blood taken from subjects participating in Cohort 3 - the CanCOLD cohort (311)- (Table 2.3). There was significantly less *AHR* mRNA in the blood of subjects with COPD relative to At Risk subjects (Fig. 2.6A). There was also significantly less *AHR* mRNA in the blood of COPD-Never Smokers (no history of smoking) compared to both At Risk and Non-smokers (Fig. 2.6B). Subjects with an emphysema score of 1 or more as assessed by computed tomography (CT) scan also had significantly less *AHR* mRNA in the blood relative to the At Risk subjects (Fig. 2.6C). Finally, systemic *AHR* mRNA levels positively correlated with the FEV_1/FVC (%) (Fig. 2.6D); higher *AHR* mRNA expression was significantly correlated with better lung function. Thus, AHR expression is reduced in COPD.

Reduced AHR expression in COPD is not associated with the *AHR* SNP Arg554Lys

The reason why AHR levels are lower in COPD is not known. A number of *AHR* variants are implicated in susceptibility to diseases associated with smoking (*e.g*. lung cancer) (317). The most widely studied SNP in the human *AHR* gene is G→A substitution in exon 10, which causes an arginine to lysine change (designated Arg554Lys [rs2066853]). This substitution (Arg554Lys) can affect AHR expression (263). Therefore, we assessed if *AHR* mRNA expression in COPD was associated with common *AHR* SNPs, including Arg554Lys (rs2066853) by conducting eQTL analysis for SNPs located 10 kb up and down-stream of *AHR* on chromosome 7 (Fig. 2.7A). rs73079669 was the top SNP associated with the expression of *AHR* (Fig. 2.7A [in red] and Fig. 2.7B) but there was no difference in the frequency of rs73079669 in patients with or without COPD (p=0.95) (data not shown). There was also no association with rs2066853 and *AHR* expression in the lung (Fig. 2.7C). Thus, it is unlikely that the reduced AHR expression in COPD can be explained by altered frequency of these *AHR* SNPs.

AHRR expression is elevated in the lungs of COPD subjects

We next turned our attention to the AhRR, a negative regulator of the AhR pathway. We assessed *AHRR* mRNA levels in the lungs of patients with and without COPD. COPD subjects had significantly higher expression of *AHRR* mRNA in the lungs relative to At Risk subjects (Fig. 2.8A). As several *AHRR* SNPs are also associated with disease (318-320), eQTL analysis was conducted for SNPs located 10 kb up and down-stream of *AHRR* on chromosome 5 (Fig. 2.8B). Interestingly, one of the top eQTL-SNPs (rs554208923) was significantly associated with COPD (p=0.0196). The COPD risk allele (G) for SNP rs554208923 was significantly associated with

increased *AHRR* mRNA expression (Fig. 2.8C). Increased *AHRR* mRNA expression in COPD subjects may be at least in part a consequence of regulatory SNPs in the *AHRR* gene. Collectively, our data support that AhR deficiency drives the pathogenesis of emphysema in the murine lung, and we further demonstrate that humans with COPD exhibit reduced AhR expression.

2.5 TABLES

Table 2.1. Clinical characteristics of lung eQTL subjects.

Variable	Control (168)	COPD (217)
Age (years)	60.3 ± 10.6	65.6 ± 8.8
Male (n)	86	131
Female (n)	82	86
FEV1% Predicted	90.7 ± 16.3	72.5 ± 17.2
FEV1/FVC	75.5 ± 4.2	61.3 ± 7.9
Smoking (%)		
Smoker	28 (16.7)	59 (27.2)
Former	117 (69.6)	151 (69.6)
Never	23 (13.7)	7 (3.2)

Data presented as the mean ± SD.

Table 2.2. Clinical characteristics of St Joseph's Healthcare Hamilton subjects.

Variable	**Non-Smoker (11)**	**At Risk (11)**	**COPD (13)**
Age (years)	68.1 ± 10.3	57.9 ± 8.7	65 ± 10.7
Male (n)	5	6	7
Female (n)	6	5	6
FEV_1/FVC (%)	79.8 ± 7.3	85.6 ± 24.5	56.2 ± 11.1*
Pack Years	0 ± 0	39.5 ± 16.2*	50.4 ± 20.2*

Data presented as the mean ± SD.

*FEV_1/FVC (%) of COPD subjects is significantly lower ($p < 0.05$) than either the At Risk or Non-Smoker subjects without COPD, which were not different from each other.

*Pack years of At Risk and COPD subjects were significantly higher ($p < 0.05$) than Non-Smoker subjects, although At Risk and COPD subjects were not different from each other.

Table 2.3. Clinical characteristics of CanCOLD subjects.

Variable	Non-Smoker (16)	At Risk (15)	COPD (32)
Age (years)	67.75 ± 5.84	65.53 ± 8.46	67.31 ± 10.86
Male (n)	4	5	18
Female (n)	12	10	14
FEV_1/FVC (%)	76.39 ± 4.22	78.61 ± 4.36	60.52 ± 12.68*
Pack Years	0 ± 0	13.40 ± 10.61*	23.57± 27.49*

Data presented as the mean ± SD.

*FEV_1/FVC (%) of COPD subjects is significantly lower ($p< 0.05$) than either the At Risk or Non-Smoker subjects without COPD, which were not different from each other.

*Pack years of At Risk and COPD subjects were significantly higher ($p< 0.05$) than Non-Smoker subjects, and the pack-years of COPD subjects were significantly higher than At Risk.

2.6 FIGURES

Figure 2.1

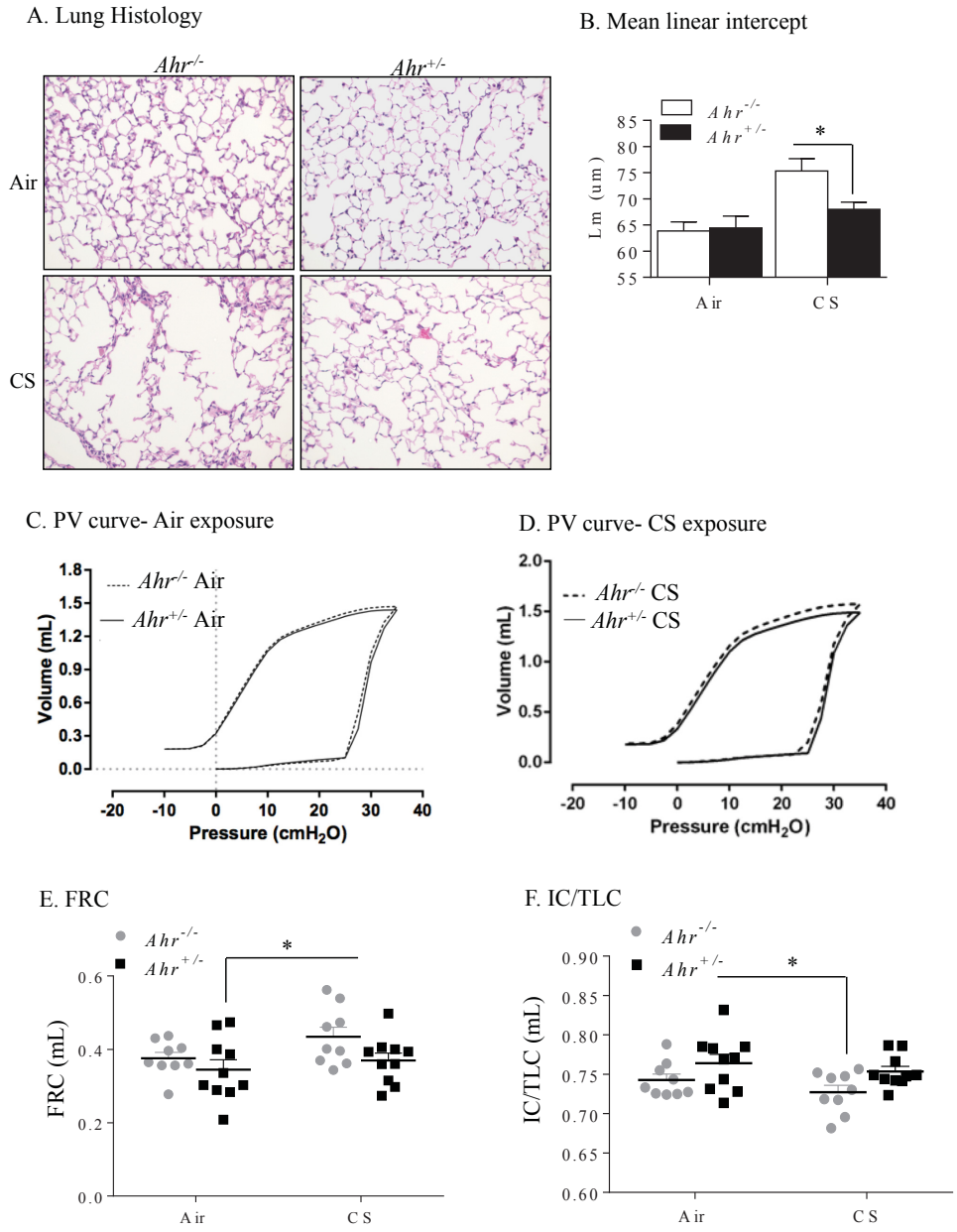

Figure 2.1. AhR deficiency drives the development of CS-induced emphysema *in vivo*. (A) Lung Histology- Representative images from the lung parenchyma of *Ahr*$^{-/-}$ and *Ahr*$^{+/-}$ mice exposed to a 4-month CS regime are shown (magnification = 20x). (B) Mean linear intercept- Lm was used to quantify airspace enlargement in the lung parenchyma of female mice. Results are expressed as mean ± SEM, n=6-8 mice per group. Representative PV-curves are shown comparing air-exposed (C) and CS-exposed (D) *Ahr*$^{+/-}$ and *Ahr*$^{-/-}$ male and female mice. There were significant changes in functional residual capacity (FRC) (E), and the ratio of inspiratory capacity to the total lung capacity (IC/TLC) (F) in CS-exposed *Ahr*$^{-/-}$ mice. Results are expressed as mean ± the SEM, n= 10-11 mice per group. Data were analyzed using a two-way ANOVA with a Tukey's test for multiple comparisons.

Figure 2.2

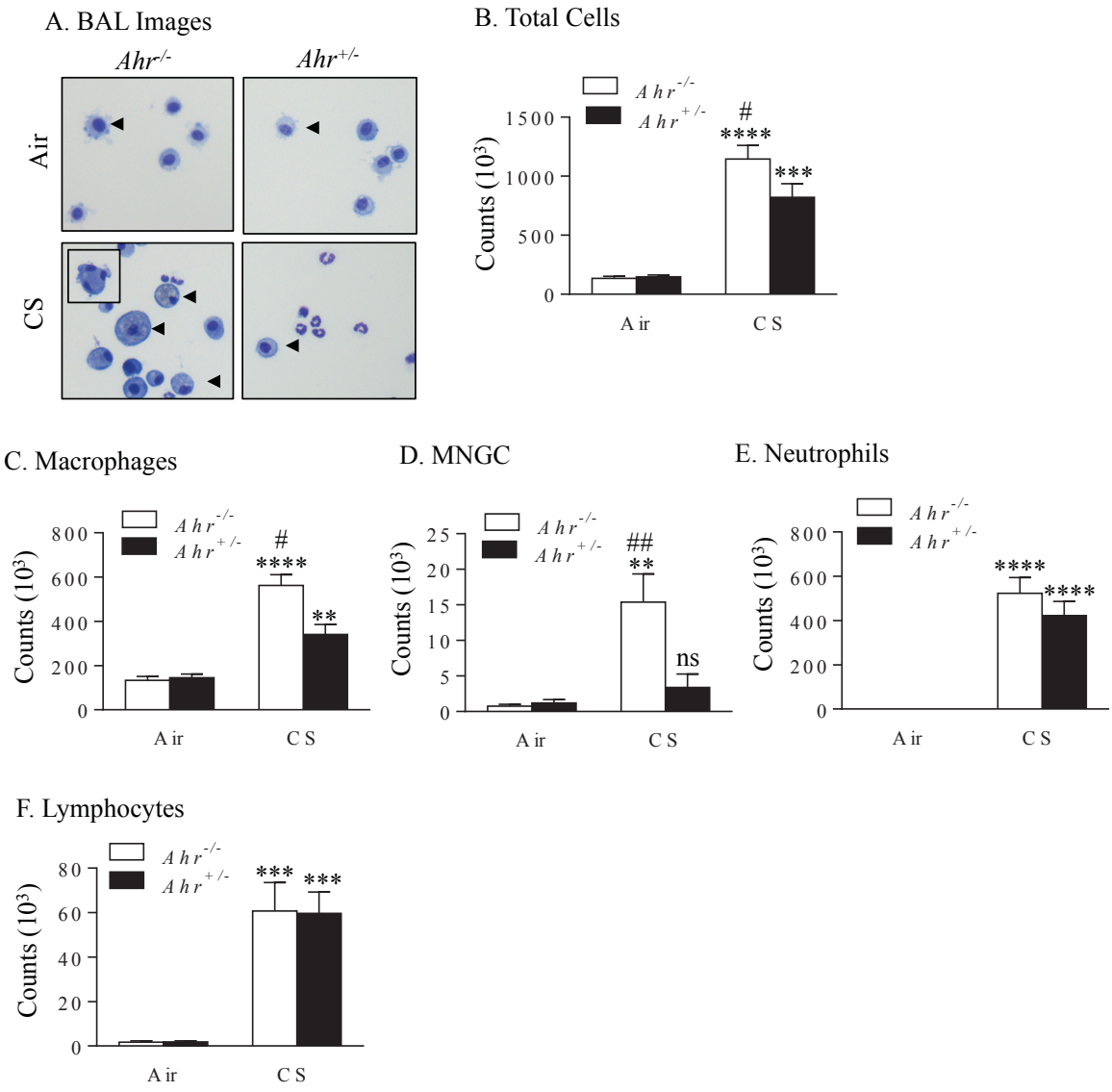

Figure 2.2. AhR deficiency results in heightened CS-induced pulmonary inflammation. (A) BAL Images- Representative images of cells from the BAL of male *Ahr*$^{+/-}$ and *Ahr*$^{-/-}$ mice exposed to an 8-week CS regime; black arrows depict BAL macrophages; inset-multi-nucleated giant cell. (B) Total Cells- There was a significant increase in cellularity in response to CS (**** $p < 0.0001$; *** $p < 0.001$ compared to air-only exposure). There were significantly more BAL cells in CS-exposed *Ahr*$^{-/-}$ mice (# $p < 0.05$ compared to CS-exposed *Ahr*$^{+/-}$ mice). **(C)** Macrophages- CS increased the number of macrophages in CS-exposed *Ahr*$^{+/-}$ and *Ahr*$^{-/-}$ mice (**** $p < 0.0001$; ** $p < 0.01$ compared to air-only exposure); macrophages were also higher in CS-exposed *Ahr*$^{-/-}$ mice (# $p < 0.05$); (C) MNGC- MNGCs were significantly increased in CS-exposed *Ahr*$^{-/-}$ mice compared to air-exposed *Ahr*$^{-/-}$ mice (** $p < 0.01$) as well as CS-exposed *Ahr*$^{+/-}$ mice (## $p < 0.01$); (E) Neutrophils- CS induced a significant increase BAL neutrophils in both *Ahr*$^{+/-}$ and *Ahr*$^{-/-}$ mice (**** $p < 0.0001$); there was no difference between *Ahr*$^{+/-}$ and *Ahr*$^{-/-}$ mice. (F) Lymphocytes- CS induced a significant increase of lymphocytes in *Ahr*$^{+/-}$ and *Ahr*$^{-/-}$ mice (**** $p < 0.0001$); there was no difference between *Ahr*$^{+/-}$ and *Ahr*$^{-/-}$ mice. Data were analyzed using a two-way ANOVA with a Tukey's test for multiple comparisons. Results are expressed as mean ± SEM, n=4-5 mice per group.

Figure 2.3

A. *Mmp9:Timp1* mRNA

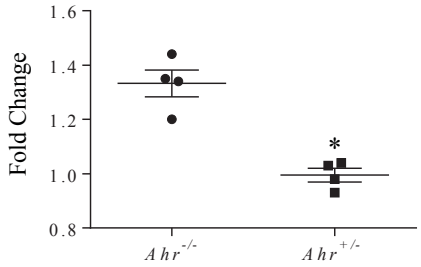

B. MMP9:TIMP1 protein

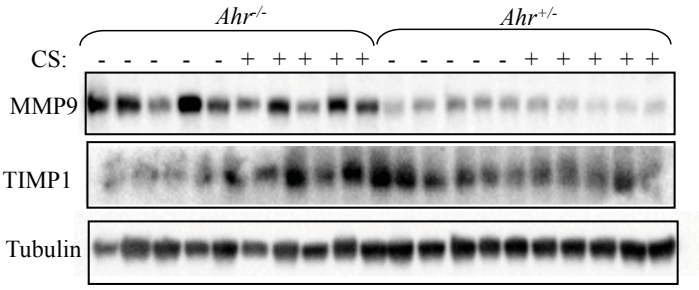

C. MMP9:TIMP1 protein quantification

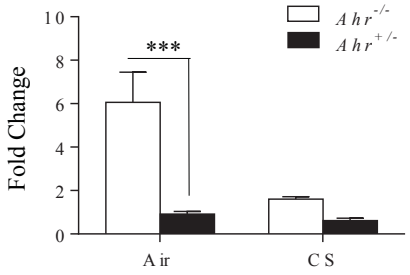

Figure 2.3. AhR deficiency results in a protease : anti-protease imbalance in the lungs. (A) *Mmp9:Timp1* mRNA- the ratio of *Mmp9:Timp1* mRNA was significantly higher in air-exposed male *Ahr*$^{-/-}$ mice relative to the air-exposed *Ahr*$^{+/-}$ mice. Data was analyzed using a Komologrov Smirnov non-parametric t-test. Results are expressed as mean ± SEM, n=4-5 mice per group. (B, C) MMP9:TIMP1 protein- the ratio of MMP9:TIMP1 protein was significantly higher in air-exposed *Ahr*$^{-/-}$ mice relative to the air-exposed *Ahr*$^{+/-}$ mice. Data was analyzed using a two-way ANOVA with a Bonferroni correction. Results are expressed as mean ± SEM, n=4-5 mice per group.

Figure 2.4

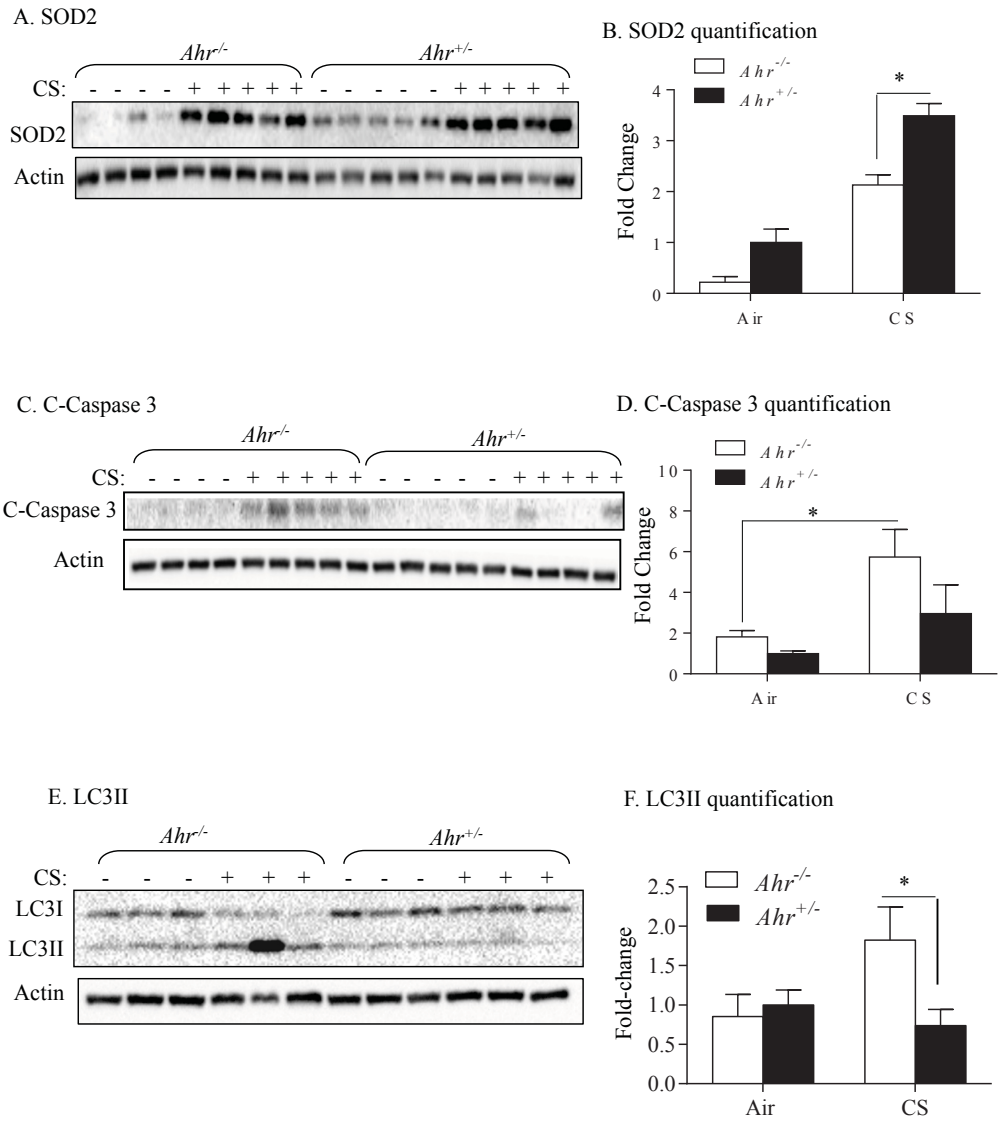

Figure 2.4. AhR deficiency impairs SOD2 upregulation and activates cell death machinery in the CS-exposed lung. (A, B) SOD2 quantification- SOD2 expression is significantly lower in the lungs of the CS-exposed male *Ahr*$^{-/-}$ mice relative to the CS-exposed *Ahr*$^{+/-}$ mice (n= 4-5 mice per group). (C, D) C-Caspase 3 quantification- C-Caspase 3 expression was significantly upregulated in the lungs of the *Ahr*$^{-/-}$ mice in response to CS, whereas no significant change in C-Caspase 3 expression was observed in the *Ahr*$^{+/-}$ mice in response to CS (n=9-10 mice per group). (E, F) LC3II quantification- LC3II is significantly higher in the lungs of the CS-exposed *Ahr*$^{-/-}$ mice compared to the CS-exposed *Ahr*$^{+/-}$ mice (n= 9-10 mice per group). Data was analyzed using a two-way ANOVA with a Bonferroni correction. Results are expressed as mean ± SEM.

Figure 2.5

A. *AHR* mRNA expression in human lung tissue

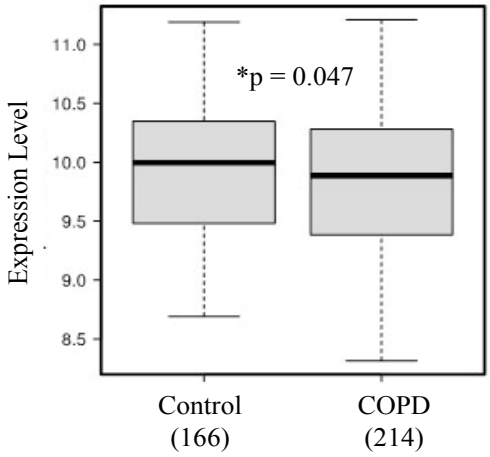

B. AHR protein in human lung tissue (mIHC)

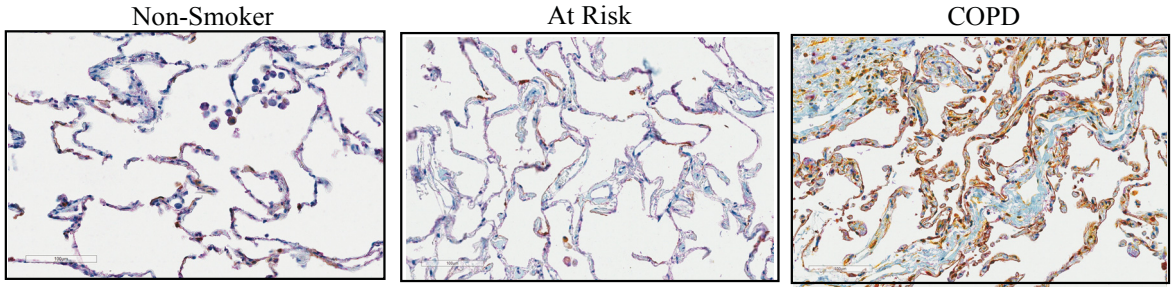

Figure 2.5. AHR expression is lower in lung tissue from human COPD subjects. (A) *AHR* mRNA in human lung tissue- There was significantly less *AHR* mRNA in the lungs of COPD subjects (n=214) compared to subjects without COPD (Control) (n=266) as analyzed using a Welch t-test. (B) AHR protein in human lung tissue (mIHC)- mIHC was used to detect AHR (purple), vimentin (fibroblasts; yellow) and cytokeratin-19 (epithelial cells; brown) in human lungs. Note the relative decrease in AHR (purple) in COPD subjects relative to Non-smokers and those At Risk (smokers without COPD); representative images are shown. Scale bars (100μm) are shown in the bottom left corner of each image.

Figure 2.6

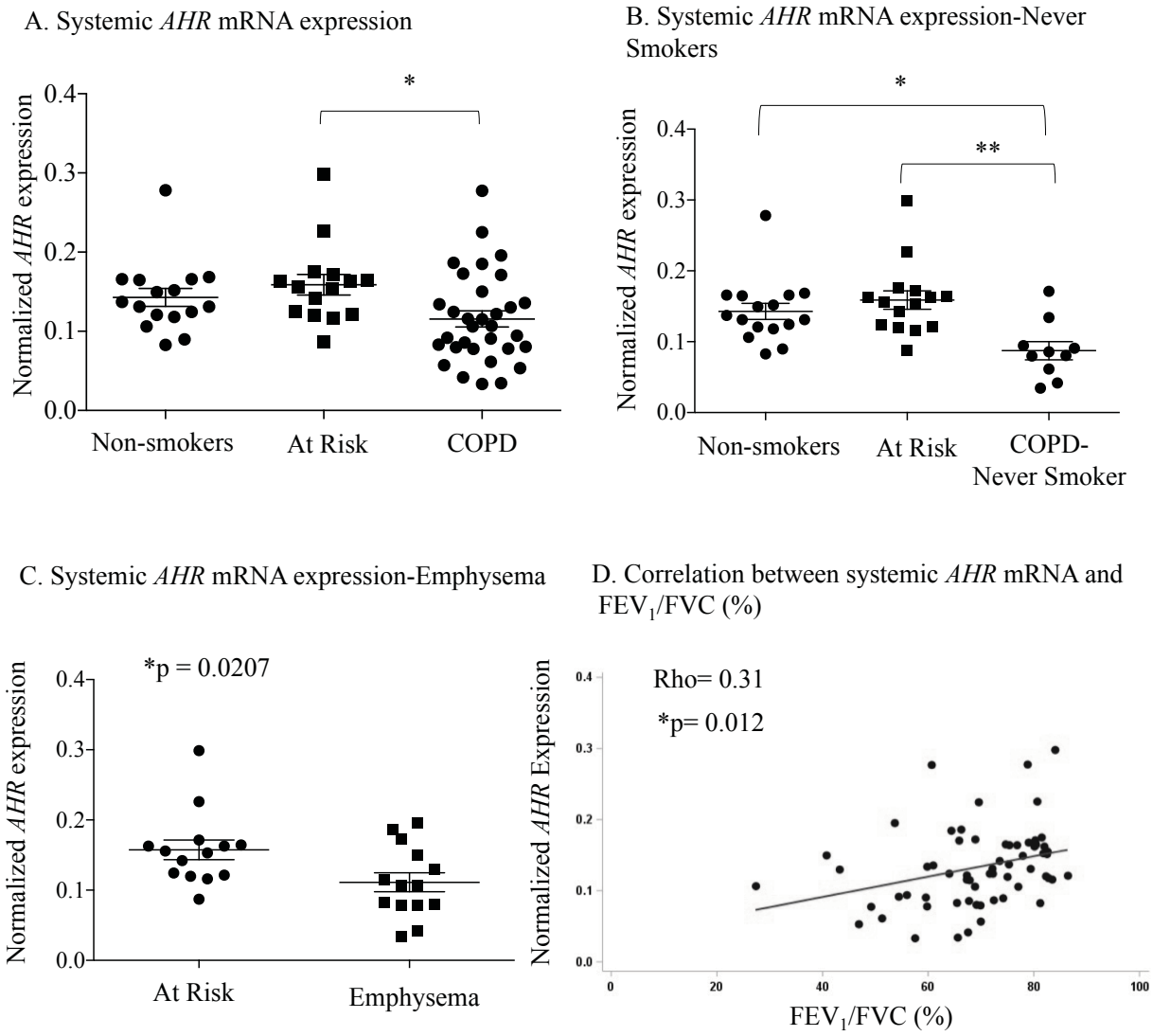

Figure 2.6. *AHR* expression is significantly reduced in the blood of human COPD subjects from the CanCOLD cohort. (A) Systemic *AHR* mRNA expression- There was significantly less systemic *AHR* mRNA in COPD subjects (n=32) relative to the At Risk subjects (n=15). (B) Systemic *AHR* mRNA expression- Never Smokers- *AHR* mRNA expression was significantly less in COPD subjects with no history of smoking (COPD-Never smokers; n=10) relative to both Non-smokers (n=16) and At Risk (n=15) control subjects. Results were analyzed using a Kruskal-Wallis non-parametric one-way ANOVA. Results are expressed as mean ± SEM. (C) Systemic *AHR* mRNA expression-Emphysema- *AHR* mRNA expression was significantly less in COPD subjects that had also been diagnosed with emphysema via CT (Emphysema; n=14) relative to At Risk control subjects (n=14). Results were analyzed using a Komologrov Smirnov non-parametric t-test. Results are expressed as mean ± SEM. (D) Correlation between systemic *AHR* mRNA and FEV_1/FVC (%)- There was a significant positive correlation between systemic *AHR* mRNA expression and lung function (FEV_1/FVC) as assessed using a Pearson's correlation coefficient.

Figure 2.7

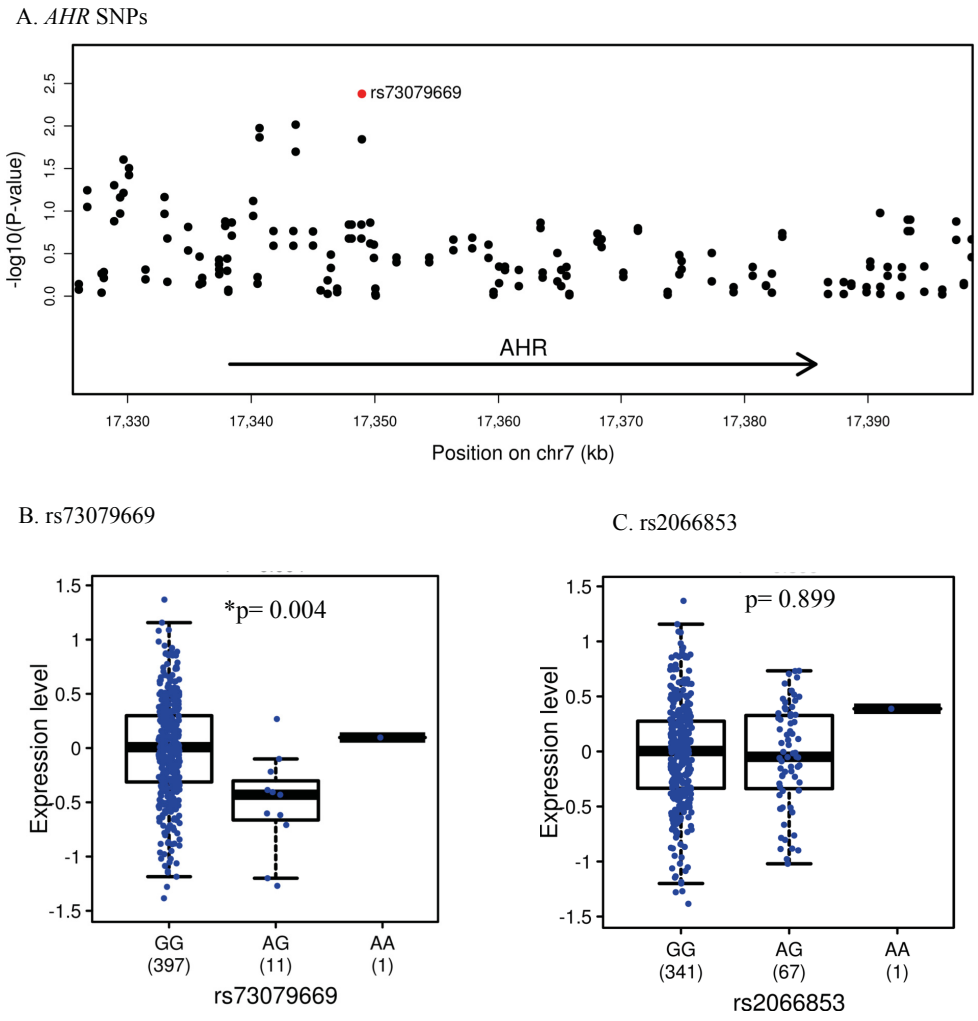

Figure 2.7. Reduced *AHR* expression is not associated with *AHR* SNPs. (A) *AHR* SNPs- Data are lung eQTL within or near the *AHR* gene on chromosome 7. Each dot represents an association test between one SNP and the expression of *AHR*. The y axis shows the P values in –log10 scale. The x axis shows the location of SNPs on chromosome 7. (B) rs73079669- Box plots of mRNA expression levels for *AHR* in human lung tissues according to genotyping for the SNP rs73079669. The y axis presents mRNA expression levels for *AHR* while the x axis represents the three groups; the number of subjects in parenthesis. (C) rs2066853- Box plots of mRNA expression levels for *AHR* in human lung tissues according to genotyping for rs2066853.

Figure 2.8

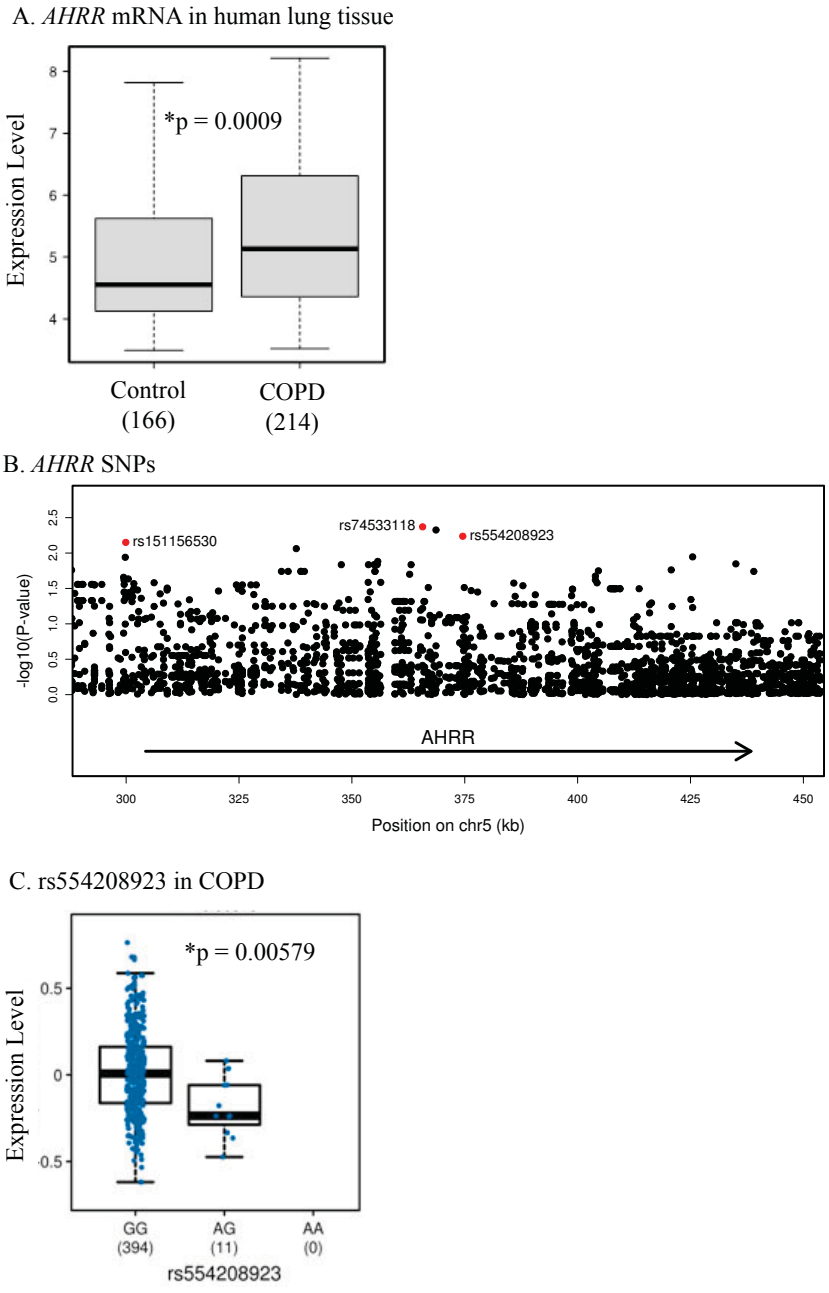

Figure 2.8. *AHRR* expression is significantly elevated in COPD. (A) *AHRR* mRNA in human lung tissue - Box plot of *AHRR* mRNA expression in the lungs of subjects with COPD (n=217) and without COPD (Control) (166). (B) *AHRR* SNPs- Lung eQTL within or near the *AHRR* gene on chromosome 5. Each dot represents an association test between one SNP and the expression of *AHRR*. The y axis shows the P values in –log10 scale. The x axis shows the location of SNPs on chromosome 5. (C) rs554208923 in COPD- Box plots of mRNA expression levels for *AHRR* in human lung tissues according to genotyping groups for SNP rs554208923. The left y axis presents *AHRR* mRNA expression levels. The x axis represents the three genotyping groups with the number of subjects in parenthesis.

2.7 DISCUSSION

Despite knowledge on the role of the AhR pathway in mediating dioxin-induced toxicity, the biological and physiological functions of the AhR remain largely unknown. The fact that the AhR is ubiquitously-expressed, evolutionarily-conserved and activated in response to endogenous ligands suggests that the AhR evolved for purposes beyond strictly mediating toxic effects to a subset of environmental contaminants. When considered with our data, we posit that the AhR pathway has evolved to be a homeostatic regulator of respiratory health against inhaled toxicants.

Along these lines, one of our most exciting observations was that *Ahr*$^{-/-}$ mice have extensive lung parenchymal destruction after only a 4-month CS-exposure. This is striking because the *Ahr*$^{-/-}$ mice are on the C57BL/6 background, a strain that requires ~6 months of CS exposure to develop the emphysematous airspace enlargement (321). It is also interesting that the *Ahr*$^{-/-}$ mice did not exhibit basal airspace enlargement. This is in contrast to a number of other murine models that spontaneously develop emphysema-like lung tissue destruction (322-324), suggesting that the emphysematous changes in response to CS are not attributable to impaired lung development or a congenital defect due to absence of the AhR.

In addition to the evident lung structural damage, CS-exposed *Ahr*$^{-/-}$ mice also exhibited emphysema-like changes in lung function, including a significant increase in the FRC and a significant decrease in the IC/TLC ratio. This is in accordance with lung function in humans with emphysema, where lung parenchymal destruction results in an outward recoil of the lung, leading to hyperinflation, air trapping and an increased FRC (314). Moreover, a reduced IC/TLC ratio is associated with worse clinical outcomes in COPD patients as well as with more severe disease (325), increased exacerbations (326) and increased mortality (327). It could be that AhR dysregulation (altered function and/or reduced expression) may predispose a susceptible individual

to the development of emphysema and subsequent deterioration in lung function.

Lung tissue destruction in COPD is thought to be a consequence of many inter-dependent mechanisms including inflammation, an anti-protease imbalance, oxidative stress and increased cell death. The goal of this study was not to establish which of these mechanism(s) is the causative driver of CS-induced airspace enlargement in *Ahr*$^{-/-}$ mice but rather, to assess the totality of AhR involvement in mechanisms relevant to COPD pathogenesis. Our data clearly indicate that there is dysregulation of multiple mechanisms when AhR is absent. For example, accelerated cell death underlies emphysematous airspace enlargement by causing alveolar wall destruction (72). We observed significant upregulation of features consistent with increased cell death in the lungs of CS-exposed *Ahr*$^{-/-}$ mice. We chose for this analysis c-caspase 3 and LC3II expression, as these are increased during apoptosis and autophagy, respectively. Experimental evidence also places these as central for emphysema development. For example, intratracheal instillation of c-caspase-3 induces epithelial cell apoptosis and emphysematous airspace enlargement in the mouse lung (98). Additionally, LC3-deficient mice are protected against the development of a CS-induced emphysema-like phenotype (109). Finally, upregulation of caspase 3 activity and LC3II expression occur in the lungs of COPD subjects (127). Although we cannot conclude that upregulation of these cell death mechanisms is, in fact, the direct cause airspace enlargement in our model, our data continue to support the assumption that the AhR protects the lung against the deleterious effects of CS.

These cell death mechanisms may be driven by inflammation. We have previously reported that the *Ahr*$^{-/-}$ mice exhibit significantly greater neutrophilia in the BAL than the *Ahr*$^{+/-}$ mice following both an acute (3 day) (301) as well as following a sub-chronic (2-4 week) CS exposure (162, 216). Leukocytosis is the main respiratory and systemic immune alteration in smokers (328,

329) and neutrophils are abundant in the bronchial lumen (330), bronchial wall and lung parenchyma of patients with COPD (331, 332). However, chronic inflammation in COPD is also typified by macrophage infiltration into the lungs and airways (76), with the macrophage believed to be one of the key effector cells that drive lung tissue destruction (46). Therefore, one of our more intriguing observations was pulmonary inflammation dominated by macrophages in *Ahr*$^{-/-}$ mice exposed to a chronic smoke regime. We consider this to be a reflection of the ability of the AhR to control the progression of inflammation over time, from one that is neutrophil-dominant (acute) to macrophage-centric (chronic).

Of note was our observation that MNGCs, regarded to be the product of monocytes/macrophage fusion, are only increased in *Ahr*$^{-/-}$ mice chronically exposed to CS. This suggests that the AhR may play a key role in the fusion of monocytes or macrophages, a phenomenon for which the mechanism(s) is unknown. MNGCs, first described in tuberculosis (333), are a hallmark of a chronic inflammatory response (334). Formation of MNGCs may also be a consequence of chronic injury (335). MCGCs have been observed in the lung in response to carbon black (336) and cigarette smoke (337), where they may contribute to the removal of debris from tissue (333). Whether MNGCs are detrimental or beneficial is only speculative. MNGCs that form on implanted material (surgical sutures, implanted devices) may degrade the biomaterial (334). Of relevance to our findings and emphysema pathogenesis, MNGCs are also important sources of reactive oxygen species (338) and MMP9 (339). While the functional significance of MNGCs in the lungs of *Ahr*$^{-/-}$ mice is unclear, it is not unreasonable to speculate that their increased presence may directly contribute to the lung tissue destruction seen in our model.

The signaling mechanism(s) by which the AhR may attenuate the development of emphysema is not currently known but may involve direct control over microRNA (miRNA). We

have shown *in vitro* and *in vivo* that the AhR controls miRNA expression, which regulates apoptosis and inflammation from CS exposure (216, 297). For example, attenuation of CS-induced lung cell death occurs via AhR-dependent regulation of miR-196a (217). Other miRNA are also regulated by the AhR in response to CS. One of these is miR-183 (216), which suppresses MMP9 expression in cancer cell lines (340). It could be that lower induction of miR-183 in *Ahr*$^{-/-}$ mice contributes to higher MMP9:TIMP1 ratio observed herein. The AhR also represses some miRNA, including miR-96, in response to CS *in vivo* (216). This could be important, as miR-96 is over-expressed in chronic lung diseases such as idiopathic pulmonary fibrosis and lung cancer (341) (342). miR-96 targets the transcription factor FOXO3a and may be why there is more inflammation in the lungs of *Ahr*$^{-/-}$ mice. Thus, it could be that dynamic regulation of miRNA is one means through which the AhR can control multiple pathogenic mechanisms implicated in COPD pathogenesis.

We and others have shown that there is dysregulation of miRNA expression in COPD (312, 343-345), including higher expression of miRNA, such as miR-146a and miR-29, which are predicted to control AhR expression. This could be of significance, given that our data demonstrate there is reduced pulmonary and systemic AHR expression in people with COPD. Although CS exposure can decrease AhR expression (162, 346), we do not believe that the reduced AHR in COPD subjects is a consequence of smoking. This is largely because AHR protein expression is reduced in the lung of COPD subjects relative to the At Risk subjects, despite there being no significant difference in the smoking histories (*i.e.* pack-years) between these two groups (Table 2.2). Furthermore, systemic *AHR* mRNA expression was also significantly reduced in COPD subjects that had never smoked.

Although we were unable to demonstrate that *AHR* SNPs account for lower AHR levels in

COPD, we did observe elevated *AHRR* expression in the lungs of COPD subjects. This raises the possibility that the AHRR could be controlling AHR expression. Part of this rationale comes from studies showing that AhRR can alter AhR expression and activity following exposure to CS and wood smoke (271). Furthermore, *Ahrr*$^{-/-}$ mouse embryonic fibroblasts have significantly higher constitutive *Ahr* mRNA expression (274, 347). When considered together with the fact that those with COPD have significantly higher expression of *AHRR* mRNA, we postulate that one additional mechanism that may explain why there is reduced AHR in COPD could be elevated AHRR levels. Future experiments to assess if blocking AhRR activity can restore AhR expression in COPD subjects may shed light on a promising therapeutic approach to restore AhR levels in COPD.

A limitation of our study is the cross-sectional nature in which our information on the AhR pathway is obtained. We currently do not have data, for example, on AHR expression in the same individual over time *(i.e.* pre- and post-COPD development). For this reason, we are unable to conclude whether reduced AHR expression predisposes individuals to the development of COPD or if the development of COPD itself is responsible for the changes in AHR expression. Based on our *in vivo* data, whereby AhR deficiency drives the development of CS-induced emphysema, we consider that low AHR precedes disease development and may even represent a susceptibility factor for COPD. It could be that low levels of AHR are inherent (from birth) or progressive, meaning that there is loss of the AHR expression over time. In an individual that smokes or is exposed to high levels of air pollution, low AHR could contribute to COPD development and overall individual susceptibility.

In conclusion, we demonstrate that AhR deficiency worsens the development of a CS-induced emphysema-like phenotype in conjunction with exacerbating mechanisms that contribute to lung tissue destruction *in vivo*. We also establish that lung and systemic AHR expression is

reduced in COPD subjects, and that low AHR levels correlate with worse lung function. Collectively our data position the AhR as a central player in the homeostatic maintenance of lung health and provide mechanistic insight into its mode of action. These findings lay the foundation for the AhR as a novel therapeutic target or biomarker in identifying those individuals susceptible to the development of COPD.

STUDY APPROVAL

Animal procedures were approved by the McGill University Animal Care Committee (Protocol Number: 5933) and human subjects were approved by the Research Ethics Board of St Joseph's Healthcare Hamilton (00-1839).

AUTHOR CONTRIBUTIONS

Data curation and analysis: NG., THT., YB., ARS., LC., CM., MZ. ML., AR., PZL; Funding acquisition: CJB, JB; Investigation: NG., CJB; Methodology: NG., YB., AR., LS., JGM., HT., SP; Project administration: NG., CJB; Resources: YB., PZL., JB., WCT., RPP., PJS., J Matthews., AR., J.Martin, PN; Supervision: NG., CJB; Intellectual contributions: NG., CJB., BMS., QH., DHE., SJ., J.Martin, AB., AR., YB; Manuscript writing, review and editing: NG., CJB., YB., THT., AR., RPP., PJS., PN, BMS.

2.8 Preface: Chapter 3

In Chapter 2 we demonstrated that AhR deficiency drives the development of a CS-induced emphysema-like phenotype in the murine lung. This conclusion was supported by our observations that AhR ablation promoted the CS-induced 1) upregulation of pathogenic mechanisms underlying emphysema development (*i.e.* inflammation, antiprotease imbalance, impaired antioxidant upregulation and activation of cell death machinery), 2) increase in lung parenchymal destruction and 3) declines in lung function in the murine lung. The translational nature of these findings is highlighted by our observation that human COPD subjects exhibit reduced pulmonary and systemic AHR expression relative to subjects without COPD. Moreover, in humans, systemic *AHR* expression is positively correlated with the lung function parameter FEV_1/FVC (%), such that less *AHR* is associated with worse lung function. Taken together, our findings presented in Chapter 2 suggest a protective role for the presence of the AhR in attenuating the pathogenesis of CS-induced emphysema/COPD. These findings could provide a foundation for the therapeutic targeting the AhR in individuals susceptible to the development of COPD. However, for the AhR to be considered as putative therapeutic molecular target in COPD, its mechanism of action to combat CS-induced lung damage must be further elucidated.

Thus, in Chapter 3 we utilized an *in vitro* model of CS exposure to assess the mechanism through which AhR deficiency may promote CS-induced lung damage. Since the loss of lung structural cells is of particular importance to the pathogenesis of emphysema (72, 97), we utilized an *in vitro* model of CS-exposure to assess the mechanism through which AhR deficiency may promote CS-induced lung structural cell death. Although we have previously shown that AhR deficiency promotes CS-induced apoptosis in lung structural cells (161), the cell death mechanisms that are induced by CS are not limited to apoptosis and may include autophagy and ER stress (109,

141, 155, 348). It is therefore important to determine whether the AhR functions as a global regulator of toxicant-induced cell death in the lung, and thus if the AhR is capable of regulating alternative cell death mechanisms- including autophagy and/or ER stress- in lung structural cells.

3 Aryl hydrocarbon receptor (AhR) deficiency promotes endoplasmic reticulum (ER) stress in lung structural cells

Necola Guerrina[1,2], Kashmira Prasade[1], Luca Cuccia[4], Jason Matthews[5,6], David H. Eidelman[1,3], Qutayba Hamid[1,3,7] and Carolyn J. Baglole[1,2,3,4]

[1]Research Institute of the McGill University Health Centre, Departments of [2]Pathology, [3]Medicine, [4]Pharmacology and Therapeutics, McGill University; [5]Department of Nutrition, University of Oslo, Oslo, Norway; [6]Department of Pharmacology & Toxicology, University of Toronto, Toronto Canada; [7]College of Medicine, University of Sharjah, United Arab Emirates.

Correspondence and requests for materials should be addressed to:
Carolyn J. Baglole
1001 Decarie Blvd (EM22248)
Montreal, Quebec H4A3J1
Telephone: (514) 934-1934 ext. 76109
E-mail: Carolyn.baglole@mcgill.ca

ACKNOWLEDGEMENTS

ImageStream® data were acquired through the Immunophenotyping platform of the Research Institute of the McGill University Health Center (RI-MUHC). Processing of samples for TEM was made possible by the Facility for Electron Microscopy Research (FEMR) of McGill University. ER stress antibodies were graciously provided by Dr. Louise Larose. We would also like to acknowledge and thank Laurent Huck, Dominique Mayaki and Kwang-Bo Joung for their expertise and assistance with optimization of gene expression protocols. This work was supported by the Canada Foundation for Innovation (CFI), Natural Sciences and Engineering Research Council of Canada (NSERC), and the Canadian Institutes for Health Research (CIHR). C.J.B. was supported by a salary award from the Fonds de recherche du Quebec-Sante (FRQ-S).

The authors declare no conflicts of interest.

3.1 ABSTRACT

The aryl hydrocarbon receptor (AhR) is a transcription factor highly expressed in barrier organs such as the skin, intestine and lung. The lungs are continuously exposed to environmental contaminants such as air pollution and cigarette smoke (CS), which may induce inter-dependent cell death mechanisms such as apoptosis, autophagy and endoplasmic reticulum (ER) stress. These cell death modalities contribute to the pathogenesis of common respiratory diseases such as chronic obstructive pulmonary disease (COPD). Moreover, CS is also a complex mixture of AhR ligands. Although we have previously shown that AhR activation protects against CS-induced apoptosis, whether the AhR attenuates alternative CS-induced cell death modalities, such as autophagy and ER stress, is unknown. Using cigarette smoke extract (CSE) as our *in vitro* surrogate of environmental contaminant exposure, we first assessed the conversion of LC3I to LC3II, a classic feature of both autophagic and ER stress-mediated cell death pathways. LC3II was elevated in CSE-exposed lung structural cells when AhR was absent. However, this heightened LC3II could not be explained by the upregulation of key autophagy genes (*Gabarapl1, Beclin-1, Lc3b*), upregulation of upstream autophagic machinery (ATG5-12, ATG3) or by impaired autophagic flux. This suggested that LC3 processing may be autophagy-independent, which was further supported by the absence of autophagosomes in $Ahr^{-/-}$ lung cells. However, $Ahr^{-/-}$ lung cells had widespread ER-dilation, elevated expression of the ER stress markers CHOP and GADD34 and an accumulation of ubiquitinated proteins. These findings collectively illustrate that AhR deficiency promotes ER stress in lung structural cells via a mechanism that is likely autophagy-independent.

3.2 INTRODUCTION

The aryl hydrocarbon receptor (AhR) is a ligand-activated transcription factor that belongs to the basic helix loop helix PER-ARNT-SIM (bHLH/PAS) family of regulatory proteins (168). Although the AhR is ubiquitously-expressed throughout the body, its expression is highest in first-line defense organs such as the lung, gut, skin, and liver (164). Historically, the AhR is best-known for its ability to mediate the detrimental effects of the man-made toxicant 2,3,7,8-tetrachlorodibenzo-p-dioxin (TCDD; dioxin) (182, 292, 293). The unligated AhR is found in the cytoplasm complexed with chaperone proteins (197). After TCDD binding, the AhR translocates to the nucleus and forms a heterodimer with the AhR nuclear transporter (ARNT). This AhR-ARNT complex binds to DNA sequences termed the dioxin response element (DRE), initiating the transcription of genes such as cytochrome P450 (CYP) CYP1A1. Persistent activation of the AhR pathway by TCDD is associated with toxic responses (183).

However, the AhR has emerged as a regulator of cellular processes independent of TCDD exposure; these processes include proliferation, differentiation and survival (243, 249, 250, 252). Perturbations in these processes can lead to prevalent diseases such as chronic obstructive pulmonary disease (COPD). COPD is a respiratory disease that is principally caused by exposure to air pollution (ambient, biomass and occupational) and cigarette smoke (CS). Given that 92% of the world's population reside in locations where air pollution levels exceed the World Health Organization (WHO) ambient air quality guidelines, and that there are still over 1 billion smokers worldwide, COPD is likely to remain a prominent health care concern for decades to come. Both air pollution and CS are a mixture of gases and particulate matter composed of metals (iron, nickel), biological agents (endotoxins), minerals (quartz) and organic chemicals such as polychlorinated dibenzodioxins and polycyclic aromatic hydrocarbons (41-44). Many of these

organic chemicals are ligands of the AhR (216, 349).

We have previously shown that loss of the AhR promotes several pathogenic effects of CS, including increased apoptosis in lung structural cells (161). While it is postulated that loss of lung cells due to enhanced apoptosis is a feature in lung diseases such as COPD, other cell death mechanisms are likely to also be important. In fact, cell death mechanisms that are induced by CS may be highly inter-dependent, and thus not limited to apoptosis. These other cell death mechanisms may include autophagy, cytoplasmic vacuolization death and paraptosis, all of which are associated with endoplasmic reticulum (ER) stress (109, 141, 155, 348).

ER stress is caused by the accumulation of misfolded protein aggregates in the ER lumen, leading to the initiation of a three-branched signaling cascade collectively referred to as the unfolded protein response (UPR). Exposure to toxicants such as CS that induce excessive or prolonged ER stress may render the UPR insufficient to restore homeostasis, such that the 'pro-death' arm of the ER stress response dominates (131). This pro-death arm depends on the upregulation of the transcription factor C/EBP homologous protein (CHOP) (136-138); CHOP can then induce both apoptosis and/or autophagy (141, 350, 351). Autophagy involves the cytoplasmic uptake of damaged proteins, substrate and organelles by autophagic vesicles (autophagosomes) and their subsequent lysosomal degradation (113). Exposure to CS causes an accumulation of autophagosomes within lung structural cells, leading to cell death (124, 127).

Another feature common to both ER stress and autophagy is the processing of microtubule-associated protein 1 light chain 3 (LC3), from the unconjugated isoform (LC3I) to the phosphatidylethanolamine-conjugated isoform (LC3II). This post-translational processing of LC3 is critical for autophagosome maturation (117). Thus, LC3 is conventionally regarded as a marker of autophagy (352). However, LC3 processing has recently been implicated in autophagy-

independent- but ER stress-mediated cell death mechanisms such as cytoplasmic vacuolation death and paraptosis (155-157). These autophagy-independent cell death mechanisms are characterized by the absence of autophagosomes and a failure to increase the expression of other autophagy markers.

Our knowledge of the mechanisms controlling these various forms cell death remains incompletely understood. We hypothesize that the AhR may be a regulator of cell survival in the harsh environment of the lung, and thus be capable of attenuating alternative cell death mechanisms- including autophagy and/or ER stress- in lung structural cells. These lung structural cells include alveolar epithelial cells and fibroblasts, which are responsible for gas exchange and the synthesis of the extracellular matrix necessary to maintain lung structure, respectively. We have used CS as a relevant environmental toxicant to understand how the AhR regulates lung structural cell death. Using an *in vitro* model of CS exposure together with AhR-deficient lung cells, we show that AhR deficiency increases ER stress by a mechanism that is likely independent of autophagy. Our data support that the AhR is critically important in promoting lung structural cell survival.

3.3 MATERIALS AND METHODS

Chemicals

All chemicals were purchased from Sigma-Aldrich (St. Louis, MO) unless otherwise indicated. Bafilomycin A1 was purchased from Enzo Life Sciences (Farmingdale, NY). Actinomycin D (ActD) was purchased from Biomol (Plymouth Meeting, PA). CH-223191 (1-Methyl-N-[2-methyl-4-[2-(2-methylphenyl) diazenyl] phenyl-1H-pyrazole-5-carboxamide) is from Tocris Bioscience (Minneapolis, MN).

Cell Culture

Primary Mouse Lung Fibroblasts (MLFs) were generated and cultured from AhR wild-type (*Ahr*$^{+/+}$), AhR heterozygous (*Ahr*$^{+/-}$) and AhR deficient (*Ahr*$^{-/-}$) male and female C57BL/6 mice (Jackson Laboratory, Bar Harbor, ME) as previously described (194, 353). Unless otherwise indicated, fibroblasts were plated at a density of 10,000 cells/cm^2.

MLE12 cells, a distal bronchiolar and alveolar epithelial cell line (ATCC, Manassas, VA) (354), were cultured in DMEM-F12 as described (194).

A549 cells were used to generate A549-AhR^{ko} cells using a zinc finger nuclease technology targeting the AhR; these cells were cultured in DMEM as described (217, 355).

All cells were maintained at 37°C, incubated in humidified 5% CO_2, 95% air and all experiments were conducted following 12-24h in serum-free media.

Preparation of Cigarette Smoke Extract (CSE)

Research grade cigarettes (3R4F) with a filter were obtained from the Kentucky Tobacco Research Council (Lexington, KT) and CSE was generated as previously described (97, 160, 356, 357). Briefly, smoke from one cigarette was bubbled into 10 ml of serum free-media and subsequently

passed through a 0.45μm sterile filter (25-mm Acrodisc; Pall Corp., Ann Arbor, MI). An optical density of 0.65 (320 nm) was considered to represent 100% CSE. This CSE preparation was diluted to 2% in the appropriate serum free-media.

Imaging Flow Cytometry

Cells were fixed with 4% paraformaldehyde (PFA) for 20 min, washed and resuspended in PBS 1x with 0.2% bovine serum albumin (BSA) (Fisher BioReagents) at 4^0C overnight. Cells were then permeabilized using 1:10 Perm/Wash buffer (BD Biosciences, Mississauga, Ontario). Anti-LC3B mAB (1:100; MBL International, Woburn MA) was then added to the samples for 30 min. Cells were next incubated with Alexa-Flour 488 goat anti-mouse (1:1000; Invitrogen) secondary antibody for 30 min. Cells were then washed and re-suspended in PBS. Images were acquired using the ImageStreamX (Amnis, Seattle, Washington). Samples were gated to remove debris, and at least 10,000 events per sample were then analyzed using the IDEAS 6.1 software. The bright detail intensity (BDI) was used to evaluate LC3 punctae.

Transfection

MLE12 cells were transiently transfected with 60 nM small interfering (si)RNA against *Ahr* (Santa Cruz) or non-targeting control siRNA (Santa Cruz) according to the manufacturer's instructions. Six hrs after the transfection, 1 mL of DMEM-F12 medium containing antibiotics/ antimycotics was added to the cells overnight. The following day the cells were switched to serum free-media prior to treatment with CSE for 3–24h.

Western Blot

Total cellular protein was prepared using RIPA lysis buffer supplemented with a protease inhibitor cocktail (Roche Diagnostics, Germany) and protein quantitation performed with the BCA method (Pierce, Rockford, IL). Five to forty μg of cellular proteins were fractionated on SDS-PAGE gels and electroblotted onto immunoblot PVDF membrane (Bio-Rad Laboratories, St. Laurent, QC, Canada). Incubation with a primary antibody (Table 3.1) followed by the HRP-conjugated secondary antibody was used to assess changes in protein levels. Protein levels were visualized by enhanced chemiluminescence (ECL) and detected using a gel documentation system (Bio-Rad). In instances where protein expression became saturated during detection, the image acquired at the exposure time immediately prior to saturation was utilized for analysis. Densitometry was performed using ImageJ.

Analysis of Gene Expression

Total RNA was isolated from media or CSE-treated cultured cells using a Qiagen miRNeasy kit (Qiagen Inc., Hilden, Germany). RNA samples were diluted to a concentration of 10 ng/μl. Following dilution, reverse transcription of total RNA was carried out in a 25-μl reaction mixture by iScript II^{TM} Reverse Transcription Supermix (Bio-Rad Laboratories, Mississauga, ON, Canada) at 25°C for 5 min, at 42°C for 30 min and at 85°C for 5 min. Quantitative PCR (qPCR) was performed with 1 μl cDNA from the media and CSE-treated cultured cells and 0.5μM primers added in Ssofast^{TM} Eva Green® Super-mix (Bio-Rad). PCR amplification was performed using a CFX96 Real-Time PCR Detection System (Bio-Rad) as described (194). Gene expression was analyzed using the $^{\Delta\Delta}$Ct method following normalization to the housekeeping gene β-actin. Primer sequences utilized for qPCR are listed in Table 3.2. *Xbp-1* mRNA splicing was assessed by PCR,

which was carried out in a 25µl reaction mixture consisting of 1µl of 10µM forward mouse Xbp-1 primer, 1µl of 10µM reverse mouse Xbp-1 primer, 2µl cDNA, 12.5µl 2x DreamTaq Green PCR Mastermix (Thermo Fisher Scientific) and 8.5µl of nuclease free water at 95°C for 15 sec, 50°C for 30 sec, and 72°C for 34 sec for a total of 35 cycles. Samples were then run using gel electrophoresis on a 3% agarose gel for 1.5h. The primers utilized for Xbp-*1* PCR flank the 26-nucleotide intron that is removed following IRE1α activation to yield sXbp-1*;* the sequence was: (forward) CCT TGT GGT TGA GAA CCA and (reverse) GTG TCA GAG TCC ATG GGA (358).

Transmission Electron Microscopy (TEM)

Following treatment with media or 2% CSE for 8h, *Ahr*$^{-/-}$ *and Ahr*$^{+/-}$ MLFs were trypsinized and centrifuged to form a pellet. Supernatant was removed and the pellets were fixed in 2.5% glutaraldehyde (Electron Microscopy Sciences, Hatfield, PA) overnight at 4^0C followed by incubation with 1% osmium tetroxide (Mecalab, Montreal, QC, Canada) and 1.5% potassium ferrocyanide (Fisher Scientific, Ottawa, ON, Canada) for 1h at 4^0C. Cells were washed and dehydrated in a graded series of ethanol/deionized water, infiltrated with a 1:1 and 3:1 Epon 812 (Mecalab, Montreal, QC, Canada) ethanol mixture for 30 min followed by 100% Epon 812 for 1h. Finally, the cells were embedded in fresh 100% Epon 812 and left to polymerize overnight at 60^0C. Blocks were cut in 100 nm ultrathin sections with an Ultracut E ultramicrotome (Reichert Jung, Cambridge, UK) and transferred onto 200-mesh copper grids (Electron Microscopy Sciences, Hatfield, PA). Sections were post-stained first with 4% aqueous uranyl acetate (Electron Microscopy Sciences, Hatfield, PA) followed by Reynold's lead citrate (Fisher Scientific, Ottawa, ON, Canada). Samples were imaged with a FEI Tecani-12 transmission electron microscope (FEI, Hillsboro, OR) operating at an accelerating voltage of 120 kV equipped with an XR-80C AMT, 8-

megapixel CCD camera.

Determination of *Chop* mRNA Stability

Ahr$^{-/-}$ and *Ahr*$^{+/-}$ MLFs were treated with 2% CSE for 2h, followed by treatment with 1μg/mL ActD for 0.5h, 2h and 6h. ActD treatment times were chosen based on the half-life of *Chop* mRNA, which ranges between 0.5h and 5h (359-361). Following treatments, *Chop* mRNA expression was assessing using qPCR as described above.

Statistical Analyses

Statistical analysis was performed using Prism 6-1 (La Jolla, CA). A two-way analysis of variance (ANOVA) was followed by a Bonferroni or Tukey multiple comparisons test. In all cases, a p-value < 0.05 is considered statistically significant.

3.4 RESULTS

AhR deficiency increases LC3 processing in lung structural cells

LC3 processing is a feature of both autophagic and ER stress-mediated cell death. Therefore, we first analyzed LC3 processing by western blot in MLE12 cells after we knocked-down AhR protein via siRNA (siAhR) (Fig. 3.1A). AhR knock-down in MLE12 cells resulted in a significant increase in LC3II in response to CSE relative to cells transfected with the control siRNA (siCtrl) (Fig. 3.1B). In both the untreated- and CSE-treated *Ahr*$^{-/-}$ MLFs, LC3 processing to LC3II was significantly higher compared to the *Ahr*$^{+/-}$ MLFs (Fig. 3.1C). Using ImageStream®, we analyzed cellular LC3 punctae using the bright detail intensity (BDI). A high BDI is reflective of cells with numerous, bright LC3 punctae, a parameter also associated with heightened LC3 expression (108). CSE-treated *Ahr*$^{-/-}$ MLFs showed the highest proportion of LC3 BDI-high cells (27.4%; Fig. 3.1D). To complement these findings, we also evaluated LC3 in the human alveolar epithelial cell line A549, whereby AhR expression was eliminated by zinc finger nuclease technology (355). In both untreated- and CSE-exposed A549-AhR^{ko} cells, LC3 processing to LC3II was significantly higher compared to the A549 Parent cells (Fig. 3.2A). A549-AhR^{ko} cells also had increased LC3 punctae as supported by a higher proportion of LC3 BDI-high cells (Fig. 3.2B). CSE-treated A549-AhR^{ko} also showed the highest proportion of LC3 BDI-high cells (70.3%; Fig. 3.2B). Collectively, these data support that reduced AhR expression (*i.e.* in both knock-down and knock-out models) increases LC3 expression and processing in lung structural cells.

Upregulation of LC3II in AhR-deficient lung cells is not due to impaired autophagic flux

LC3 processing is well-recognized as a hallmark of autophagy. Therefore, we next sought

to determine if the increased LC3II in CSE-treated AhR-deficient cells was due to impairment in autophagic flux. We first evaluated the expression of p62 (118). Although CSE increased p62 protein expression in the *Ahr*$^{+/-}$ MLFs, there was no significant difference in p62 expression between CSE-exposed *Ahr*$^{-/-}$ and *Ahr*$^{+/-}$ cells (Fig. 3.3A). There was also no difference in p62 expression between CSE-treated A549-AhR^{ko} and AhR Parent cells (Fig. 3.3B). To establish if the AhR regulates autophagic flux we utilized Bafilomycin A1, an inhibitor of autophagosome-lysosome fusion (362). We assessed LC3II protein in A549-AhR^{ko} and AhR Parent cells treated with CSE in the presence or absence of Bafilomycin A1. Although Bafilomycin A1 induced a significant increase in LC3II expression, LC3II in the untreated and CSE-treated A549-AhR^{ko} cells was significantly less than when in the presence of Bafilomycin A1 (Fig. 3.3C). Taken together, these results suggest that an impairment in autophagic flux does not explain the heightened LC3 processing in AhR-deficient cells.

Increased LC3II in AhR-deficient lung structural cells is not due to an upregulation of upstream autophagy-related proteins

Given that LC3II was elevated in the absence of AhR, we reasoned that this might be accompanied by an increase in the upstream autophagic markers ULK1, ATG5-12 and ATG3. Of these, only ULK1 expression changed in response to CSE in *Ahr*$^{+/-}$ MLFs (Fig. 3.4A- left panel). There was no significant difference in the expression ATG5-12 or ATG3 (Fig. 3.4B-C- left panels). Similar results were obtained in A549 cells, where there was no significant difference in the expression of these autophagy-related proteins either in response to CSE or based on AhR expression (Fig. 3.4A-C- right panels). Collectively, these results support that the elevated LC3 processing in AhR-deficient lung structural cells cannot be explained by an upregulation of

upstream autophagic machinery.

Elevated LC3II in AhR-deficient lung structural cells is not due to an upregulation of autophagic genes

The canonical AhR signaling pathway involves the translocation of the AhR to the nucleus and subsequent alterations in gene expression due to DRE-dependent transcription (183, 292). We therefore reasoned that the AhR attenuation of LC3 processing may be related to its function as a transcription factor. Thus, we chose for analysis autophagic markers known to be regulated at the transcriptional level, which included *Gabarapl1, Beclin-1* and *Lc3b* (363). However, there was no significant difference in expression of *Gabarapl1* (Fig. 3.5A), *Beclin-1* (*Becn1*) (Fig. 3.5B) or *Lc3b* mRNA (Fig. 3.5C) between the $Ahr^{-/-}$ and $Ahr^{+/-}$ MLFs (Fig. 3.5- left panels) or between A549-AhR^{ko} and A549 Parent cells (Fig. 3.5-right panels). To ensure that the lack of induction of the autophagy genes was not due to impaired AhR activation by CSE, we assessed levels of *Cyp1a1* mRNA, whose induction by CSE is dependent on the AhR (194). These data show that in both MLFs and A549 cells, there was significant upregulation in *Cyp1a1* mRNA only in CSE-treated AhR-expressing cells (Fig. 3.5D). Therefore, we conclude that the AhR does not transcriptionally-regulate these autophagy-related genes despite strong activation by CSE.

AhR deficiency results in ER stress

In an attempt to establish whether the elevated LC3 processing in $Ahr^{-/-}$ MLFs was associated with autophagy, we assessed transmission electron micrographs (TEM) for the presence of autophagosomes, a technique/read-out considered to be the gold standard for validating autophagy (364). However, there was a distinct absence of an accumulation of autophagosomes in

the *Ahr*$^{-/-}$ MLFs, although some autophagosomes (black arrowheads) were observed (Fig. 3.6A). What was striking was the existence of extensive dilation in the rough ER (white arrowheads) only in the *Ahr*$^{-/-}$ MLFs (Fig. 3.6A). This is a morphological hallmark of ER stress that occurs in response to an accumulation of misfolded proteins (131). Other features of ER stress-mediated cell death include the accumulation of ubiquitinated proteins, UPR activation and the upregulation of UPR targets. We also observed a dramatic increase in ubiquitinated proteins in *Ahr*$^{-/-}$ MLFs that was further exacerbated following CSE exposure (Fig. 3.6B). Treatment of MLFs with the proteasome inhibitor MG-132 (10μM for 2 hours) was used as a positive control for detecting ubiquitinated proteins by western blot (data not shown).

We next assessed the expression of proteins involved in the three branches of the UPR signaling cascade. These included the phosphorylated form of the eukaryotic translation initiation factor 2α (p-eIF2α), activating transcription factor 4 (ATF4), inositol-requiring enzyme 1α (IRE1α) and activating transcription factor 6 (ATF6). In the first UPR branch, protein kinase RNA-like endoplasmic reticulum kinase (PERK) activation induces the phosphorylation of eIF2α. This phosphorylation event results in the general inhibition of translation (132), while favoring the translation of the ATF4 (133). In the second UPR branch, IRE1α activation triggers the splicing of X-box binding 1 (*sXbp-1*) mRNA. In the third UPR branch, ATF6 activation results in its proteolytic cleavage at the golgi apparatus, yielding a 50 kDa ATF6 subunit (C-ATF6). There was little perceptible difference in p-eIF2α, ATF4 or C-ATF6 in response to CSE or between *Ahr*$^{-/-}$ and *Ahr*$^{+/-}$ MLFs (Fig. 3.6C); only IRE1α showed a perceptible increase in *Ahr*$^{+/-}$ MLFs exposed to CSE (Fig. 3.6C). However, there was no change in *sXbp-1* (Fig. 3.6D). Treatment of MLFs with the ER-stress inducers- Tunicamycin (7μg/mL for 1 hour) and Thapsigargin (1μM for 4 hours)- were used as positive controls for detecting these UPR proteins by western blot (data not shown).

These data support that the *Ahr*$^{-/-}$ MLFs do not exhibit activation of any of the three classical UPR branches despite features of ER stress.

ER stress-mediated cell death is dependent on the upregulation of UPR targets CHOP and growth arrest and DNA damage-inducible gene 34 (GADD34) (136-138, 361). CHOP expression was significantly higher in the CSE-treated *Ahr*$^{-/-}$ MLFs compared to the CSE-treated *Ahr*$^{+/-}$ MLFs (Fig. 3.6E). CHOP expression was also significantly higher in *Ahr*$^{+/-}$ MLFs that had been treated with the pharmacological AhR antagonist CH-223191 (Fig. 3.6F). This suggests that AhR activation is necessary to attenuate this increase in CHOP. GADD34 was also significantly higher in *Ahr*$^{-/-}$ MLFs (Fig. 3.6G). Collectively, these data support that the elevated LC3 processing caused by AhR deficiency is associated with ER stress and likely occurs through an autophagy-independent mechanism.

Increased CHOP in *Ahr*$^{-/-}$ MLFs is not due to enhanced transcription of *Chop* mRNA or altered *Chop* mRNA stability

We next sought to address the mechanism for the elevated CHOP protein expression in the *Ahr*$^{-/-}$ MLFs. We first focused on mRNA expression, but there was no significant difference in *Chop* mRNA between the untreated or CSE-treated *Ahr*$^{-/-}$ and *Ahr*$^{+/-}$ MLFs (Fig. 3.7A). As we have previously shown that the AhR controls cyclooxygenase-2 (COX-2) protein by destabilizing *Cox-2* mRNA (194), we next assessed if the lower CHOP protein expression in the *Ahr*$^{+/-}$ MLFs was a consequence of AhR-mediated mRNA instability. Therefore, an ActD-chase experiment was conducted whereby we treated cells with CSE followed by ActD for 0.5, 2 or 6 hours. Although there was significant *Chop* mRNA degradation by 6h after ActD, there was no differences in the rate of *Chop* mRNA degradation observed between *Ahr*$^{-/-}$ and *Ahr*$^{+/-}$ MLFs (Fig. 3.7B). Our data

collectively show that AhR deficiency results in autophagy-independent LC3 processing and ER stress that is characterized by ER dilation, elevated ubiquitinated proteins and increased CHOP and GADD34 protein expression.

3.5 TABLES

Table 3.1. Antibodies used for western blot.

Primary Antibody	Dilution	Company	Catalog Number
AhR	1:5000	Enzo Life Sciences	**BML-SA210**
Actin	1:50000	Millipore	**MAB1501**
LC3B	1:1000	Cell Signaling	**3868**
ULK1	1:1000	Cell Signaling	**8054**
ATG5-12	1:1000	Cell Signaling	**12994, 4180**
ATG3	1:1000	Cell Signaling	**3415**
p62	1:1000	Cell Signaling	**5114**
p-EIF2α	1:1000	Cell Signaling	**3398**
ATF4	5µg/mL	Sigma Aldrich	**WH0000468M1**
IRE1α	1:1000	Cell Signaling	**3294**
ATF6	1:1000	Santa Cruz	**SC-166659**
CHOP	1:1000	Cell Signaling	**2895**
GADD34	1:250	Santa Cruz	**SC-8327**
Ubiquitin	1:1000	Cell Signaling	**3933**

Table 3.2. Primer sequences used for qRT-PCR.

Target Gene	Species	Forward Sequence	Reverse Sequence
Beclin-1	mouse	CTT-GGA-GGA-GGA-GAG-GCT-GA	TGT-GGA-AGG-TGG-CAT-TGA-AG
Beclin-1	human	AAC-CTC-AGC-GGA-AGA-CTG-AA	GAC-GTT-GAG-CTG-ACT-GTC-CA
Gabarapl1	mouse	GAT-GCC-TGC-AAT-GTG-AGA-GC	AAG-CAG-CGG-AGA-GGA-AAC-AG
Gabarapl1	human	GGT-CCC-CGT-GAT-TGT-AGA-GA	GGA-GGG-ATG-GTG-TTG-TTG-AC
Lc3b	mouse	CGA-TAC-AAG-GGG-GAG-AAG-CA	ACT-TCG-GAG-ATG-GGA-GTG-GA
Lc3b	human	ACA-CAG-CAT-GGT-CAG-CGT-CT	TTT-CAT-CCC-GAA-CGT-CTC-CT
Cyp1a1	human	TTG-GTC-TCC-CTT-CTC-TAC-ACT-CTT-GTA-ATA	GCA-AGC-TCA-ATG-CAG-GCT-AGA-ATA-G
Cyp1a1	mouse	CCT-TAC-CAA-GTG-CTA-GGA-TAC-AGT-CAT	CAG-TAA-AGA-AGA-GAG-ACC-AAG-AGC-TGA-T
Chop	mouse	AAC-AGA-GGT-CAC-ACG-CAC-AT	ACT-TTC-CGC-TCG-TTC-TCC-TG
β -Actin	mouse/human	CTA-CAA-TGG-CTG-CGT-GTG	TGG-GGT-GTT-GAA-GGT-CTC

3.6 FIGURES

Figure 3.1

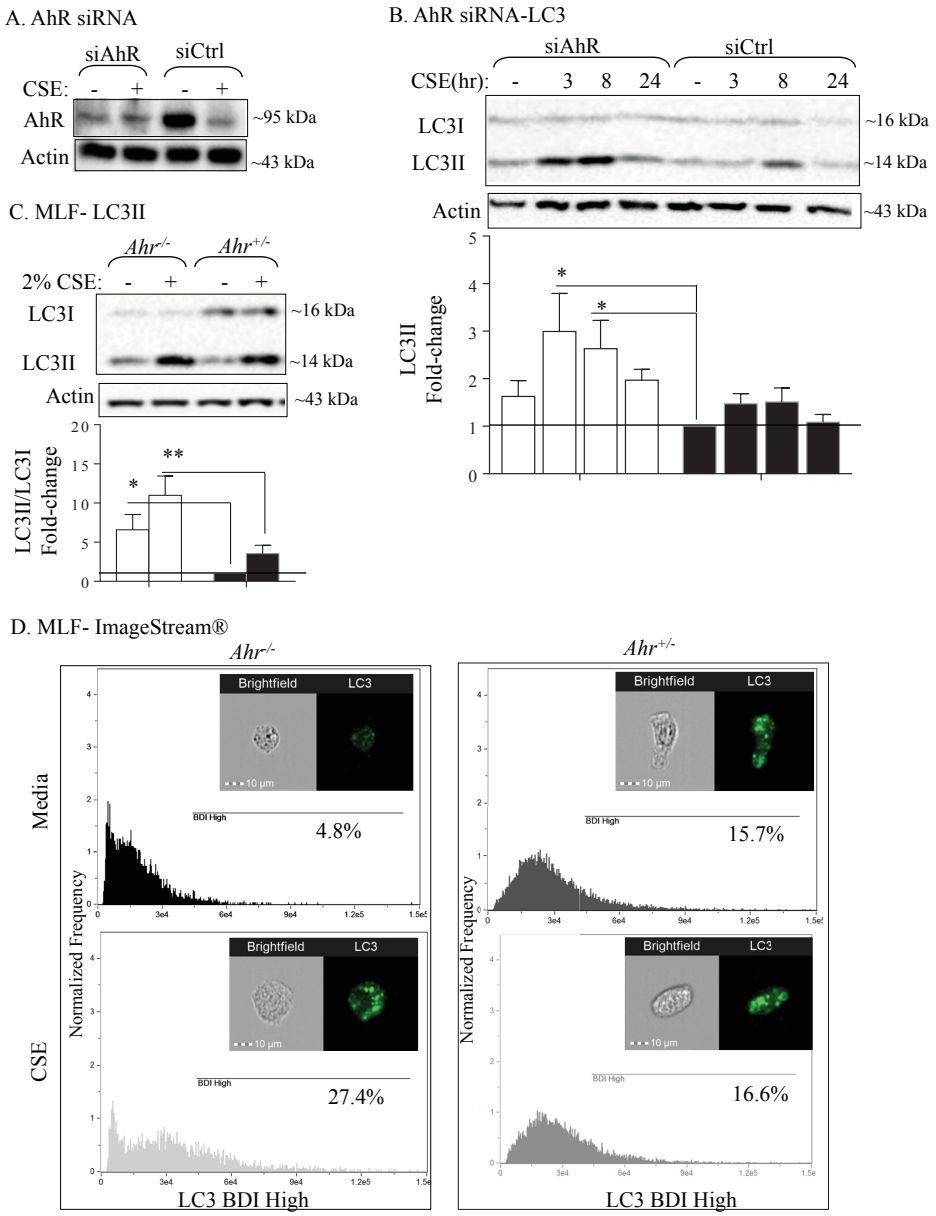

Figure 3.1. AhR deficiency increases LC3 processing in lung structural cells. (A) AhR siRNA: Representative western blot of AhR knock-down in MLE12 cells. **(B)** AhR siRNA-LC3: AhR knock-down in the MLE12 cells leads to higher LC3II expression following treatment with CSE. Untreated media-only negative controls are denoted by the absence of CSE (-). Representative western blot is shown, and results are expressed as mean ± SEM (n=4-6). Data was analyzed using a 2-way ANOVA followed by Tukey multiple comparisons test. **(C)** MLF-LC3II: There was significantly more LC3I to LC3II processing in CSE-treated *Ahr*$^{-/-}$ MLFs relative to the CSE-treated *Ahr*$^{+/-}$ MLFs. Untreated media-only negative controls are denoted by the absence of CSE (-). Representative western blot is shown (n=14 replicate experiments). Data was analyzed using a 2-way ANOVA followed by Bonferroni correction for multiple comparisons. **(D)** MLF-ImageStream®: Imaging flow cytometry was used to assess LC3 expression in *Ahr*$^{+/-}$ and *Ahr*$^{-/-}$ MLFs; a representative image shows there is more LC3 punctae (green) in CSE-exposed *Ahr*$^{-/-}$ MLFs (27.4% of population with LC3 BDI High).

Figure 3.2

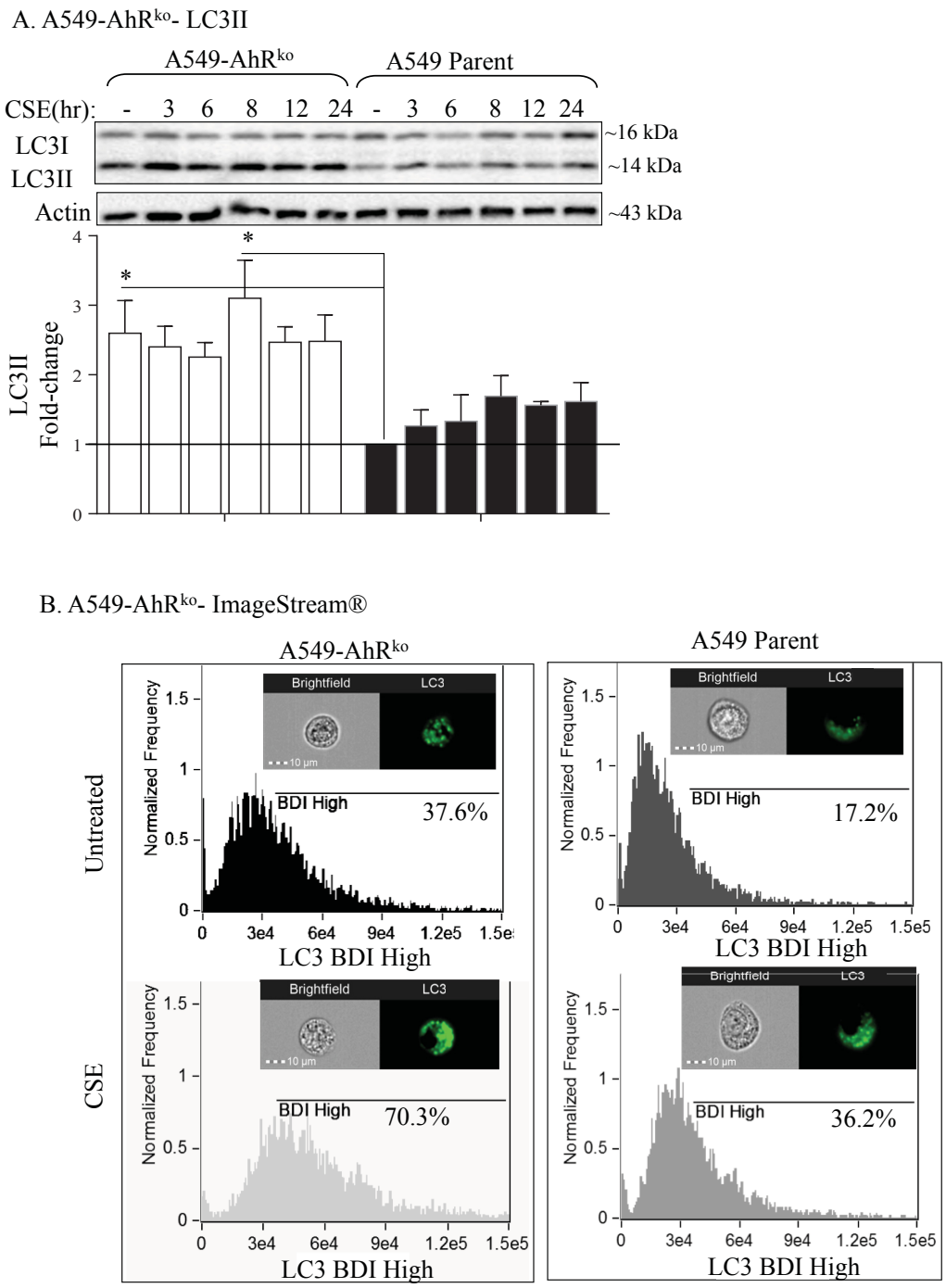

Figure 3.2. AhR deficiency increases LC3 processing in human alveolar epithelial cells. (A) A549-AhR^{ko}- LC3II: There is significantly more LC3II in the A549-AhR^{ko} both at baseline and upon treatment with CSE for 8h. Untreated media-only negative controls are denoted by the absence of CSE (-). Representative western blot is shown (n=4 replicate experiments). Results are expressed as mean ± SEM. Data was analyzed using a 2-way ANOVA followed by a Tukey multiple comparisons test. **(B)** A549-AhR^{ko}-ImageStream®: Imaging flow cytometry was used to assess LC3 expression, which was quantified by assessing the proportion (%) of cells within each treatment that exhibited a high LC3 bright detail intensity (BDI High). A representative cellular image is shown. CSE-treated A549-AhR^{ko} cells exhibit a markedly elevated proportion of LC3 BDI High cells relative to the CSE-treated A549 Parent cells (70.3% and 36.2% of population with LC3 BDI High, respectively).

Figure 3.3

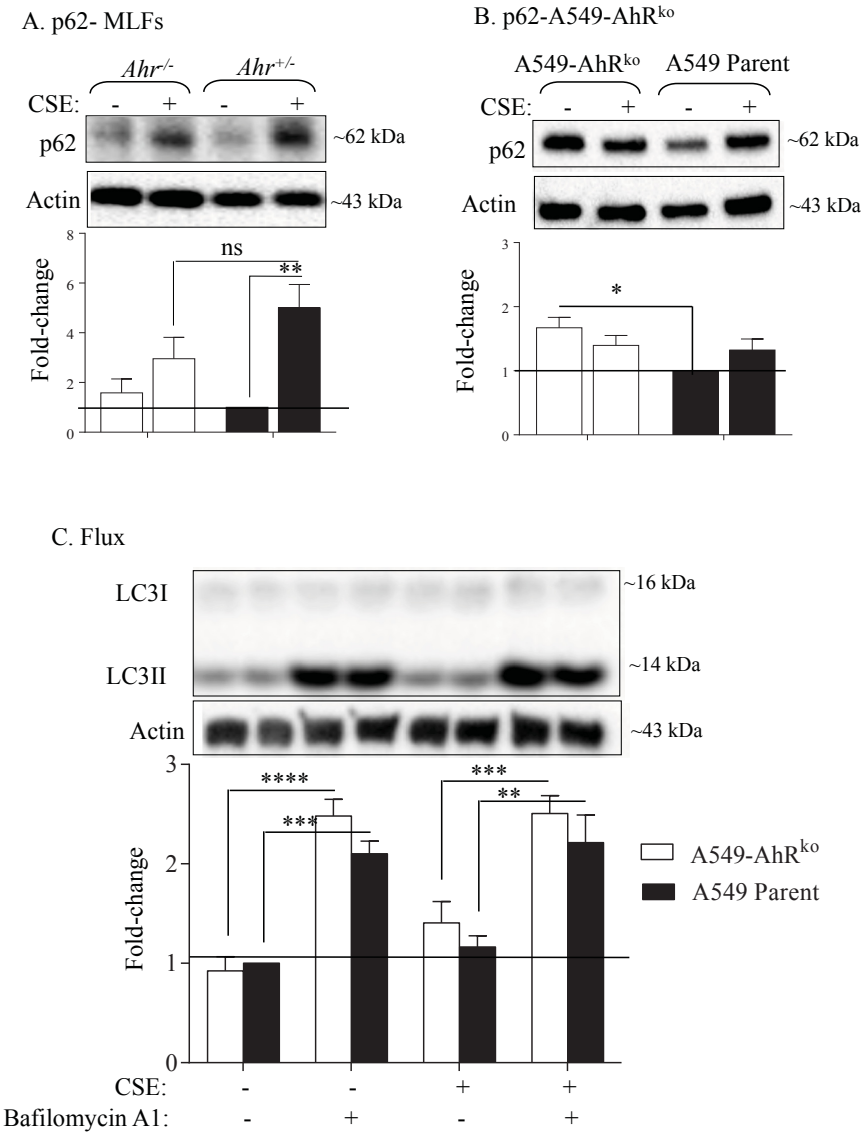

Figure 3.3. Increased LC3II in AhR-deficient lung structural cells is not due to impaired autophagic flux. (A) p62- MLFs: Expression of p62 was higher in the *Ahr*$^{+/-}$ MLFs upon treatment with CSE, but there was no difference in p62 expression between CSE-treated *Ahr*$^{+/-}$ and *Ahr*$^{-/-}$ MLFs. Representative western blot of n=5 independent experiments is shown. **(B)** p62-A549-AhR^{ko}: There was no difference in p62 expression between the CSE-treated A549-AhR^{ko} and A549 Parent cells. Representative western blot of n=4 independent experiments is shown. Results are expressed as mean ± SEM. Data was analyzed using a 2-way ANOVA followed by Bonferroni correction for multiple comparisons. **(C)** Flux: A549-AhR^{ko} and A549 Parent cells were treated with 2% CSE for 8h with or without Bafilomycin A1 for an additional 2h. For both the A549-AhR^{ko} and A549 Parent cells, there was a significant increase in LC3II upon the addition of Bafilomycin A1. LC3II expression in the untreated or CSE-treated cells was significantly less than in the presence of Bafilomycin A1. Untreated media-only negative controls are denoted by the absence of CSE and Bafilomycin A1 (-). Western blot is representative of n=8 independent experiments. Results are expressed as mean ± SEM. Data was analyzed using a 2-way ANOVA followed by Tukey multiple comparisons test.

Figure 3.4

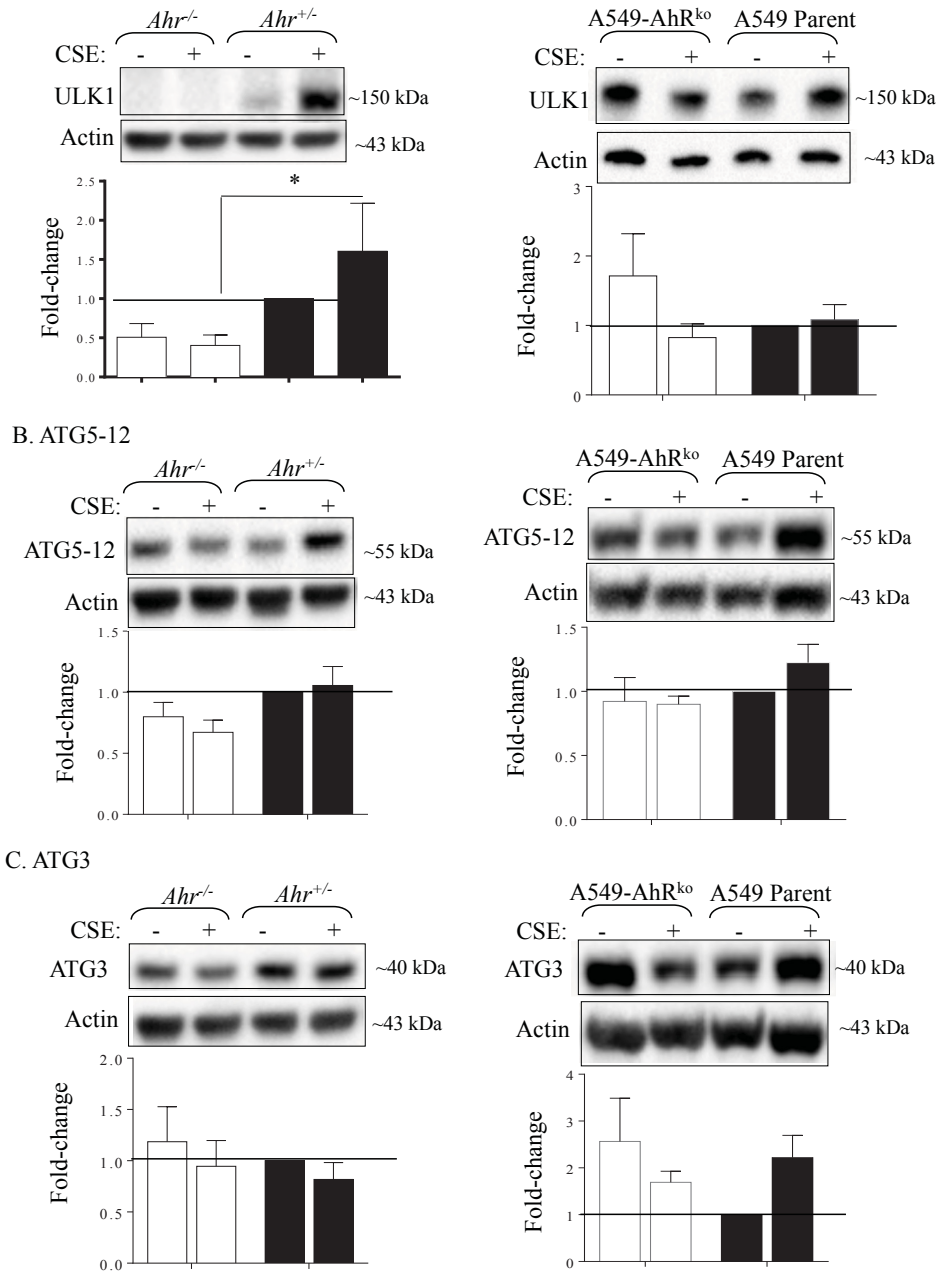

Figure 3.4. Increased LC3II in AhR-deficient lung structural cells is not due to increases in upstream autophagic machinery. (A) ULK1 expression was higher in the CSE-treated *Ahr*$^{+/-}$ MLFs relative to the CSE-treated *Ahr*$^{-/-}$ MLFs *(left panel)*, although there was no difference in ULK1 expression between the CSE-treated A549-AhR^{ko} and A549 Parent cells *(right panel).* There was no significant difference in the autophagy proteins ATG5-12 **(B)** or ATG3 **(C)** in *Ahr*$^{+/-}$ and *Ahr*$^{-/-}$ MLFs (*left panels*) or A549-AhR^{ko} and A549 Parent cells (*right panels*) exposed to 2% CSE for 8h. Results are expressed as mean ± SEM of n=5-10 independent experiments. Data was analyzed using a 2-way ANOVA followed by Bonferroni correction for multiple comparisons.

Figure 3.5

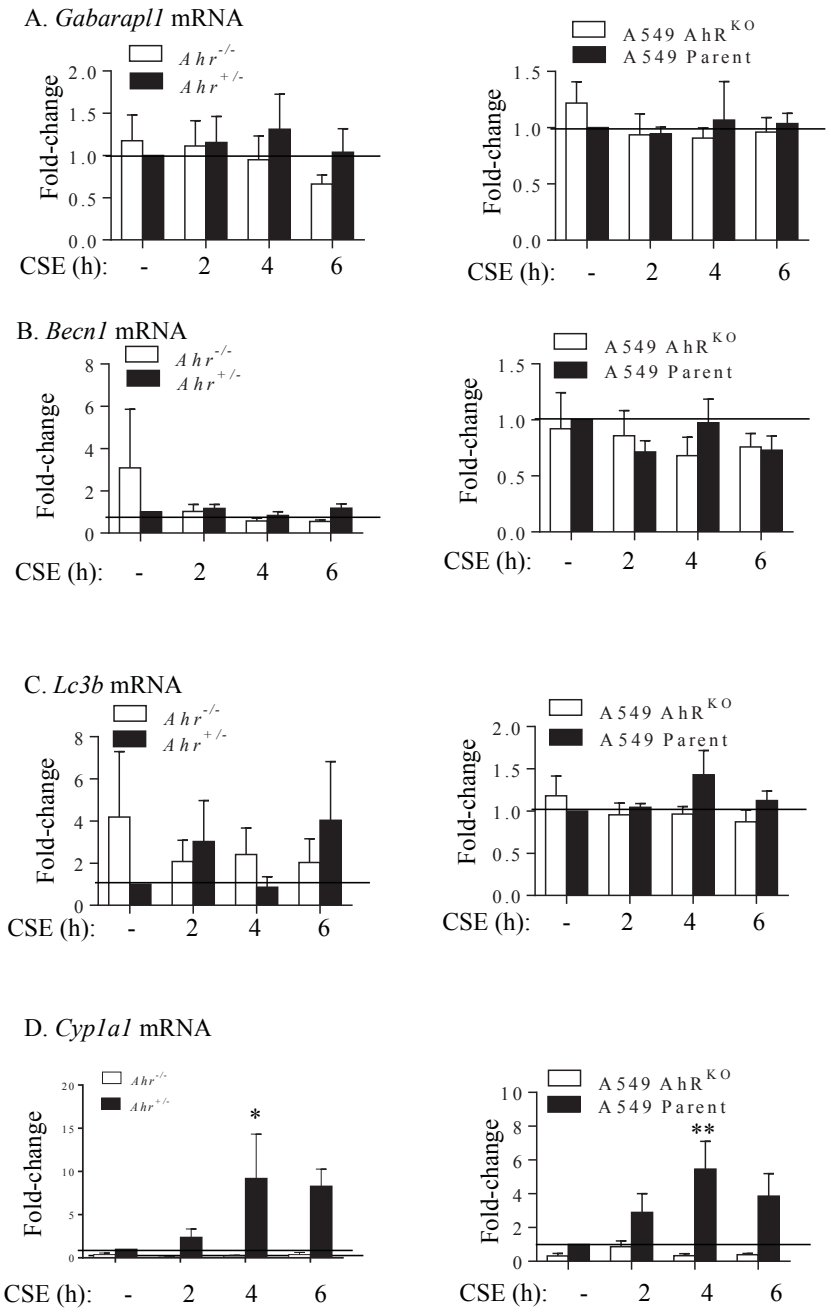

Figure 3.5. AhR does not alter the transcriptional upregulation of genes associated with autophagy. mRNA expression of **(A)** *Gabarapl1*, **(B)** *Beclin-1* (*Becn1*) and **(C)** *Lc3b* were assessed in *Ahr*$^{+/-}$ and *Ahr*$^{-/-}$ MLFs (*left panels*) and A549-AhR^{ko} and A549 Parent cells (*right panels*) following treatment with 2% CSE for 2, 4, and 6h. There was no difference in the expression of these autophagy genes at baseline or after treatment with CSE. **(D)** *Cyp1a1* mRNA: There was a significant increase in *Cyp1a1* mRNA expression in response to treatment with CSE only in *Ahr*$^{+/-}$ MLFs and A549 Parent cells. Results are expressed as mean ± SEM of n=4-7 independent experiments. Data was analyzed using a 2-way ANOVA followed by Bonferroni correction for multiple comparisons.

Figure 3.6

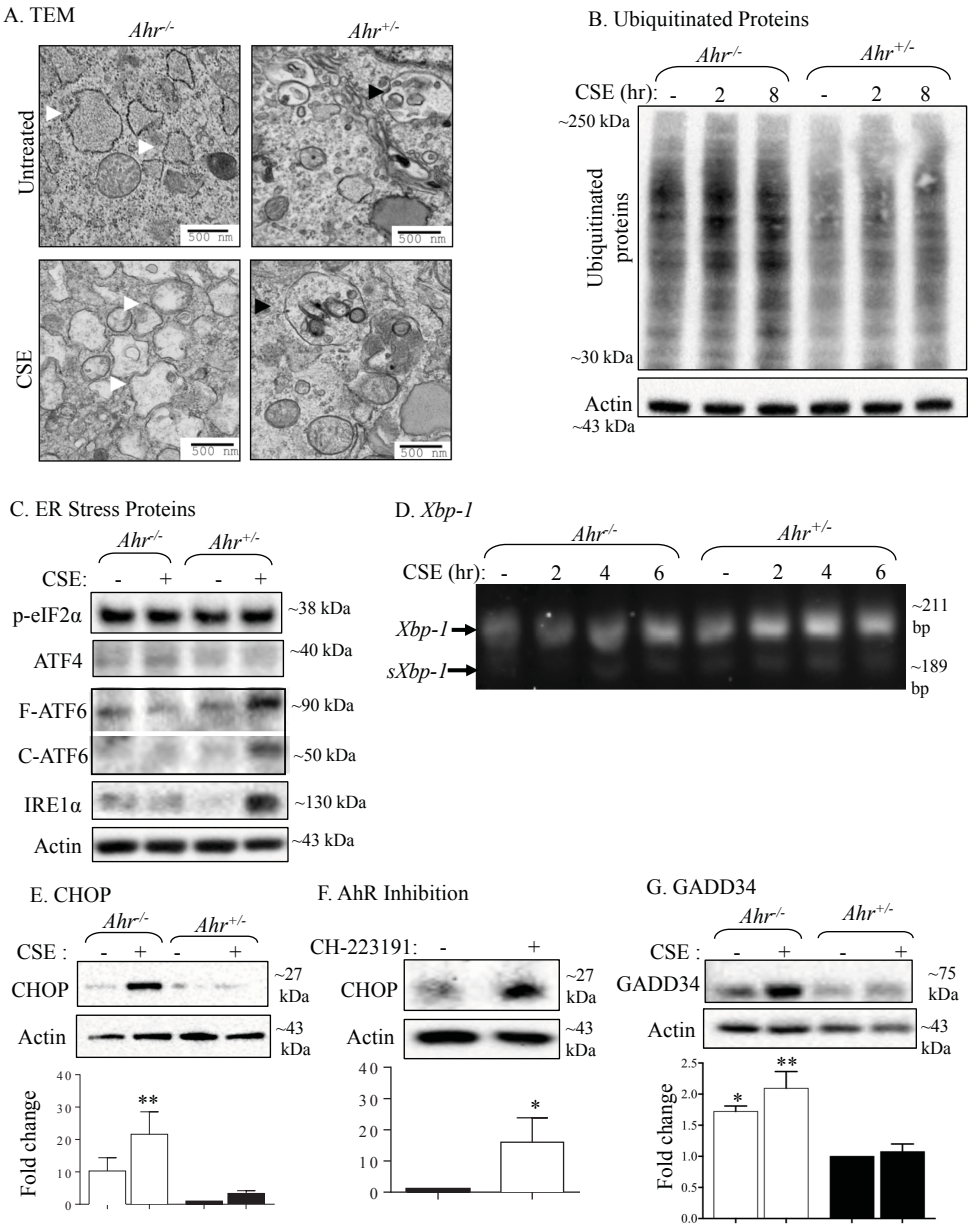

Figure 3.6. AhR deficiency causes ER stress and an accumulation of ubiquitinated proteins in lung fibroblasts. **(A)** TEM: Both untreated and CSE-treated *Ahr*$^{-/-}$ MLFs exhibit extensively dilated ER (white arrow heads) throughout the cytoplasm, which is not observed in the *Ahr*$^{+/-}$ MLFs (6800x magnification). **(B)** Ubiquitinated proteins were higher in the untreated and 2% CSE-treated *Ahr*$^{-/-}$ MLFs relative to the *Ahr*$^{+/-}$ MLFs (n=4). **(C)** ER Stress Proteins: Protein expression of p-eIF2α, ATF4, Full (F) and cleaved (C)-ATF6 and IRE1α were assessed by western blot following treatment with 2% CSE for 8h. Representative western blots are of at least n=4 independent experiments. **(D)** *Xpb-1*: *Xpb-1* mRNA splicing was assessed in the *Ahr*$^{-/-}$ and *Ahr*$^{+/-}$ following treatment with 2% CSE for 2, 4 and 6h. *Xbp-1* image is representative of n=4 independent experiments. **(E)** CHOP protein expression was significantly higher in CSE-treated *Ahr*$^{-/-}$ cells. **(F)** AhR Inhibition: *Ahr*$^{+/-}$ MLFs were treated with 10 μM of CH-223191 or equivalent volume of vehicle (DMSO) for 8h. CHOP protein expression was significantly higher in the CH-223191 treated cells. **(G)** GADD34 expression was significantly higher in both the untreated and CSE-treated *Ahr*$^{-/-}$ MLFs. Results are expressed as mean ± SEM of n=4-14 independent experiments. Data was analyzed using a 2-way ANOVA followed by Bonferroni correction for multiple comparisons.

Figure 3.7

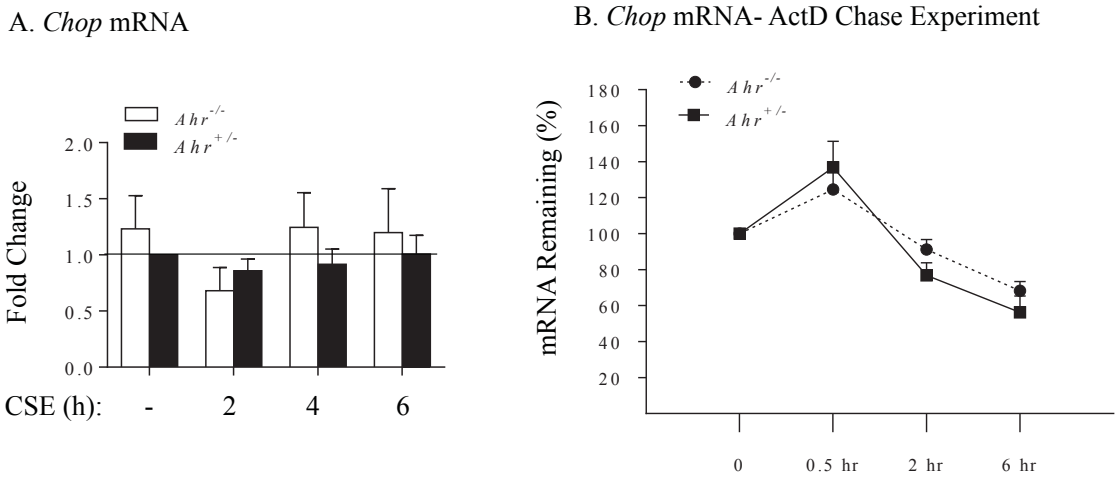

Figure 3.7. Elevated CHOP protein expression in *Ahr*$^{-/-}$ MLFs is not due to an upregulation of *Chop* mRNA or alterations in *Chop* mRNA stability. (A) *Chop* mRNA expression was assessed in *Ahr*$^{+/-}$ and *Ahr*$^{-/-}$ MLFs following treatment with 2% CSE for 2, 4, and 6h. There was no significant difference in *Chop* mRNA expression between *Ahr*$^{+/-}$ and *Ahr*$^{-/-}$ MLFs. Results are expressed as mean ± SEM of n=9 independent experiments. Data was analyzed using a 2-way ANOVA followed by Bonferroni correction for multiple comparisons. **(B)** *Chop* mRNA- ActD chase experiment: *Ahr*$^{+/-}$ and *Ahr*$^{-/-}$ MLFs were pre-treated with 2% CSE for 2h (time 0) followed by treatment with 1µg/mL of ActD for 0.5h, 2h and 6h. The amount of *Chop* mRNA remaining was significantly reduced in both genotypes following 6h ActD treatment, but there were no differences in mRNA expression between the genotypes. Results are expressed as mean ± SEM of n=4 independent experiments. Data was analyzed using a 2-way ANOVA followed by a Tukey's multiple comparisons test.

3.7 DISCUSSION

Although much is known about the toxicological response of the AhR to TCDD, considerably less is known about its physiological functions. Our lab has previously demonstrated that the AhR suppresses CS-induced apoptotic cell death in lung structural cells (161). Toxicant-induced cell death is mediated by a variety of inter-dependent cell death processes, including apoptosis, autophagy as well as ER stress. Herein, we show that the AhR controls LC3 processing in what is likely an autophagy-independent manner. Given that LC3 processing is also critical for ER stress-mediated cell death, we evaluated the contribution of the AhR towards controlling the ER stress response. Consistent with classic features of ER stress, cellular absence of the AhR was characterized by ER dilation, the accumulation of ubiquitinated proteins and an increase in the downstream UPR targets CHOP and GADD34. These features are largely consistent with two ER stress-mediated cell death mechanisms termed cytoplasmic vacuolation death and paraptosis (155-157). These processes are also characterized by the absence of autophagosomes and elevated LC3 processing- but without changes in the expression of other autophagy-related proteins (155, 157), features that are also prevented by AhR expression. As a whole, we consider these to be compelling evidence that the AhR controls a novel cell death mechanism consistent with ER stress-induced cytoplasmic vacuolation death.

We have not ruled out a role for the AhR in paraptosis however. The major distinguishing feature between cytoplasmic vacuolation death and paraptosis is that paraptosis is also associated with swelling of the mitochondria (157). Although not evaluated in the present study, we have previously reported that *Ahr*$^{-/-}$ MLFs exhibit a significant reduction in mitochondrial membrane potential following treatment with CSE (161). One feature of both cytoplasmic vacuolation death and paraptosis that is not consistent with absence of AhR expression is that these mechanisms do

not typically present with apoptotic-like changes or caspase activation (155, 157). We have also previously reported that the CSE-treated *Ahr*$^{-/-}$ MLFs exhibit morphological hallmarks of apoptosis and caspase 3 activation (161). This suggests that CSE-treated *Ahr*$^{-/-}$ MLFs may be undergoing "paraptosis-like" cell death based on a phenotype that does not entirely fit all of the hallmarks of paraptosis or apoptosis. This should not be entirely surprising however as the AhR likely regulates multiple cell death mechanisms that could be occurring simultaneously (107). Our results support that the AhR is a global regulator of cell death in lung structural cells.

It was also intriguing that ULK1 expression was significantly lower in the CSE-treated *Ahr*$^{-/-}$ MLFs. ULK1 is important for the initiation of the early autophagosomal membrane (116). Therefore, we thought that ULK1 expression would be higher in the CSE-treated *Ahr*$^{-/-}$ MLFs because of heightened autophagy. Recently, a noncanonical- and autophagy-independent role for ULK1 in the trafficking of proteins from the ER to the golgi has been described (150). Here, ULK1/2 was necessary for the formation of the coatomer protein complex II. This complex functions to bundle and transport newly synthesized proteins from the ER to the golgi apparatus. Thus, ULK1/2 deficiency may cause ER stress through the impairment of ER-to-golgi trafficking. Lower ULK1 in *Ahr*$^{-/-}$ MLFs is therefore consistent with ER stress.

It is also intriguing that CHOP protein expression was significantly higher after inhibition of AhR activation by the antagonist CH-223191 (194). This suggests that the AhR attenuation of CHOP requires the nuclear presence of the AhR or some other form of AhR activity. Currently we are not sure how the AhR controls CHOP expression, as this was not associated with transcriptional control of *Chop* mRNA or alterations in *Chop* mRNA stability. We speculate that the AhR regulation of CHOP may be occurring via a non-canonical signaling mechanism that requires AhR nuclear localization but is independent of AhR transcriptional activities. In line with this

observation, it has been previously reported that the AhR regulation of the antioxidant sulfiredoxin1 (287) and the acute phase response gene serum amyloid A (365) require AhR nuclear translocation but are independent of DNA-binding. A non-canonical AhR-mediated regulatory mechanism is also supported by our own data, particularly those that show elevated CHOP expression in the *Ahr*$^{-/-}$ MLFs occurring in the absence of the activation of the three UPR branches. It is possible that the AhR may attenuate CHOP expression via regulation of micro RNA (miRNA). We have shown that the AhR attenuation of CS-induced apoptosis is mediated via its regulation of mir-196a (217). Similarly, CHOP expression can be non-canonically regulated by miR-183-5p-mediated binding to the 3'-untranslated region of CHOP mRNA (366).

An alternative possibility is that elevated CHOP expression is a consequence of increased translation. GADD34 forms a complex with protein phosphatase 1c to dephosphorylate eIF2α, which drives the resumption of protein synthesis (131). Consistent with this, we observe elevated GADD34 expression in the *Ahr*$^{-/-}$ MLFs without an increase eIF2α phosphorylation or elevated ATF4 expression. Increased protein synthesis results in the production of reactive oxygen species due to oxidative protein folding in the ER (367). The pathogenic effects of increased protein synthesis in ER stressed cells is also illustrated by the finding that inhibition of translation with cycloheximide (CHX) protects against ER stress-induced cell death (155). Further studies to mechanistically evaluate how the AhR controls CHOP are ongoing.

In conclusion, our data support that the AhR is a regulator of lung structural cell survival by regulating various cell death mechanisms. We report for the first time that AhR deficiency predisposes cells to ER stress and autophagy-independent LC3 processing. It may be that subsequent exposure of AhR-deficient cells to an environmental toxicant such as CS overwhelms the clearing capacity of the ER, which ultimately results in heightened expression of the pro-death

ER stress mediator CHOP, further accumulation of ubiquinitated protein aggregates and ultimately cell death. These findings support that the AhR may maintain lung health by attenuating toxicant-induced death of lung structural cells. These findings could provide the foundation for the therapeutic targeting of the AhR for the treatment of toxicant-induced lung diseases characterized by excessive cell death, such as COPD.

AUTHOR CONTRIBUTIONS

Data curation and analysis: NG., KP., LC.; Funding acquisition: CJB; Investigation: NG., CJB; Methodology: NG.; Project administration: NG., CJB; Resources: J.M. Supervision: NG., CJB; Intellectual contributions: NG., CJB., QH., DHE., Manuscript writing, review and editing: NG., CJB.

4 Contribution to Original Knowledge

This work is the first to demonstrate that AHR expression is reduced in both the lung tissue and blood of COPD subjects, and that reduced systemic *AHR* expression is significantly correlated with reduced lung function in these individuals. We also experimentally demonstrate that AhR-deficiency drives the development of a CS-induced emphysema-like phenotype using a preclinical model of chronic CS exposure. Moreover, our findings are also the first to show that AhR-deficiency promotes ER-stress cell death, through a mechanism that appears to be autophagy-independent. Collectively, this data demonstrates an important role for the AhR in the homeostatic maintenance of lung health by attenuating the development of CS-induced emphysema.

5 General Discussion

Using a multi-disciplinary approach, our findings collectively support that reduced AhR expression promotes the pathogenesis of CS-induced emphysema, suggesting a protective role for the AhR in the maintenance of lung health. These observations may open up new avenues to manage a disorder for which no therapeutic options currently exist to stop or slow its progression. However, to harness the therapeutic potential of the AhR in the context of emphysema/COPD, it is first necessary to address an important dichotomy. The AhR is able to mediate protective effects in some contexts and pathogenic effects in others. This phenomenon may be a consequence of ligand-dependent differences, which can differentially influence several aspects of AhR activation, including the type of AhR signaling pathway induced (*i.e.* canonical or non-canonical). Alternatively, this phenomenon may also be the product of dysregulated AhR expression (*i.e.* over- or under-expressed relative to physiological conditions), which is observed in several different diseases. This general discussion explores these concepts in the context of our findings, as well as the broader implications of the AhR in COPD.

5.1 Dual Roles of the AhR: Protective vs Pathogenic

To date, our knowledge about the AhR is largely centralized around its ability to mediate the toxic effects of TCDD (181, 368). However, there is growing evidence to support the notion that the AhR is required for the maintenance of health. The AhR has been critically implicated in numerous physiological processes including xenobiotic metabolism, organ development and the regulation of immunity (see *1.3.4 "Outcomes of AhR signaling: Physiologic Functions of the AhR").* Furthermore, our data establish that the presence of the AhR dampens CS-induced lung damage by attenuating the development of an emphysema-like phenotype *in vivo* (**Fig. 2.1**). This dichotomy between TCDD and CS raises an important question: how can the AhR act as both a

mediator of toxicity (*i.e.* TCDD) and a protector of lung health (*i.e.* CS)?

One potential explanation is that ligand-dependent differences can induce both pathogenic or protective effects of the AhR. An important difference between TCDD and CS relates to its metabolism and clearance from the body. Whereas TCDD is persistent- with a half-life of approximately 7-12 years in humans (174, 175), CS is rapidly metabolized. One study reported that in humans, the half-life of nicotine, and its primary metabolite cotinine, is 2-3 hours and 17 hours, respectively (369). Thus, perhaps AhR-mediated pathogenicity vs protection in response to TCDD or CS, respectively, is a consequence of the chronicity of AhR activation. This possibility is further strengthened by observations that although TCDD, FICZ and ITE are all high affinity AhR agonists (164), FICZ and ITE are rapidly metabolized and non-toxic (370), whereas TCDD is persistent and toxic.

Another difference between TCDD and CS is that TCDD is a single compound whereas CS is a complex mixture of more than 5,000 chemicals including metals, gases, biological agents, and organic chemicals such as nicotine, PCDDs (*e.g.* TCDD) and PAHs (*e.g.* benzo[a]pyrene) (41-44). Although the AhR mediates carcinogenicity induced by components of CS, such as TCDD (182) and benzo[a]pyrene (305), it simultaneously protects against the pathogenic effects of CS in the lung. This demonstrates that CS is more than simply the sum of its parts, and that CS represents an AhR agonist that is structurally and functionally distinct from TCDD. This distinction is important to consider as different AhR ligands induce different conformational changes in the AhR protein upon binding (371). More specifically, the conformational changes observed in the AhR protein differ depending on whether or not the ligand induces canonical AhR activation ((371).

Therefore, another important consideration when comparing differences between TCDD and CS is the signaling mechanism through which the activated AhR exerts its effects. The canonical

AhR signaling pathway is characterized by 1) ligand binding, 2) AhR nuclear translocation, 3) AhR-ARNT heterodimerization and 4) AhR binding to the DRE in target genes to induce transcription of mRNA. It is well-established that TCDD-induced pathogenicity is mediated through the canonical AhR signaling pathway. This is supported by evidence that TCDD-induced toxicity requires not only AhR expression, but also AhR nuclear translocation (184) and DRE-binding (183). Furthermore, mice with reduced expression of ARNT (*i.e.* ARNT hypomorphs) are also largely protected against TCDD-induced toxicity (372). In contrast, many of the reported protective effects of the AhR against CS-induced injury are mediated through non-canonical AhR signaling mechanisms.

5.2 How may the AhR Protect against CS-induced Emphysema?

Although the mechanisms(s) through which the AhR protect against the pathogenesis of CS-induced emphysema are currently unknown, there is evidence to support that it may involve AhR-dependent regulation of non-canonical signaling mechanisms. The development of emphysema is mediated by several interdependent pathogenic processes in the lung, including inflammation, an anti-protease imbalance, oxidative stress and increased cell death. Given the complexity of emphysema pathogenesis, it is unlikely that the AhR attenuates these pathogenic processes (and thus the development of emphysema) via the regulation of a single signaling mechanism. Instead, it is more likely that the ability of the AhR to protect against the development of CS-induced emphysema involves the AhR-dependent regulation of a combination of these non-canonical signaling mechanisms.

5.2.1 Protein Interactions

One non-canonical mechanism through which the AhR may protect against CS-induced emphysema is via direct or indirect interactions with other proteins. The AhR can form dimers

with a variety of proteins that are involved in processes including cell cycle progression, cell death and immunity (209). For example, the AhR physically interacts with the NF*κB* transcription factor RelB (253, 373). An anti-inflammatory role for RelB is supported by findings that RelB attenuates CS-induced cyclooxygenase 2 (COX-2) expression (312). In line with this, the AhR-mediated suppression of CS-induced neutrophilia in the murine lung is associated with the nuclear retention of RelB (162). These AhR-RelB dimers have also been reported to initiate transcription of target genes via binding to a unique and DRE-independent response element termed the RelBAHRE (374). Collectively, these findings raise the possibility that the AhR-mediated nuclear retention of RelB may represent one way through which the AhR can suppress acute CS-induced inflammation. Perhaps this AhR-dependent regulation of RelB also contributes to the AhR attenuation of CS-induced macrophage infiltration that we observed in response to a chronic CS-regime (**Fig. 2.2**).

Another example of an AhR-dependent protein interaction is the regulation of Human Antigen R (HuR). HuR is an RNA-binding protein that functions to stabilize target mRNA when localized to the cytoplasm. The AhR attenuates CS-induced COX-2 expression via the nuclear sequestration of HuR, resulting in the destabilization and degradation of *Cox-2* mRNA *in vitro* (194). Moreover, another established target gene of HuR is *Mmp9* (375, 376). Thus, it is not unreasonable to postulate that similar to *Cox*-2, perhaps the elevated protease expression (*i.e.* increased MMP9:TIMP1 ratio [**Fig. 2.3**]) we observed in the lungs of the *Ahr*$^{-/-}$ mice is a consequence of the cytoplasmic shuttling of the HuR, resulting in enhanced *Mmp9* mRNA stability and expression. These examples serve to highlight that one of the mechanisms through which the AhR may be acting to attenuate the pathogenesis of CS-induced emphysema is via the regulation of, and interaction with, proteins not associated with canonical AhR signaling (*e.g* RelB and HuR).

As non-canonical protein interactions may contribute to the AhR attenuation of CS-induced

emphysema pathogenesis, we considered whether the AhR may be interacting with nuclear factor erythroid 2 (NRF2), a master regulator of antioxidants. This consideration is relevant based on our finding that the upregulation of the antioxidant SOD2 is impaired in CS-exposed *Ahr*$^{-/-}$ mice (**Fig. 2.4**). Although the AhR and NRF2 regulate several common antioxidant genes, such as *Nqo1* (287, 377), we speculate that the AhR regulation of antioxidant defenses in the murine lung is likely independent of NRF2. This assertion is supported by previous reports demonstrating no difference in either the expression or nuclear localization of NRF2 between AhR-deficient and AhR-expressing lung structural cells (161). However, it may be that dampened upregulation of the mitochondrial antioxidant SOD2 in the lungs of the CS-exposed *Ahr*$^{-/-}$ mice is an indirect result of mitochondrial dysfunction that ensues as a consequence of AhR ablation (161).

5.2.2 AhR-dependent Regulation of miRNA

Another non-canonical mechanism through which the AhR may attenuate the pathogenesis of CS-induced emphysema is via regulation of ncRNA. One type of ncRNA is miRNA, which target mRNA for degradation. A number of miRNA, including miR-196a, miR-96, miR-137 and miR-133b are significantly reduced in the lungs of *Ahr*$^{-/-}$ mice (216), illustrating that the AhR regulates miRNA expression in the lung. In line with this, the attenuation of CS-induced apoptosis *in vitro* is mediated by the AhR-dependent regulation of miR-196a (217). Thus, perhaps the ability of the AhR to attenuate the activation of CS-induced apoptotic cell death machinery in the lung (**Fig. 2.4**) is a consequence of AhR-dependent regulation of miR-196a.

We also found that the AhR suppresses CS-induced LC3II expression (*i.e.* a marker involved in both autophagy and ER stress mediated cell death modalities) in murine lung (**Fig. 2.4**). Moreover, our *in vitro* data suggest that this AhR-mediated suppression of LC3II in the lung likely reflects the AhR attenuation of ER stress, as opposed to autophagy (**Fig. 3.3-3.6**). Our *in*

vitro data further suggest that the AhR-dependent attenuation of ER stress may be mediated via a non-canonical signaling mechanism. This is supported by our observation that the upregulation of the ER stress markers -CHOP and GADD34- were not accompanied by the classical activation of the UPR arms in the AhR-deficient cells (**Fig. 3.6**). Thus, perhaps similar to apoptosis, the AhR-attenuation of ER stress involves AhR-dependent regulation of miRNA. The plausibility of this is supported by evidence that CHOP expression is non-canonically regulated by miR-183-5p (366). Additionally, the expression of both GADD34 and CHOP are also regulated by mir-199a-5p in monocytes from subjects with AAT deficiency (378). Collectively, these data raise the possibility that the AhR-dependent regulation of miRNA may represent another non-canonical mechanism through which the AhR protects against the development of CS-induced emphysema.

5.3 Homeostatic Levels of AhR are Necessary for the Maintenance of Lung Health

As discussed above, pathogenic or protective AhR-mediated outcomes are often observed in response to different AhR ligands (*e.g.* TCDD vs CS, respectively). These differential outcomes induced by ligands may be a consequence of the ligand itself (single compound vs complex mixture), the persistence of AhR activation (chronic vs acute), or the AhR signaling pathway induced (canonical vs non-canonical). Although AhR-activation by different ligands represent one example of how the AhR may be pathogenic in one context and protective in another, changes in AhR expression may represent another. This notion is supported by evidence that changes in AhR expression are associated with a number of different disease states. Thus, the potential role of the AhR in disease (*i.e.* pathogenic or protective) may be largely attributable to whether it is over- or under-expressed relative to physiological conditions.

The importance of homeostatic levels of AhR expression in the maintenance of lung health is underscored by the dichotomy between COPD and lung cancer. While both COPD and lung cancer

are diseases primarily caused by the inhalational exposure of CS, AHR overexpression is consistently observed in subjects with lung cancer (215, 275), while we demonstrate that emphysema/COPD subjects exhibit reduced AHR expression (**Fig. 2.5 and 2.6**). In line with this, the AhR mediates pathogenic and pro-oncogenic effects in numerous cancer cell lines (276), while our *in vivo* data support that AhR-deficiency promotes the pathogenesis of CS-induced emphysema/COPD (**Fig. 2.1-2.4**). This raises the question: how can the AHR be pathogenic in lung cancer and protective in emphysema/COPD?

The answer to this question may involve homeostatic levels of AHR. The emphysema component of COPD, which is associated with reduced AHR expression, is largely a consequence of reduced cell proliferation and excessive cell death, culminating in the loss of lung parenchyma. It has been previously reported that AhR-deficiency causes reduced cellular proliferation (379), and our data support that AhR-deficiency exacerbates both CSE-induced lung structural cell death (**Fig. A1)** and the destruction of lung parenchyma (**Fig. 2.1**). This information collectively highlights the pathogenic nature of reduced AHR expression in the context of emphysema. In contrast to emphysema, lung cancer, which is associated with increased AHR expression, is characterized by excessive cell proliferation and resistance to cell death. Moreover, AhR overexpression or constitutive activation in cancer cell lines induces tumor growth, whereas AhR inhibition in these cells leads to reduced cell proliferation and migration (276). Thus, too little AHR appears to cause excessive cell death and the concomitant development of emphysema/COPD, whereas too much AHR appears to promote excessive cell proliferation thereby contributing to the development of lung cancer. Taken together, these findings collectively provide a foundation to support that homeostatic levels of AHR expression and activation may be critical for the maintenance of lung health.

5.4 Mechanistic Insights into the AhR Attenuation of CS-induced Emphysema

The loss of lung structural cells is of particular importance in the pathogenesis of the emphysema component of COPD (72, 97) and involves a variety of cell death modalities (see *1.2.4 "Cell Death"*). In addition, macrophages are an immune cell type that contributes to emphysematous lung destruction (46). Using a preclinical model of CS exposure, we are the first to demonstrate that AhR deficiency drives the development of a CS-induced emphysema-like phenotype (**Fig. 2.1**), implicating the AhR in the pathogenesis of emphysema. In line with mechanisms known to contribute to emphysema, we also observed that AhR deficiency renders lung structural cells significantly more vulnerable to CSE-induced cell death (**Fig. A1)** (161), and that AhR deficiency is associated with significantly elevated numbers of macrophages in the lung following a chronic CS regime **(Fig.2.2)**.

Similar to the AhR, the protein LC3 also plays an important role in the development of CS-induced emphysema. While the loss of AhR expression drives development of an emphysema-like phenotype, loss of LC3 expression protects against it. This is supported by several lines of evidence, including that LC3-deficiency protects against the development of a CS-induced emphysema-like phenotype and apoptotic cell death in the murine lung (109). Interestingly, macrophages from the lungs of cigarette smokers also exhibit elevated LC3II expression, which is associated with impaired phagocytic capacities resulting in defective pathogen clearance (124). This prompted us to ask the question: is AhR deficiency associated with heightened LC3 expression/processing (*i.e.* conversion from LC3I to LC3II)?

Our findings consistently demonstrate this to be true. We observed that AhR deficiency drives CS-induced LC3II upregulation. This LC3II upregulation was observed in both AhR-deficient mouse lung tissue (**Fig. 2.4 C, D**) and lung structural cells, including alveolar epithelial

cells and lung fibroblasts of mouse and human origin (**Fig. 3.1 and 3.2**). This upregulation of CS-induced LC3 in AhR-deficient models was not restricted to lung structural cells, as it was also upregulated in CS-exposed BAL macrophages (**Fig. A2A and A2C**). Finally, the expression of LC3 in bone marrow derived macrophages (BMDM), which are postulated to be the primary source of infiltrating macrophages in response to CS-induced lung injury, is also significantly greater in the absence of AhR (**Fig. A2B and A2D**). Thus, increases in CS-induced LC3 expression/processing in the absence of AhR is not specific to the lung but is also observed in cells of extra-pulmonary origin. This suggests that the AhR may attenuate CS-induced LC3 expression/processing throughout the body.

Moreover, the reduced AHR expression we report in COPD is observed in both the lungs and blood of COPD subjects (**Fig. 2.5, 2.6**). Collectively, this raises the possibility that the protective effects of the AhR against CS may not be specific to the lung, but rather, that the AhR may represent a protector against CS-induced injury throughout the body. In other words, in addition to our data demonstrating that AhR deficiency worsens CS-induced lung parenchymal destruction and declines in lung function (**Fig. 2.1**), reduced AhR expression may also contribute to other aspects of COPD extra-pulmonary manifestations such as weight loss (18) and skeletal muscle dysfunction (19, 20) (see *1.1.1.4 "Extra-Pulmonary Manifestations"*). Although the literature regarding the role of the AhR in skeletal muscle functionality is lacking, reports from murine models have demonstrated that AhR deficiency attenuates diet-induced obesity (380, 381). These reports provide grounds to speculate that reduced AhR expression in patients with COPD may be associated with an increased propensity to be underweight. The potential implications of the AhR in attenuating these extra-pulmonary features of COPD are clinically significant given that they are associated with fatigue, reduced exercise capacity, and negatively impact these

patient's quality of life. Moreover, weight loss represents a poor prognostic sign in COPD, as patients who are underweight have a significantly higher mortality than patients who are or normal weight (382). Taken together, our data position the AhR as a protector of toxicant-induced lung damage, and evidence from our *in vitro* CS models suggest that the AhR could have broader implications in other features of COPD pathogenesis in addition to lung parenchymal destruction.

5.5 Clinical Implications for the AHR in COPD

Currently, no disease modifying agents exist that are capable of changing the natural history of COPD (96). This highlights the need for a novel molecular target that can: 1) identify individuals who are susceptible to COPD development, and/or 2) be therapeutically targeted to attenuate COPD progression. We believe that our data presented here within may provide a basis for the potential use of the AhR as a novel biomarker and/or therapeutic target for emphysema/COPD.

5.5.1 AHR as a Novel Biomarker in COPD

A biomarker is defined as a characteristic that can be objectively measured in the body, which influences or predicts the presence or progression of a disease (383). Furthermore, this "characteristic" can be a substance, structure or physiological process (383). To date, the only biomarker consistently utilized for COPD is the measurement of the lung function parameter FEV_1 (384). Although FEV_1 is intrinsically reproducible and relatively easy to measure (384), it has several major drawbacks as a biomarker for COPD. Firstly, given that FEV_1 is a measure of airway obstruction, significant lung structural damage has typically occurred before appreciable declines in FEV_1 become evident. Moreover, FEV_1 is not specific to COPD (384), as it can also be reduced in other lung diseases associated with airway obstruction such as asthma and cystic fibrosis. Additionally, FEV_1 cannot be obtained from all COPD patients as it is dependent on patient cooperation. In addition to FEV_1, HRCT scans are also used to assess the presence of lung

structural damage and thus serve as a biomarker to identify patients with the emphysema component of COPD. Despite the fact that FEV_1 and HRCT scans are useful tools for the diagnosis of COPD and emphysema, detectable changes in these biomarkers only become evident once lung damage has occurred. This highlights the fact that there currently lacks a predictive biomarker capable of identifying individuals most susceptible to the development of COPD.

We propose that our data position the AHR as a potential novel biomarker, with predictive capabilities in COPD. Firstly, the AHR is a molecular substance that we have established can be objectively measured in both the blood (*i.e. AHR* mRNA expression) and lungs (*i.e.* AHR mRNA and protein expression) of humans. Secondly, we also show that reduced AHR expression in both the lungs (**Fig. 2.5**) and blood (**Fig. 2.6**) is significantly associated with the presence of COPD. Moreover, our finding that *AHR* expression is also significantly reduced in COPD subjects with no history of smoking (**Fig. 2.6B**), demonstrates that reduced AHR expression in COPD is not a consequence of cigarette smoking, but rather a consequence of the disease. Thirdly, we also established that reduced systemic *AHR* expression is significantly correlated with reduced lung function (FEV_1/FVC) in humans (**Fig. 2.6D**). This demonstrates that a change in *AHR* is associated with a change in a clinical outcome of COPD, which is a proposed requirement for the identification of novel COPD biomarkers (385). Lastly, our pre-clinical model of CS exposure supports that AhR deficiency exacerbates the development of an emphysema-like phenotype (**Fig. 2.1-2.4**). It is important to appreciate that this finding *in vivo* does not demonstrate that low AHR expression in humans will predict the development of COPD. However, it does suggest that reduced AHR expression in humans may precede, and thereby increase an individual's susceptibility, to the development of COPD. To determine if low AHR is truly predictive of

whether or not an individual will develop COPD, AHR expression would need to be assessed in the same individual over time *(i.e.* pre- and post-COPD development).

Collectively, our findings raise the possibility that reduced AHR expression (when combined with evidence of COPD-associated risk factors such as exposure to inhalational toxicants) could be a useful biomarker to identify individuals who are most susceptible to the development of COPD. A simple blood-test indicating reduced AHR expression could potentially identify the individuals particularly at risk of toxicant-induced lung damage and the development of COPD. However, the AHR cannot by itself represent the sole biomarker to diagnose individuals with COPD as low AHR expression is also observed in several other inflammatory diseases affecting barrier organs including Crohn's disease (277), ocular Behçet's disease (278), and chronic rhinosinusitis (279). Nevertheless, the fact that 25-30% of all COPD patients have never smoked (45, 52) highlights the need to understand the factors that predispose to the development of COPD. Our work supports that the AHR may represent one of these factors, which could enable it to serve as a predicative biomarker for COPD thereby making preventative therapeutic intervention a possibility.

5.5.2 Therapeutically Targeting the AHR in COPD

The AHR could also potentially serve as a novel target for pharmacological intervention to prevent or slow COPD pathogenesis. Although no AHR-targeted therapies are currently clinically approved, the AHR has been proposed as an attractive therapeutic target for many pathological conditions. Many food and drug administration (FDA) approved drugs have been demonstrated to induce AhR activation (386). These include drugs such as leuflunomide, flutamide and nimodipine, which are used to treat rheumatoid arthritis, prostate cancer and high blood pressure, respectively (386). The availability of these compounds raises the possibility of testing whether

an AhR agonist could be used to increase the activity of AHR in susceptible individuals (*i.e.* those with reduced AHR expression and COPD-associated risk-factors). AhR activation is known to elicit protective effects in inflammatory conditions. For example, FICZ attenuates psoriasis-like skin inflammation *in vivo* (280), pulmonary inflammation in a mouse model of asthma (281, 282) and gastrointestinal inflammation in a murine model of colitis (283, 284). Additionally, ITE administration dampens Th17 mediated inflammatory responses in patients with allergic rhinitis (285), and attenuates inflammation associated with a murine model of colitis (286) and multiple sclerosis (387). Moreover, even AhR activation by TCDD alleviates inflammation in experimental colitis (246) and in a murine model of multiple sclerosis (388).

However, before embarking on such studies, it is important to take into account which AhR ligand is to be used therapeutically to activate the AHR and attenuate COPD pathogenesis. For example, although TCDD has potentially desirable immunosuppressive properties, it would not be suitable for therapeutic usage due to its toxic and carcinogenic effects (181, 368). Additionally, although FICZ alleviates inflammation in several experimental disease models affecting barrier organs including the skin, lungs and gut (280, 282, 283), it also promotes inflammation in a mouse model of multiple sclerosis (388). What may underlie these differential effects of AhR ligands- such as FICZ- across diseases and organ systems is the focus of many ongoing studies in the AhR field.

Concerns as to whether or not the AHR could serve as a possible therapeutic target have been raised, mostly due to CYP1A1-mediated toxicity observed *in vitro* and/or following chronic AhR over-activation (370). The role of CYP1A1 is the subject of ongoing debate, as it mediates both the bioactivation of environmental pollutants such as benzo[a]pyrene into DNA-adduct forming carcinogenic metabolites (389), and benzo[a]pyrene detoxification (390). Recent work has

revealed a paradoxical role for CYP1A1, whereby *in vitro* it is more important in xenobiotic bioactivation (391), whereas *in vivo* it is more important for xenobiotic detoxification.

The beneficial role for CYP1A1 *in vivo* is highlighted by the finding that benzo[a]pyrene is cleared from the bloodstream much more rapidly in CYP1A1 expressing mice relative to CYP1A1-deficient mice (392). Furthermore, although TCDD-mediated activation of the AhR results in the induction of CYP1A1, it is important to appreciate that the toxic effects elicited by TCDD are CYP1A1-independent (202, 393). Despite this limitation, pursuing studies to evaluate the therapeutic potential of the AhR in COPD is warranted. In support of this, the fact that the AhR is evolutionarily conserved, ubiquitiously expressed, and activated in response to endogenous ligands underscores its physiological importance beyond the mediation of toxic effects in response to compounds such as TCDD. Moreover, *in vivo* models have consistently demonstrated that experimental intervention using AhR agonists to increase AhR activity is effective in attenuating the pathogenesis of many chronic inflammatory conditions affecting barrier organs (280, 282-284, 286).

A potential solution to overcome these limitations regarding the therapeutic use of the AHR in COPD may be a newly characterized class of AhR ligands called selective AhR modulators (SAhRMs). AhR ligands were traditionally classified as either agonists or antagonists based on whether they result in the activation or inhibition of AhR-mediated transcriptional activities (*i.e.* CYP1A1 induction). However, SAhRMs represent a class of AhR ligands that can bind to the AhR and induce its activation through non-canonical signaling mechanisms that are independent of CYP1A1 induction (394). A number of these SAhRMs have been identified and have shown promise in slowing the progression of cancer cell growth, including breast cancer (395), gastric cancer (396), pancreatic cancer (397) and prostate cancer (398). Furthermore, several of these

SAhRMs also exhibit anti-inflammatory properties (394, 399), making them attractive in the context of COPD pathogenesis.

5.6 Future Directions

Although this work is the first to establish a role for reduced AhR expression in promoting the pathogenesis of CS-induced emphysema, these findings have also raised several important questions that represent exciting avenues for future research.

5.6.1 AhR Attenuation of CS-induced Airspace Enlargement: Canonical or Non-canonical?

While our findings collectively illustrate that AhR-deficiency drives the development of an emphysema-like phenotype, they do not address the signaling mechanism through which the presence of the AhR may be exerting these protective effects. Thus, future work could elucidate if the AhR attenuation of CS-induced emphysema is mediated via a canonical or non-canonical AhR signaling mechanism *in vivo*. One way that this could be determined is by assessing airspace enlargement in the lungs of mice that either harbour a mutation in the AhR nuclear localization signal (*Ahr*$^{nls/nls}$) or in the AhR DNA-binding domain (*Ahr*$^{dbd/dbd}$) (183, 184). If the AhR attenuation of CS-induced emphysema is mediated via canonical AhR signaling (*i.e.* requiring AhR nuclear translocation and DRE-binding), one would expect a significant increase in airspace enlargement following a 4-month CS-regime in the *Ahr*$^{nls/nls}$ and *Ahr*$^{dbd/dbd}$ mice, comparable to that observed in the CS-exposed *Ahr*$^{-/-}$ mice.

A complementary approach to gain insight into the AhR mechanism of action would be to utilize an AhR antagonist *in vivo.* More specifically, AhR-expressing mice could be administered CH-223191 to inhibit canonical AhR activity by preventing nuclear translocation and DRE-binding of the AhR. If CS-exposed CH-223191-treated mice exhibit increased airspace enlargement relative to CS-exposed control mice (*i.e.* with functional AhR signaling capabilities),

this would indicate that canonical AhR signaling is required for the AhR to protect against CS-induced lung injury.

5.6.2 Is the AhR Attenuation of Emphysema Dependent on ER stress?

We consistently observed that AhR deficiency was associated with an upregulation of CS-induced LC3 expression and/or processing (*i.e.* mouse lung tissue, MLFs, A549s, MLE12s, BAL macrophages, BMDM). We initially thought that this finding reflected an AhR-dependent regulation of CS-induced autophagy. However, we discovered this was unlikely, as we observed that the heightened LC3II observed in AhR-deficient cells was unaccompanied by 1) an increased presence of autophagosomes (**Fig. 3.6A**); 2) an upregulation of autophagic genes (**Fig. 3.5**); 3) an upregulation of upstream autophagic machinery (**Fig. 3.4**) or 4) impaired autophagic flux (**Fig. 3.3**). LC3 has been implicated in autophagy-independent- but ER stress-mediated cell death mechanisms such as cytoplasmic vacuolation death and paraptosis (155-157). In line with this, our data presented here within are the first to demonstrate that AhR deficiency is associated with ER stress (**Fig. 3.6**). Furthermore, ER stress observed in AhR-deficient cells is further exacerbated following exposure to CSE and is associated with increased CSE-induced cell death (**Fig. A1**).

An important point illustrated by these studies on ER stress-induced cell death is that LC3 is not specific to autophagy, as LC3 knock-down also protects cells against cytoplasmic vacuolation death (155). This fact calls into question whether or not autophagy is actually a causal mechanism underlying emphysema pathogenesis, given that the only publication to support this assertion did so by demonstrating that LC3-deficient mice are protected against the development of CS-induced experimental emphysema (109). This understanding of LC3, coupled with our own findings, collectively provides a foundation to postulate that perhaps ER stress, and not autophagy, drives emphysema pathogenesis. Currently, only two studies exist demonstrating a relationship

between ER stress and emphysema. One study demonstrated that subjects with severe emphysema have significantly higher expression of ER stress proteins, p-EIF2α and CHOP, in their lungs relative to those with mild emphysema or control subjects (144). The second study reported a role for ER stress in emphysema pathogenesis upon demonstrating that pharmacological alleviation of ER stress prevents CS-induced airspace enlargement, inflammation and apoptosis in the murine lung (110). When considered collectively, these data support the idea that ER stress may be a critical mechanism underlying emphysema pathogenesis.

Future studies should identify whether ER stress and/or LC3 processing is simply associated with, or causally implicated in, the development of emphysema in AhR-deficient models. This could be addressed by knocking-down critical ER-stress mediators such as CHOP in AhR-deficient cells or mice to determine if the mechanism through which the AhR attenuates CS-induced cell death (*in* vitro) and/or experimental emphysema (*in vivo*), respectively, is mediated by its regulation of ER stress. Similarly, knocking-down LC3 would also elucidate if LC3 upregulation is simply associated with, or causally driving, the pathogenic phenotype observed in the AhR-deficient models.

5.6.3 How Much AhR is Enough?

Finally, our findings establish that AhR deficiency drives the development of experimental emphysema, and that emphysema/COPD subjects exhibit reduced AHR expression, which together suggest a protective role for the presence of the AhR in attenuating the pathogenesis of emphysema/COPD. It remains unknown, however, how much AhR is enough to elicit these protective effects against CS-induced lung damage.

Although we demonstrate a protective role for the presence of the AhR in the pathogenesis of an emphysema-like phenotype using AhR knockout (*Ahr*$^{-/-}$) mice, one approach to this question

would be to utilize AhR hypomorphic mice that exhibit reduced AhR expression (372). Manipulating AhR expression (*i.e.* 25% reduction, 50% reduction, 75% reduction *etc.*) in hypomorphic mice and exposing them to CS could establish the quantity of AhR required to protect against CS-induced lung parenchymal destruction. Perhaps CS-induced lung injury progressively and linearly worsens as AhR expression is reduced. Alternatively, perhaps there is a critical threshold of AhR expression below which an emphysema-like phenotype typically develops. Although our findings demonstrating a positive correlation between systemic *AHR* expression and lung function (FEV_1/FVC) in humans (**Fig. 2.6D**) is suggestive of the former, *in vivo* studies using AhR hypomorphic mice could further elucidate these questions.

5.7 Conclusions: Implications Beyond CS

We believe that our findings may have implications beyond the development of CS-induced emphysema. The fact that never-smokers account for approximately 25-30% of COPD cases illustrates the importance of factors other than strictly exposure to mainstream CS in the development of COPD (45, 52). Perhaps low levels of AHR from birth, or progressive loss of the AHR over-time, represent a genetic susceptibility factor that predisposes individuals to the development of COPD. Progressive loss of AHR in these individuals could be akin to the multiple hit hypothesis used to explain the loss of dopaminergic neurons as a driver of Parkinson's disease pathogenesis (400). It could be that reduced AHR expression represents "one hit" and chronic exposure to inhalational toxicants represents another "hit", which together drive COPD pathogenesis in susceptible individuals. This is similar to AAT deficiency, where concomitant exposure to CS accelerates the development of emphysema in these individuals and is associated with a 10-20 yr. shorter lifespan than AAT deficient persons who have never-smoked (401). As previously discussed, inhalational toxicants (see *1.1.2.1.3 "Inhalation of Toxicants")* other than

CS, likely contribute to the development of COPD. Thus, this second “hit” may also come in the form of exposure to ambient or occupational air pollution. Taken together, this provides the grounds to postulate that the AhR may serve as a universal protector against toxicant-induced insults. Given that no therapeutic options currently exist to stop or slow COPD progression, these findings could provide the basis for the development of new therapeutic agents or biomarkers for COPD.

6 APPENDIX

Figure A1

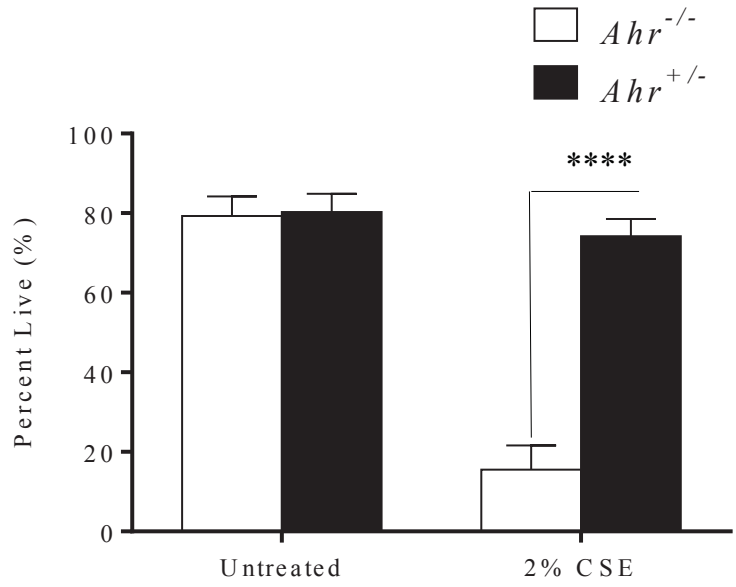

Figure A1. AhR-deficient lung structural cells exhibit reduced viability in response to CSE-treatment. Cell viability was determined in *Ahr*$^{+/-}$ and *Ahr*$^{-/-}$ MLFs following treatment with 2% CSE for 24h. Cell viability was significantly less in the CSE-treated *Ahr*$^{-/-}$ MLFs relative to the CSE-treated *Ahr*$^{+/-}$ MLFs. Results are expressed as mean ± SEM of n=4 independent experiments. Data was analyzed using a 2-way ANOVA followed by Bonferroni correction for multiple comparisons.

Figure A2

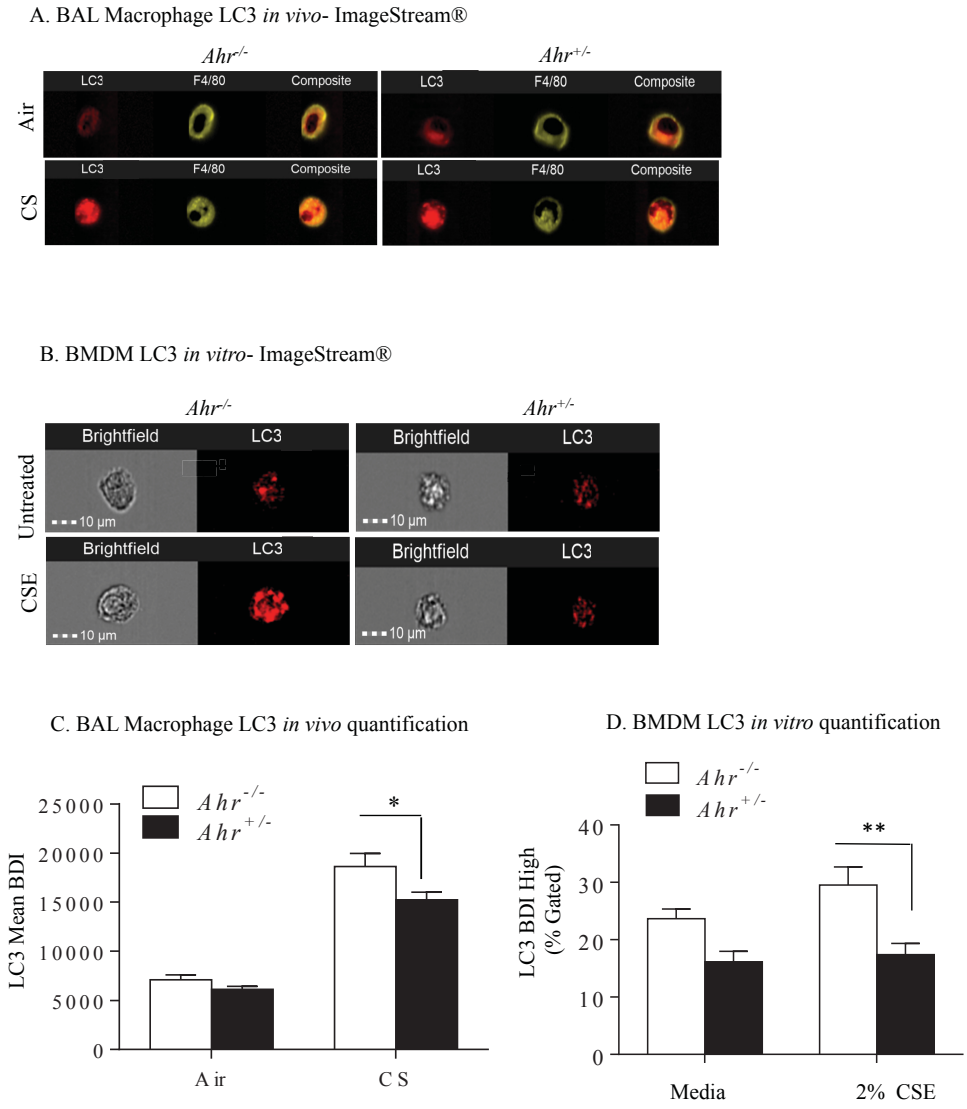

Figure A2. AhR deficiency increases CS-induced LC3 upregulation in lung and BMDM macrophages.
(A) BAL Macrophages LC3- ImageStream®: Representative images of the increased LC3 punctae in BAL macrophages are shown. **(C)** BAL Macrophages quantification- ImageStream®: LC3 expression was quantified in F4/80^{+} BAL cells (macrophages). The mean LC3 BDI was significantly higher in BAL macrophages from the CS-exposed *Ahr*$^{-/-}$ mice relative to the CS-exposed *Ahr*$^{+/-}$ mice (n=3-5 mice per group). **(B)** BMDM LC3- ImageStream®: Cultured BMDM from *Ahr*$^{+/-}$ and *Ahr*$^{-/-}$ mice were treated with 2% CSE for 8h and LC3 expression was assessed by ImageStream®. Representative images of LC3 expression are shown. **(D)** BMDM LC3 Quantification- ImageStream®: The proportion of LC3 high BDI cells was significantly higher in BMDM from *Ahr*$^{-/-}$ mice exposed to CSE (n=3-5 mice per group). All data was analyzed using a 2-way ANOVA with a Bonferroni correction. Results are expressed as mean ± SEM.

7 REFERENCES

1. Kemp SV, Polkey MI, & Shah PL (2009) The epidemiology, etiology, clinical features, and natural history of emphysema. *Thorac Surg Clin* 19(2):149-158.
2. Kim V & Criner GJ (2013) Chronic bronchitis and chronic obstructive pulmonary disease. *Am J Respir Crit Care Med* 187(3):228-237.
3. Aoshiba K & Nagai A (2004) Differences in airway remodeling between asthma and chronic obstructive pulmonary disease. *Clin Rev Allergy Immunol* 27(1):35-43.
4. Jones RL, Noble PB, Elliot JG, & James AL (2016) Airway remodelling in COPD: It's not asthma! *Respirology* 21(8):1347-1356.
5. Berg K & Wright JL (2016) The Pathology of Chronic Obstructive Pulmonary Disease: Progress in the 20th and 21st Centuries. *Arch Pathol Lab Med* 140(12):1423-1428.
6. Friedman PJ (2008) Imaging studies in emphysema. *Proc Am Thorac Soc* 5(4):494-500.
7. Anderson AE, Jr. & Foraker AG (1973) Centrilobular emphysema and panlobular emphysema: two different diseases. *Thorax* 28(5):547-550.
8. Laitinen LA & Koskela K (1999) Chronic bronchitis and chronic obstructive pulmonary disease: Finnish National Guidelines for Prevention and Treatment 1998-2007. *Respir Med* 93(5):297-332.
9. Pauwels RA & Rabe KF (2004) Burden and clinical features of chronic obstructive pulmonary disease (COPD). *Lancet* 364(9434):613-620.
10. Vestbo J, Hurd SS, Rodriguez-Roisin R, & Committee GS (2012) [An overview of Global Strategy for the Diagnosis, Management and Prevention of Chronic Obstructive Pulmonary Disease (GOLD) (revised 2011)]. *Zhonghua Yi Xue Za Zhi* 92(14):937-938.
11. GOLD (2017) *Global Strategy for the Diagnosis, Management and Prevention of COPD, Global Initiative for Chronic Obstructive Lung Disease (GOLD)*.
12. Miravitlles M*, et al.* (2004) Effect of exacerbations on quality of life in patients with chronic obstructive pulmonary disease: a 2 year follow up study. *Thorax* 59(5):387-395.
13. Sapey E & Stockley RA (2006) COPD exacerbations . 2: aetiology. *Thorax* 61(3):250-258.
14. Zielinski J*, et al.* (1997) Causes of death in patients with COPD and chronic respiratory failure. *Monaldi Arch Chest Dis* 52(1):43-47.
15. Sethi S (2010) Infection as a comorbidity of COPD. *Eur Respir J* 35(6):1209-1215.
16. Rawal G & Yadav S (2015) Nutrition in chronic obstructive pulmonary disease: A review. *J Transl Int Med* 3(4):151-154.
17. Muers MF & Green JH (1993) Weight loss in chronic obstructive pulmonary disease. *Eur Respir J* 6(5):729-734.
18. Eriksson B*, et al.* (2016) Only severe COPD is associated with being underweight: results from a population survey. *ERJ Open Res* 2(3).
19. Seymour JM*, et al.* (2010) The prevalence of quadriceps weakness in COPD and the relationship with disease severity. *Eur Respir J* 36(1):81-88.
20. Kharbanda S, Ramakrishna A, & Krishnan S (2015) Prevalence of quadriceps muscle weakness in patients with COPD and its association with disease severity. *Int J Chron Obstruct Pulmon Dis* 10:1727-1735.
21. Ottenheijm CA*, et al.* (2005) Diaphragm dysfunction in chronic obstructive pulmonary disease. *Am J Respir Crit Care Med* 172(2):200-205.

22. Putcha N, Drummond MB, Wise RA, & Hansel NN (2015) Comorbidities and Chronic Obstructive Pulmonary Disease: Prevalence, Influence on Outcomes, and Management. *Semin Respir Crit Care Med* 36(4):575-591.
23. Cavailles A*, et al.* (2013) Comorbidities of COPD. *Eur Respir Rev* 22(130):454-475.
24. Lee SJ*, et al.* (2015) Risk factors for chronic obstructive pulmonary disease among never-smokers in Korea. *Int J Chron Obstruct Pulmon Dis* 10:497-506.
25. Islam MS, Hossain MM, Pasha MM, Azad AK, & Murshed KM (2013) Prevalence and risk factors of chronic obstructive pulmonary disease (COPD) in Dhaka city population. *Mymensingh Med J* 22(3):547-551.
26. Crighton EJ, Ragetlie R, Luo J, To T, & Gershon A (2015) A spatial analysis of COPD prevalence, incidence, mortality and health service use in Ontario. *Health Rep* 26(3):10-18.
27. van Durme Y*, et al.* (2009) Prevalence, incidence, and lifetime risk for the development of COPD in the elderly: the Rotterdam study. *Chest* 135(2):368-377.
28. Camp PG, O'Donnell DE, & Postma DS (2009) Chronic obstructive pulmonary disease in men and women: myths and reality. *Proc Am Thorac Soc* 6(6):535-538.
29. Han MK*, et al.* (2007) Gender and chronic obstructive pulmonary disease: why it matters. *Am J Respir Crit Care Med* 176(12):1179-1184.
30. de Torres JP*, et al.* (2005) Gender and COPD in patients attending a pulmonary clinic. *Chest* 128(4):2012-2016.
31. Dransfield MT*, et al.* (2007) Gender differences in the severity of CT emphysema in COPD. *Chest* 132(2):464-470.
32. Seifart C & Plagens A (2007) Genetics of chronic obstructive pulmonary disease. *Int J Chron Obstruct Pulmon Dis* 2(4):541-550.
33. Lieberman J, Winter B, & Sastre A (1986) Alpha 1-antitrypsin Pi-types in 965 COPD patients. *Chest* 89(3):370-373.
34. Russo R*, et al.* (2016) Prevalence of alpha-1 antitrypsin deficiency and allele frequency in patients with COPD in Brazil. *J Bras Pneumol* 42(5):311-316.
35. Stockley RA (2014) Alpha1-antitrypsin review. *Clin Chest Med* 35(1):39-50.
36. NIH (2013) *Alpha-1 antitrypsin deficiency*, ((NIH) NIoH).
37. Janciauskiene SM*, et al.* (2011) The discovery of alpha1-antitrypsin and its role in health and disease. *Respir Med* 105(8):1129-1139.
38. Al Ashry HS & Strange C (2017) COPD in individuals with the PiMZ alpha-1 antitrypsin genotype. *Eur Respir Rev* 26(146).
39. Kelly E, Greene CM, Carroll TP, McElvaney NG, & O'Neill SJ (2010) Alpha-1 antitrypsin deficiency. *Respir Med* 104(6):763-772.
40. Takubo Y*, et al.* (2002) Alpha1-antitrypsin determines the pattern of emphysema and function in tobacco smoke-exposed mice: parallels with human disease. *Am J Respir Crit Care Med* 166(12 Pt 1):1596-1603.
41. Valavanidis A, Fiotakis K, & Vlachogianni T (2008) Airborne particulate matter and human health: toxicological assessment and importance of size and composition of particles for oxidative damage and carcinogenic mechanisms. *J Environ Sci Health C Environ Carcinog Ecotoxicol Rev* 26(4):339-362.
42. Ghio AJ (2014) Particle exposures and infections. *Infection* 42(3):459-467.

43. Council NR (2010) *Review of the Department of Defence Enhanced Particulate Matter Surveillance Program Report* (The National Academies Press, Washington), (Defence Do).
44. Nemmar A, Holme JA, Rosas I, Schwarze PE, & Alfaro-Moreno E (2013) Recent advances in particulate matter and nanoparticle toxicology: a review of the in vivo and in vitro studies. *Biomed Res Int* 2013:279371.
45. Tan WC*, et al.* (2015) Characteristics of COPD in never-smokers and ever-smokers in the general population: results from the CanCOLD study. *Thorax* 70(9):822-829.
46. Beckett EL*, et al.* (2013) A new short-term mouse model of chronic obstructive pulmonary disease identifies a role for mast cell tryptase in pathogenesis. *J Allergy Clin Immunol* 131(3):752-762.
47. Hogg JC (2004) Pathophysiology of airflow limitation in chronic obstructive pulmonary disease. *Lancet* 364(9435):709-721.
48. Stratelis G, Fransson SG, Schmekel B, Jakobsson P, & Molstad S (2008) High prevalence of emphysema and its association with BMI: a study of smokers with normal spirometry. *Scand J Prim Health Care* 26(4):241-247.
49. Flouris AD*, et al.* (2009) Acute and short-term effects of secondhand smoke on lung function and cytokine production. *Am J Respir Crit Care Med* 179(11):1029-1033.
50. Goldklang MP, Marks SM, & D'Armiento JM (2013) Second hand smoke and COPD: lessons from animal studies. *Front Physiol* 4:30.
51. Reid JL, Rynard VL, Czoli CD, & Hammond D (2015) Who is using e-cigarettes in Canada? Nationally representative data on the prevalence of e-cigarette use among Canadians. *Prev Med* 81:180-183.
52. Lamprecht B*, et al.* (2011) COPD in never smokers: results from the population-based burden of obstructive lung disease study. *Chest* 139(4):752-763.
53. Andersen ZJ*, et al.* (2012) Stroke and long-term exposure to outdoor air pollution from nitrogen dioxide: a cohort study. *Stroke* 43(2):320-325.
54. DeVries R, Kriebel D, & Sama S (2016) Low level air pollution and exacerbation of existing copd: a case crossover analysis. *Environ Health* 15(1):98.
55. Hu G*, et al.* (2010) Risk of COPD from exposure to biomass smoke: a metaanalysis. *Chest* 138(1):20-31.
56. Fullerton DG, Bruce N, & Gordon SB (2008) Indoor air pollution from biomass fuel smoke is a major health concern in the developing world. *Trans R Soc Trop Med Hyg* 102(9):843-851.
57. Boschetto P*, et al.* (2006) Chronic obstructive pulmonary disease (COPD) and occupational exposures. *J Occup Med Toxicol* 1:11.
58. Santo Tomas LH (2011) Emphysema and chronic obstructive pulmonary disease in coal miners. *Curr Opin Pulm Med* 17(2):123-125.
59. Thoren K, Jarvholm B, & Morgan U (1989) Mortality from asthma and chronic obstructive pulmonary disease among workers in a soft paper mill: a case-referent study. *Br J Ind Med* 46(3):192-195.
60. Cho Y*, et al.* (2015) Work-related COPD after years of occupational exposure. *Ann Occup Environ Med* 27:6.
61. Rabe KF & Watz H (2017) Chronic obstructive pulmonary disease. *Lancet* 389(10082):1931-1940.

62. Adeloye D*, et al.* (2015) Global and regional estimates of COPD prevalence: Systematic review and meta-analysis. *J Glob Health* 5(2):020415.
63. Collaborators GBDCRD (2017) Global, regional, and national deaths, prevalence, disability-adjusted life years, and years lived with disability for chronic obstructive pulmonary disease and asthma, 1990-2015: a systematic analysis for the Global Burden of Disease Study 2015. *Lancet Respir Med* 5(9):691-706.
64. Lopez-Campos JL, Tan W, & Soriano JB (2016) Global burden of COPD. *Respirology* 21(1):14-23.
65. Evans J, Chen Y, Camp PG, Bowie DM, & McRae L (2014) Estimating the prevalence of COPD in Canada: Reported diagnosis versus measured airflow obstruction. *Health Rep* 25(3):3-11.
66. Ancochea J*, et al.* (2013) Underdiagnosis of chronic obstructive pulmonary disease in women: quantification of the problem, determinants and proposed actions. *Arch Bronconeumol* 49(6):223-229.
67. Hill K*, et al.* (2010) Prevalence and underdiagnosis of chronic obstructive pulmonary disease among patients at risk in primary care. *CMAJ* 182(7):673-678.
68. Labonte LE*, et al.* (2016) Undiagnosed Chronic Obstructive Pulmonary Disease Contributes to the Burden of Health Care Use. Data from the CanCOLD Study. *Am J Respir Crit Care Med* 194(3):285-298.
69. Bryan SaN, T. (2015) *Deaths from Chronic Obstructive Pulmonary Disease in Canada, 1950 to 2011*, (Catalogue SC).
70. Reid DJ & Pham NT (2013) Emerging Therapeutic Options for the Management of COPD. *Clin Med Insights Circ Respir Pulm Med* 7:7-15.
71. Babu KS, Kastelik JA, & Morjaria JB (2014) Inhaled corticosteroids in chronic obstructive pulmonary disease: a pro-con perspective. *Br J Clin Pharmacol* 78(2):282-300.
72. Sharafkhaneh A, Hanania NA, & Kim V (2008) Pathogenesis of emphysema: from the bench to the bedside. *Proc Am Thorac Soc* 5(4):475-477.
73. Martin TR & Frevert CW (2005) Innate immunity in the lungs. *Proc Am Thorac Soc* 2(5):403-411.
74. Tamimi A, Serdarevic D, & Hanania NA (2012) The effects of cigarette smoke on airway inflammation in asthma and COPD: therapeutic implications. *Respir Med* 106(3):319-328.
75. D'Hulst A I, Vermaelen KY, Brusselle GG, Joos GF, & Pauwels RA (2005) Time course of cigarette smoke-induced pulmonary inflammation in mice. *Eur Respir J* 26(2):204-213.
76. MacNee W (2005) Pathogenesis of chronic obstructive pulmonary disease. *Proc Am Thorac Soc* 2(4):258-266; discussion 290-251.
77. Finkelstein R, Fraser RS, Ghezzo H, & Cosio MG (1995) Alveolar inflammation and its relation to emphysema in smokers. *Am J Respir Crit Care Med* 152(5 Pt 1):1666-1672.
78. Podolin PL*, et al.* (2013) T cell depletion protects against alveolar destruction due to chronic cigarette smoke exposure in mice. *Am J Physiol Lung Cell Mol Physiol* 304(5):L312-323.
79. Keatings VM, Collins PD, Scott DM, & Barnes PJ (1996) Differences in interleukin-8 and tumor necrosis factor-alpha in induced sputum from patients with chronic obstructive pulmonary disease or asthma. *Am J Respir Crit Care Med* 153(2):530-534.
80. Majo J, Ghezzo H, & Cosio MG (2001) Lymphocyte population and apoptosis in the lungs of smokers and their relation to emphysema. *Eur Respir J* 17(5):946-953.

81. Taraseviciene-Stewart L & Voelkel NF (2008) Molecular pathogenesis of emphysema. *J Clin Invest* 118(2):394-402.
82. Taggart CC, Greene CM, Carroll TP, O'Neill SJ, & McElvaney NG (2005) Elastolytic proteases: inflammation resolution and dysregulation in chronic infective lung disease. *Am J Respir Crit Care Med* 171(10):1070-1076.
83. Houghton AM (2015) Matrix metalloproteinases in destructive lung disease. *Matrix Biol* 44-46:167-174.
84. Brew K & Nagase H (2010) The tissue inhibitors of metalloproteinases (TIMPs): an ancient family with structural and functional diversity. *Biochim Biophys Acta* 1803(1):55-71.
85. Lindner D*, et al.* (2012) Differential expression of matrix metalloproteases in human fibroblasts with different origins. *Biochem Res Int* 2012:875742.
86. Russell RE*, et al.* (2002) Release and activity of matrix metalloproteinase-9 and tissue inhibitor of metalloproteinase-1 by alveolar macrophages from patients with chronic obstructive pulmonary disease. *Am J Respir Cell Mol Biol* 26(5):602-609.
87. Funada Y, Nishimura Y, & Yokoyama M (2004) Imbalance of matrix metalloproteinase-9 and tissue inhibitor of matrix metalloproteinase-1 is associated with pulmonary emphysema in Klotho mice. *Kobe J Med Sci* 50(3-4):59-67.
88. Atkinson JJ*, et al.* (2011) The role of matrix metalloproteinase-9 in cigarette smoke-induced emphysema. *Am J Respir Crit Care Med* 183(7):876-884.
89. Aoshiba K, Yasuda K, Yasui S, Tamaoki J, & Nagai A (2001) Serine proteases increase oxidative stress in lung cells. *Am J Physiol Lung Cell Mol Physiol* 281(3):L556-564.
90. Boukhenouna S, Wilson MA, Bahmed K, & Kosmider B (2018) Reactive Oxygen Species in Chronic Obstructive Pulmonary Disease. *Oxid Med Cell Longev* 2018:5730395.
91. Church DF & Pryor WA (1985) Free-radical chemistry of cigarette smoke and its toxicological implications. *Environ Health Perspect* 64:111-126.
92. Hanta I, Kocabas A, Canacankatan N, Kuleci S, & Seydaoglu G (2006) Oxidant-antioxidant balance in patients with COPD. *Lung* 184(2):51-55.
93. Tavilani H, Nadi E, Karimi J, & Goodarzi MT (2012) Oxidative stress in COPD patients, smokers, and non-smokers. *Respir Care* 57(12):2090-2094.
94. Cristovao C, Cristovao L, Nogueira F, & Bicho M (2013) Evaluation of the oxidant and antioxidant balance in the pathogenesis of chronic obstructive pulmonary disease. *Rev Port Pneumol* 19(2):70-75.
95. Elmasry SA-A, M.; Ghoneim, A.; Nasr, M.; AboZaid, M. (2015) Role of oxidant–antioxidant imbalance in the pathogenesis of chronic obstructive pulmonary disease. *Egyptian Journal of Chest Diseases and Tuberculosis* 64:813–820.
96. Kirkham PA & Barnes PJ (2013) Oxidative stress in COPD. *Chest* 144(1):266-273.
97. Baglole CJ*, et al.* (2006) Differential induction of apoptosis by cigarette smoke extract in primary human lung fibroblast strains: implications for emphysema. *Am J Physiol Lung Cell Mol Physiol* 291(1):L19-29.
98. Aoshiba K, Yokohori N, & Nagai A (2003) Alveolar wall apoptosis causes lung destruction and emphysematous changes. *Am J Respir Cell Mol Biol* 28(5):555-562.
99. Morissette MC, Parent J, & Milot J (2009) Alveolar epithelial and endothelial cell apoptosis in emphysema: what we know and what we need to know. *Int J Chron Obstruct Pulmon Dis* 4:19-31.

100. Plantier L, Boczkowski J, & Crestani B (2007) Defect of alveolar regeneration in pulmonary emphysema: role of lung fibroblasts. *Int J Chron Obstruct Pulmon Dis* 2(4):463-469.
101. Elmore S (2007) Apoptosis: a review of programmed cell death. *Toxicol Pathol* 35(4):495-516.
102. Kosmider B, Messier EM, Chu HW, & Mason RJ (2011) Human alveolar epithelial cell injury induced by cigarette smoke. *PLoS One* 6(12):e26059.
103. Hu W*, et al.* (2009) Involvement of Bcl-2 family in apoptosis and signal pathways induced by cigarette smoke extract in the human airway smooth muscle cells. *DNA Cell Biol* 28(1):13-22.
104. Zhang L*, et al.* (2015) Resveratrol exerts an anti-apoptotic effect on human bronchial epithelial cells undergoing cigarette smoke exposure. *Mol Med Rep* 11(3):1752-1758.
105. Nana-Sinkam SP*, et al.* (2007) Prostacyclin prevents pulmonary endothelial cell apoptosis induced by cigarette smoke. *Am J Respir Crit Care Med* 175(7):676-685.
106. Demedts IK, Demoor T, Bracke KR, Joos GF, & Brusselle GG (2006) Role of apoptosis in the pathogenesis of COPD and pulmonary emphysema. *Respir Res* 7:53.
107. Fink SL & Cookson BT (2005) Apoptosis, pyroptosis, and necrosis: mechanistic description of dead and dying eukaryotic cells. *Infect Immun* 73(4):1907-1916.
108. de la Calle C, Joubert PE, Law HK, Hasan M, & Albert ML (2011) Simultaneous assessment of autophagy and apoptosis using multispectral imaging cytometry. *Autophagy* 7(9):1045-1051.
109. Chen ZH*, et al.* (2010) Autophagy protein microtubule-associated protein 1 light chain-3B (LC3B) activates extrinsic apoptosis during cigarette smoke-induced emphysema. *Proc Natl Acad Sci U S A* 107(44):18880-18885.
110. Wang Y, Wu ZZ, & Wang W (2017) Inhibition of endoplasmic reticulum stress alleviates cigarette smoke-induced airway inflammation and emphysema. *Oncotarget* 8(44):77685-77695.
111. Wang CW & Klionsky DJ (2003) The molecular mechanism of autophagy. *Mol Med* 9(3-4):65-76.
112. Mizumura K, Cloonan SM, Haspel JA, & Choi AMK (2012) The emerging importance of autophagy in pulmonary diseases. *Chest* 142(5):1289-1299.
113. Galluzzi L*, et al.* (2008) To die or not to die: that is the autophagic question. *Curr Mol Med* 8(2):78-91.
114. He C & Klionsky DJ (2009) Regulation mechanisms and signaling pathways of autophagy. *Annu Rev Genet* 43:67-93.
115. Ryter SW & Choi AM (2015) Autophagy in lung disease pathogenesis and therapeutics. *Redox Biol* 4:215-225.
116. Mack HI, Zheng B, Asara JM, & Thomas SM (2012) AMPK-dependent phosphorylation of ULK1 regulates ATG9 localization. *Autophagy* 8(8):1197-1214.
117. Nakatogawa H (2013) Two ubiquitin-like conjugation systems that mediate membrane formation during autophagy. *Essays Biochem* 55:39-50.
118. Lippai M & Low P (2014) The role of the selective adaptor p62 and ubiquitin-like proteins in autophagy. *Biomed Res Int* 2014:832704.
119. Choi AM, Ryter SW, & Levine B (2013) Autophagy in human health and disease. *N Engl J Med* 368(19):1845-1846.

120. Kuma A & Mizushima N (2010) Physiological role of autophagy as an intracellular recycling system: with an emphasis on nutrient metabolism. *Semin Cell Dev Biol* 21(7):683-690.
121. Klionsky DJ & Codogno P (2013) The mechanism and physiological function of macroautophagy. *J Innate Immun* 5(5):427-433.
122. Yang ZJ, Chee CE, Huang S, & Sinicrope FA (2011) The role of autophagy in cancer: therapeutic implications. *Mol Cancer Ther* 10(9):1533-1541.
123. Govindaraju VK, Bodas M, & Vij N (2017) Cigarette smoke induced autophagy-impairment regulates AMD pathogenesis mechanisms in ARPE-19 cells. *PLoS One* 12(8):e0182420.
124. Monick MM*, et al.* (2010) Identification of an autophagy defect in smokers' alveolar macrophages. *J Immunol* 185(9):5425-5435.
125. Jia L*, et al.* (1997) Inhibition of autophagy abrogates tumour necrosis factor alpha induced apoptosis in human T-lymphoblastic leukaemic cells. *Br J Haematol* 98(3):673-685.
126. Kim HP*, et al.* (2008) Autophagic proteins regulate cigarette smoke-induced apoptosis: protective role of heme oxygenase-1. *Autophagy* 4(7):887-895.
127. Chen ZH*, et al.* (2008) Egr-1 regulates autophagy in cigarette smoke-induced chronic obstructive pulmonary disease. *PLoS One* 3(10):e3316.
128. Pereira CMF (2013) Crosstalk between Endoplasmic Reticulum Stress and Protein Misfolding in Neurodegenerative Diseases. *ISRN Cell Biology* 2013:22.
129. Xu C, Bailly-Maitre B, & Reed JC (2005) Endoplasmic reticulum stress: cell life and death decisions. *J Clin Invest* 115(10):2656-2664.
130. Szegezdi E, Logue SE, Gorman AM, & Samali A (2006) Mediators of endoplasmic reticulum stress-induced apoptosis. *EMBO Rep* 7(9):880-885.
131. Schonthal AH (2012) Endoplasmic reticulum stress: its role in disease and novel prospects for therapy. *Scientifica (Cairo)* 2012:857516.
132. Mokas S*, et al.* (2009) Uncoupling stress granule assembly and translation initiation inhibition. *Mol Biol Cell* 20(11):2673-2683.
133. Wek RC & Cavener DR (2007) Translational control and the unfolded protein response. *Antioxid Redox Signal* 9(12):2357-2371.
134. Oslowski CM & Urano F (2011) Measuring ER stress and the unfolded protein response using mammalian tissue culture system. *Methods Enzymol* 490:71-92.
135. Celli J & Tsolis RM (2015) Bacteria, the endoplasmic reticulum and the unfolded protein response: friends or foes? *Nat Rev Microbiol* 13(2):71-82.
136. Marciniak SJ*, et al.* (2004) CHOP induces death by promoting protein synthesis and oxidation in the stressed endoplasmic reticulum. *Genes Dev* 18(24):3066-3077.
137. Lei Y*, et al.* (2017) CHOP favors endoplasmic reticulum stress-induced apoptosis in hepatocellular carcinoma cells via inhibition of autophagy. *PLoS One* 12(8):e0183680.
138. Zinszner H*, et al.* (1998) CHOP is implicated in programmed cell death in response to impaired function of the endoplasmic reticulum. *Genes Dev* 12(7):982-995.
139. Han J*, et al.* (2013) ER-stress-induced transcriptional regulation increases protein synthesis leading to cell death. *Nat Cell Biol* 15(5):481-490.
140. Kelsen SG*, et al.* (2008) Cigarette smoke induces an unfolded protein response in the human lung: a proteomic approach. *Am J Respir Cell Mol Biol* 38(5):541-550.

141. Tagawa Y, *et al.* (2008) Induction of apoptosis by cigarette smoke via ROS-dependent endoplasmic reticulum stress and CCAAT/enhancer-binding protein-homologous protein (CHOP). *Free Radic Biol Med* 45(1):50-59.
142. Jorgensen E, *et al.* (2008) Cigarette smoke induces endoplasmic reticulum stress and the unfolded protein response in normal and malignant human lung cells. *BMC Cancer* 8:229.
143. Geraghty P, Wallace A, & D'Armiento JM (2011) Induction of the unfolded protein response by cigarette smoke is primarily an activating transcription factor 4-C/EBP homologous protein mediated process. *Int J Chron Obstruct Pulmon Dis* 6:309-319.
144. Min T, Bodas M, Mazur S, & Vij N (2011) Critical role of proteostasis-imbalance in pathogenesis of COPD and severe emphysema. *J Mol Med (Berl)* 89(6):577-593.
145. Kelsen SG (2016) The Unfolded Protein Response in Chronic Obstructive Pulmonary Disease. *Ann Am Thorac Soc* 13 Suppl 2:S138-145.
146. Dunn WA, Jr. (1990) Studies on the mechanisms of autophagy: formation of the autophagic vacuole. *J Cell Biol* 110(6):1923-1933.
147. Karanasios E, *et al.* (2016) Autophagy initiation by ULK complex assembly on ER tubulovesicular regions marked by ATG9 vesicles. *Nat Commun* 7:12420.
148. Nishimura T & Mizushima N (2017) The ULK complex initiates autophagosome formation at phosphatidylinositol synthase-enriched ER subdomains. *Autophagy* 13(10):1795-1796.
149. Nishimura T, *et al.* (2017) Autophagosome formation is initiated at phosphatidylinositol synthase-enriched ER subdomains. *EMBO J* 36(12):1719-1735.
150. Joo JH, *et al.* (2016) The Noncanonical Role of ULK/ATG1 in ER-to-Golgi Trafficking Is Essential for Cellular Homeostasis. *Mol Cell* 62(6):982.
151. Sano R & Reed JC (2013) ER stress-induced cell death mechanisms. *Biochim Biophys Acta* 1833(12):3460-3470.
152. Rajesh K, *et al.* (2015) Phosphorylation of the translation initiation factor eIF2alpha at serine 51 determines the cell fate decisions of Akt in response to oxidative stress. *Cell Death Dis* 6:e1591.
153. Salazar M, *et al.* (2009) Cannabinoid action induces autophagy-mediated cell death through stimulation of ER stress in human glioma cells. *J Clin Invest* 119(5):1359-1372.
154. Csordas A, *et al.* (2011) Cigarette smoke extract induces prolonged endoplasmic reticulum stress and autophagic cell death in human umbilical vein endothelial cells. *Cardiovasc Res* 92(1):141-148.
155. Kar R, Singha PK, Venkatachalam MA, & Saikumar P (2009) A novel role for MAP1 LC3 in nonautophagic cytoplasmic vacuolation death of cancer cells. *Oncogene* 28(28):2556-2568.
156. Sperandio S, de Belle I, & Bredesen DE (2000) An alternative, nonapoptotic form of programmed cell death. *Proc Natl Acad Sci U S A* 97(26):14376-14381.
157. Lee WJ, *et al.* (2015) Nonautophagic cytoplasmic vacuolation death induction in human PC-3M prostate cancer by curcumin through reactive oxygen species -mediated endoplasmic reticulum stress. *Sci Rep* 5:10420.
158. Busch R, *et al.* (2017) Genetic Association and Risk Scores in a Chronic Obstructive Pulmonary Disease Meta-analysis of 16,707 Subjects. *Am J Respir Cell Mol Biol* 57(1):35-46.
159. Hancock DB, *et al.* (2010) Meta-analyses of genome-wide association studies identify multiple loci associated with pulmonary function. *Nat Genet* 42(1):45-52.

160. Baglole CJ*, et al.* (2008) The aryl hydrocarbon receptor attenuates tobacco smoke-induced cyclooxygenase-2 and prostaglandin production in lung fibroblasts through regulation of the NF-kappaB family member RelB. *J Biol Chem* 283(43):28944-28957.
161. Rico de Souza A*, et al.* (2011) Genetic ablation of the aryl hydrocarbon receptor causes cigarette smoke-induced mitochondrial dysfunction and apoptosis. *J Biol Chem* 286(50):43214-43228.
162. de Souza AR, Zago M, Eidelman DH, Hamid Q, & Baglole CJ (2014) Aryl hydrocarbon receptor (AhR) attenuation of subchronic cigarette smoke-induced pulmonary neutrophilia is associated with retention of nuclear RelB and suppression of intercellular adhesion molecule-1 (ICAM-1). *Toxicol Sci* 140(1):204-223.
163. Williams EG*, et al.* (2014) An evolutionarily conserved role for the aryl hydrocarbon receptor in the regulation of movement. *PLoS Genet* 10(9):e1004673.
164. Esser C & Rannug A (2015) The aryl hydrocarbon receptor in barrier organ physiology, immunology, and toxicology. *Pharmacol Rev* 67(2):259-279.
165. Flaveny C, Perdew GH, & Miller CA, 3rd (2009) The Aryl-hydrocarbon receptor does not require the p23 co-chaperone for ligand binding and target gene expression in vivo. *Toxicol Lett* 189(1):57-62.
166. Jones S (2004) An overview of the basic helix-loop-helix proteins. *Genome Biol* 5(6):226.
167. Ramadoss P & Perdew GH (2005) The transactivation domain of the Ah receptor is a key determinant of cellular localization and ligand-independent nucleocytoplasmic shuttling properties. *Biochemistry* 44(33):11148-11159.
168. Nebert DW (2017) Aryl hydrocarbon receptor (AHR): "pioneer member" of the basic-helix/loop/helix per-Arnt-sim (bHLH/PAS) family of "sensors" of foreign and endogenous signals. *Prog Lipid Res* 67:38-57.
169. Stevens EA, Mezrich JD, & Bradfield CA (2009) The aryl hydrocarbon receptor: a perspective on potential roles in the immune system. *Immunology* 127(3):299-311.
170. Nguyen LP & Bradfield CA (2008) The search for endogenous activators of the aryl hydrocarbon receptor. *Chem Res Toxicol* 21(1):102-116.
171. Stejskalova L, Dvorak Z, & Pavek P (2011) Endogenous and exogenous ligands of aryl hydrocarbon receptor: current state of art. *Curr Drug Metab* 12(2):198-212.
172. Backlund M & Ingelman-Sundberg M (2004) Different structural requirements of the ligand binding domain of the aryl hydrocarbon receptor for high- and low-affinity ligand binding and receptor activation. *Mol Pharmacol* 65(2):416-425.
173. van Leeuwen FX*, et al.* (2000) Dioxins: WHO's tolerable daily intake (TDI) revisited. *Chemosphere* 40(9-11):1095-1101.
174. Pirkle JL*, et al.* (1989) Estimates of the half-life of 2,3,7,8-tetrachlorodibenzo-p-dioxin in Vietnam Veterans of Operation Ranch Hand. *J Toxicol Environ Health* 27(2):165-171.
175. Wolfe WH*, et al.* (1994) Determinants of TCDD half-life in veterans of operation ranch hand. *J Toxicol Environ Health* 41(4):481-488.
176. Sweeney MH & Mocarelli P (2000) Human health effects after exposure to 2,3,7,8-TCDD. *Food Addit Contam* 17(4):303-316.
177. Armitage JM*, et al.* (2015) Environmental fate and dietary exposures of humans to TCDD as a result of the spraying of Agent Orange in upland forests of Vietnam. *Sci Total Environ* 506-507:621-630.

178. Bertazzi PA, Bernucci I, Brambilla G, Consonni D, & Pesatori AC (1998) The Seveso studies on early and long-term effects of dioxin exposure: a review. *Environ Health Perspect* 106 Suppl 2:625-633.
179. Caramaschi F*, et al.* (1981) Chloracne following environmental contamination by TCDD in Seveso, Italy. *Int J Epidemiol* 10(2):135-143.
180. Sorg O*, et al.* (2009) 2,3,7,8-tetrachlorodibenzo-p-dioxin (TCDD) poisoning in Victor Yushchenko: identification and measurement of TCDD metabolites. *Lancet* 374(9696):1179-1185.
181. Schecter A, Birnbaum L, Ryan JJ, & Constable JD (2006) Dioxins: an overview. *Environ Res* 101(3):419-428.
182. Fernandez-Salguero PM, Hilbert DM, Rudikoff S, Ward JM, & Gonzalez FJ (1996) Aryl-hydrocarbon receptor-deficient mice are resistant to 2,3,7,8-tetrachlorodibenzo-p-dioxin-induced toxicity. *Toxicol Appl Pharmacol* 140(1):173-179.
183. Bunger MK*, et al.* (2008) Abnormal liver development and resistance to 2,3,7,8-tetrachlorodibenzo-p-dioxin toxicity in mice carrying a mutation in the DNA-binding domain of the aryl hydrocarbon receptor. *Toxicol Sci* 106(1):83-92.
184. Bunger MK*, et al.* (2003) Resistance to 2,3,7,8-tetrachlorodibenzo-p-dioxin toxicity and abnormal liver development in mice carrying a mutation in the nuclear localization sequence of the aryl hydrocarbon receptor. *J Biol Chem* 278(20):17767-17774.
185. Moura-Alves P*, et al.* (2014) AhR sensing of bacterial pigments regulates antibacterial defence. *Nature* 512(7515):387-392.
186. Schaldach CM, Riby J, & Bjeldanes LF (1999) Lipoxin A4: a new class of ligand for the Ah receptor. *Biochemistry* 38(23):7594-7600.
187. Mezrich JD*, et al.* (2010) An interaction between kynurenine and the aryl hydrocarbon receptor can generate regulatory T cells. *J Immunol* 185(6):3190-3198.
188. Seok SH*, et al.* (2018) Trace derivatives of kynurenine potently activate the aryl hydrocarbon receptor (AHR). *J Biol Chem* 293(6):1994-2005.
189. Smith KJ*, et al.* (2011) Identification of a high-affinity ligand that exhibits complete aryl hydrocarbon receptor antagonism. *J Pharmacol Exp Ther* 338(1):318-327.
190. Casper RF*, et al.* (1999) Resveratrol has antagonist activity on the aryl hydrocarbon receptor: implications for prevention of dioxin toxicity. *Mol Pharmacol* 56(4):784-790.
191. Puppala D, Gairola CG, & Swanson HI (2007) Identification of kaempferol as an inhibitor of cigarette smoke-induced activation of the aryl hydrocarbon receptor and cell transformation. *Carcinogenesis* 28(3):639-647.
192. Gasiewicz TA & Rucci G (1991) Alpha-naphthoflavone acts as an antagonist of 2,3,7, 8-tetrachlorodibenzo-p-dioxin by forming an inactive complex with the Ah receptor. *Mol Pharmacol* 40(5):607-612.
193. Kim SH*, et al.* (2006) Novel compound 2-methyl-2H-pyrazole-3-carboxylic acid (2-methyl-4-o-tolylazo-phenyl)-amide (CH-223191) prevents 2,3,7,8-TCDD-induced toxicity by antagonizing the aryl hydrocarbon receptor. *Mol Pharmacol* 69(6):1871-1878.
194. Zago M*, et al.* (2013) Aryl hydrocarbon receptor-dependent retention of nuclear HuR suppresses cigarette smoke-induced cyclooxygenase-2 expression independent of DNA-binding. *PLoS One* 8(9):e74953.
195. Zhao B, Degroot DE, Hayashi A, He G, & Denison MS (2010) CH223191 is a ligand-selective antagonist of the Ah (Dioxin) receptor. *Toxicol Sci* 117(2):393-403.

196. Rowlands JC & Gustafsson JA (1997) Aryl hydrocarbon receptor-mediated signal transduction. *Crit Rev Toxicol* 27(2):109-134.
197. Petrulis JR & Perdew GH (2002) The role of chaperone proteins in the aryl hydrocarbon receptor core complex. *Chem Biol Interact* 141(1-2):25-40.
198. Pappas B*, et al.* (2018) p23 protects the human aryl hydrocarbon receptor from degradation via a heat shock protein 90-independent mechanism. *Biochem Pharmacol* 152:34-44.
199. McGuire J, Whitelaw ML, Pongratz I, Gustafsson JA, & Poellinger L (1994) A cellular factor stimulates ligand-dependent release of hsp90 from the basic helix-loop-helix dioxin receptor. *Mol Cell Biol* 14(4):2438-2446.
200. Tsuji N*, et al.* (2014) The activation mechanism of the aryl hydrocarbon receptor (AhR) by molecular chaperone HSP90. *FEBS Open Bio* 4:796-803.
201. Hall JM (2014) The Aryl-hydrocarbon Receptor (AhR) as a Therapeutic Target in Human Breast Cancer. *Journal of Steroids & Hormonal Science* 5(140).
202. Nukaya M, Moran S, & Bradfield CA (2009) The role of the dioxin-responsive element cluster between the Cyp1a1 and Cyp1a2 loci in aryl hydrocarbon receptor biology. *Proc Natl Acad Sci U S A* 106(12):4923-4928.
203. Li S, Pei X, Zhang W, Xie HQ, & Zhao B (2014) Functional analysis of the dioxin response elements (DREs) of the murine CYP1A1 gene promoter: beyond the core DRE sequence. *Int J Mol Sci* 15(4):6475-6487.
204. Hestermann EV & Brown M (2003) Agonist and chemopreventative ligands induce differential transcriptional cofactor recruitment by aryl hydrocarbon receptor. *Mol Cell Biol* 23(21):7920-7925.
205. Ikuta T, Eguchi H, Tachibana T, Yoneda Y, & Kawajiri K (1998) Nuclear localization and export signals of the human aryl hydrocarbon receptor. *J Biol Chem* 273(5):2895-2904.
206. Davarinos NA & Pollenz RS (1999) Aryl hydrocarbon receptor imported into the nucleus following ligand binding is rapidly degraded via the cytosplasmic proteasome following nuclear export. *J Biol Chem* 274(40):28708-28715.
207. Chang X*, et al.* (2007) Ligand-independent regulation of transforming growth factor beta1 expression and cell cycle progression by the aryl hydrocarbon receptor. *Mol Cell Biol* 27(17):6127-6139.
208. Beischlag TV, Luis Morales J, Hollingshead BD, & Perdew GH (2008) The aryl hydrocarbon receptor complex and the control of gene expression. *Crit Rev Eukaryot Gene Expr* 18(3):207-250.
209. Tappenden DM, Hwang HJ, Yang L, Thomas RS, & Lapres JJ (2013) The Aryl-Hydrocarbon Receptor Protein Interaction Network (AHR-PIN) as Identified by Tandem Affinity Purification (TAP) and Mass Spectrometry. *J Toxicol* 2013:279829.
210. Wang F, Hoivik D, Pollenz R, & Safe S (1998) Functional and physical interactions between the estrogen receptor Sp1 and nuclear aryl hydrocarbon receptor complexes. *Nucleic Acids Res* 26(12):3044-3052.
211. Ahmed S, Valen E, Sandelin A, & Matthews J (2009) Dioxin increases the interaction between aryl hydrocarbon receptor and estrogen receptor alpha at human promoters. *Toxicol Sci* 111(2):254-266.
212. Ohtake F*, et al.* (2007) Dioxin receptor is a ligand-dependent E3 ubiquitin ligase. *Nature* 446(7135):562-566.
213. Ohtake F, Fujii-Kuriyama Y, & Kato S (2007) [Transcription factor AhR is a ligand-dependcnt E3 ubiquitin ligase]. *Tanpakushitsu Kakusan Koso* 52(15):1973-1979.

214. Kim DW*, et al.* (2000) The RelA NF-kappaB subunit and the aryl hydrocarbon receptor (AhR) cooperate to transactivate the c-myc promoter in mammary cells. *Oncogene* 19(48):5498-5506.
215. Chen PH, Chang H, Chang JT, & Lin P (2012) Aryl hydrocarbon receptor in association with RelA modulates IL-6 expression in non-smoking lung cancer. *Oncogene* 31(20):2555-2565.
216. Rogers S*, et al.* (2017) Aryl hydrocarbon receptor (AhR)-dependent regulation of pulmonary miRNA by chronic cigarette smoke exposure. *Sci Rep* 7:40539.
217. Hecht E*, et al.* (2014) Aryl hydrocarbon receptor-dependent regulation of miR-196a expression controls lung fibroblast apoptosis but not proliferation. *Toxicol Appl Pharmacol* 280(3):511-525.
218. Hu W, Zhao J, & Pei G (2013) Activation of aryl hydrocarbon receptor (ahr) by tranilast, an anti-allergy drug, promotes miR-302 expression and cell reprogramming. *J Biol Chem* 288(32):22972-22984.
219. Hanieh H (2015) Aryl hydrocarbon receptor-microRNA-212/132 axis in human breast cancer suppresses metastasis by targeting SOX4. *Mol Cancer* 14:172.
220. Grimaldi G, Rajendra S, & Matthews J (2017) The aryl hydrocarbon receptor regulates the expression of TIPARP and its cis long non-coding RNA, TIPARP-AS1. *Biochem Biophys Res Commun*.
221. Nebert DW*, et al.* (2000) Role of the aromatic hydrocarbon receptor and [Ah] gene battery in the oxidative stress response, cell cycle control, and apoptosis. *Biochem Pharmacol* 59(1):65-85.
222. Nebert DW & Karp CL (2008) Endogenous functions of the aryl hydrocarbon receptor (AHR): intersection of cytochrome P450 1 (CYP1)-metabolized eicosanoids and AHR biology. *J Biol Chem* 283(52):36061-36065.
223. Whitlock JP, Jr. (1999) Induction of cytochrome P4501A1. *Annu Rev Pharmacol Toxicol* 39:103-125.
224. Whitlock JP, Jr.*, et al.* (1996) Cytochromes P450 5: induction of cytochrome P4501A1: a model for analyzing mammalian gene transcription. *FASEB J* 10(8):809-818.
225. Oladapo OO & Forkert PG (1995) Detection and localization of CYP1A1/CYP1A2 in murine liver: electrophoresis, immunoblotting and immunocytochemistry. *Afr J Med Med Sci* 24(4):395-402.
226. Park JW, Reed JR, Brignac-Huber LM, & Backes WL (2014) Cytochrome P450 system proteins reside in different regions of the endoplasmic reticulum. *Biochem J* 464(2):241-249.
227. Kohle C & Bock KW (2007) Coordinate regulation of Phase I and II xenobiotic metabolisms by the Ah receptor and Nrf2. *Biochem Pharmacol* 73(12):1853-1862.
228. Jancova P, Anzenbacher P, & Anzenbacherova E (2010) Phase II drug metabolizing enzymes. *Biomed Pap Med Fac Univ Palacky Olomouc Czech Repub* 154(2):103-116.
229. Fleck C & Braunlich H (1990) Factors determining the relationship between renal and hepatic excretion of xenobiotics. *Arzneimittelforschung* 40(8):942-946.
230. Caldwell J, Gardner I, & Swales N (1995) An introduction to drug disposition: the basic principles of absorption, distribution, metabolism, and excretion. *Toxicol Pathol* 23(2):102-114.

231. Schmidt JV, Su GH, Reddy JK, Simon MC, & Bradfield CA (1996) Characterization of a murine Ahr null allele: involvement of the Ah receptor in hepatic growth and development. *Proc Natl Acad Sci U S A* 93(13):6731-6736.
232. Walisser JA, Glover E, Pande K, Liss AL, & Bradfield CA (2005) Aryl hydrocarbon receptor-dependent liver development and hepatotoxicity are mediated by different cell types. *Proc Natl Acad Sci U S A* 102(49):17858-17863.
233. Jacob S, Farr G, De Vun D, Takiff H, & Mason A (1999) Hepatic manifestations of familial patent ductus venosus in adults. *Gut* 45(3):442-445.
234. Carreira VS*, et al.* (2015) Ah Receptor Signaling Controls the Expression of Cardiac Development and Homeostasis Genes. *Toxicol Sci* 147(2):425-435.
235. Qin H & Powell-Coffman JA (2004) The Caenorhabditis elegans aryl hydrocarbon receptor, AHR-1, regulates neuronal development. *Dev Biol* 270(1):64-75.
236. Latchney SE, Hein AM, O'Banion MK, DiCicco-Bloom E, & Opanashuk LA (2013) Deletion or activation of the aryl hydrocarbon receptor alters adult hippocampal neurogenesis and contextual fear memory. *J Neurochem* 125(3):430-445.
237. Kimura E, Ding Y, & Tohyama C (2016) AhR signaling activation disrupts migration and dendritic growth of olfactory interneurons in the developing mouse. *Sci Rep* 6:26386.
238. Kimura E*, et al.* (2017) Excessive activation of AhR signaling disrupts neuronal migration in the hippocampal CA1 region in the developing mouse. *J Toxicol Sci* 42(1):25-30.
239. Kimura E & Tohyama C (2017) Embryonic and Postnatal Expression of Aryl Hydrocarbon Receptor mRNA in Mouse Brain. *Front Neuroanat* 11:4.
240. Chevallier A*, et al.* (2013) Oculomotor deficits in aryl hydrocarbon receptor null mouse. *PLoS One* 8(1):e53520.
241. Juricek L*, et al.* (2017) AhR-deficiency as a cause of demyelinating disease and inflammation. *Sci Rep* 7(1):9794.
242. Bessede A*, et al.* (2014) Aryl hydrocarbon receptor control of a disease tolerance defence pathway. *Nature* 511(7508):184-190.
243. Villa M*, et al.* (2017) Aryl hydrocarbon receptor is required for optimal B-cell proliferation. *EMBO J* 36(1):116-128.
244. Vaidyanathan B*, et al.* (2017) The aryl hydrocarbon receptor controls cell-fate decisions in B cells. *J Exp Med* 214(1):197-208.
245. Mohinta S*, et al.* (2015) Differential regulation of Th17 and T regulatory cell differentiation by aryl hydrocarbon receptor dependent xenobiotic response element dependent and independent pathways. *Toxicol Sci* 145(2):233-243.
246. Singh NP*, et al.* (2011) Activation of aryl hydrocarbon receptor (AhR) leads to reciprocal epigenetic regulation of FoxP3 and IL-17 expression and amelioration of experimental colitis. *PLoS One* 6(8):e23522.
247. Desaulniers D*, et al.* (2005) Comparisons of brain, uterus, and liver mRNA expression for cytochrome p450s, DNA methyltransferase-1, and catechol-o-methyltransferase in prepubertal female Sprague-Dawley rats exposed to a mixture of aryl hydrocarbon receptor agonists. *Toxicol Sci* 86(1):175-184.
248. Murray IA, Nichols RG, Zhang L, Patterson AD, & Perdew GH (2016) Expression of the aryl hydrocarbon receptor contributes to the establishment of intestinal microbial community structure in mice. *Sci Rep* 6:33969.

249. Morales-Hernandez A, *et al.* (2016) Alu retrotransposons promote differentiation of human carcinoma cells through the aryl hydrocarbon receptor. *Nucleic Acids Res* 44(10):4665-4683.
250. Shimba S, Komiyama K, Moro I, & Tezuka M (2002) Overexpression of the aryl hydrocarbon receptor (AhR) accelerates the cell proliferation of A549 cells. *J Biochem* 132(5):795-802.
251. Yin XF, Chen J, Mao W, Wang YH, & Chen MH (2013) Downregulation of aryl hydrocarbon receptor expression decreases gastric cancer cell growth and invasion. *Oncol Rep* 30(1):364-370.
252. Bekki K, *et al.* (2015) The aryl hydrocarbon receptor (AhR) mediates resistance to apoptosis induced in breast cancer cells. *Pestic Biochem Physiol* 120:5-13.
253. Iu M, *et al.* (2017) RelB attenuates cigarette smoke extract-induced apoptosis in association with transcriptional regulation of the aryl hydrocarbon receptor. *Free Radic Biol Med* 108:19-31.
254. Tan NY & Khachigian LM (2009) Sp1 phosphorylation and its regulation of gene transcription. *Mol Cell Biol* 29(10):2483-2488.
255. Fitzgerald CT, Nebert DW, & Puga A (1998) Regulation of mouse Ah receptor (Ahr) gene basal expression by members of the Sp family of transcription factors. *DNA Cell Biol* 17(9):811-822.
256. Wang F, Wang W, & Safe S (1999) Regulation of constitutive gene expression through interactions of Sp1 protein with the nuclear aryl hydrocarbon receptor complex. *Biochemistry* 38(35):11490-11500.
257. Okey AB, *et al.* (2005) Toxicological implications of polymorphisms in receptors for xenobiotic chemicals: the case of the aryl hydrocarbon receptor. *Toxicol Appl Pharmacol* 207(2 Suppl):43-51.
258. Koyano S, *et al.* (2005) Functional analysis of six human aryl hydrocarbon receptor variants in a Japanese population. *Drug Metab Dispos* 33(8):1254-1260.
259. Zhao L, *et al.* (2015) Lanosterol reverses protein aggregation in cataracts. *Nature* 523(7562):607-611.
260. Chen D, *et al.* (2009) Association of human aryl hydrocarbon receptor gene polymorphisms with risk of lung cancer among cigarette smokers in a Chinese population. *Pharmacogenet Genomics* 19(1):25-34.
261. Chen Y, *et al.* (2006) Association of polymorphisms in AhR, CYP1A1, GSTM1, and GSTT1 genes with levels of DNA damage in peripheral blood lymphocytes among coke-oven workers. *Cancer Epidemiol Biomarkers Prev* 15(9):1703-1707.
262. Sangrajrang S, *et al.* (2009) Genetic polymorphisms of estrogen metabolizing enzyme and breast cancer risk in Thai women. *Int J Cancer* 125(4):837-843.
263. Helmig S, Seelinger JU, Dohrel J, & Schneider J (2011) RNA expressions of AHR, ARNT and CYP1B1 are influenced by AHR Arg554Lys polymorphism. *Mol Genet Metab* 104(1-2):180-184.
264. Wong JM, *et al.* (2001) Ethnic variability in the allelic distribution of human aryl hydrocarbon receptor codon 554 and assessment of variant receptor function in vitro. *Pharmacogenetics* 11(1):85-94.
265. Englert NA, *et al.* (2012) Genetic and epigenetic regulation of AHR gene expression in MCF-7 breast cancer cells: role of the proximal promoter GC-rich region. *Biochem Pharmacol* 84(5):722-735.

266. Wei Y*, et al.* (2008) Loss of trimethylation at lysine 27 of histone H3 is a predictor of poor outcome in breast, ovarian, and pancreatic cancers. *Mol Carcinog* 47(9):701-706.
267. Mulero-Navarro S*, et al.* (2006) The dioxin receptor is silenced by promoter hypermethylation in human acute lymphoblastic leukemia through inhibition of Sp1 binding. *Carcinogenesis* 27(5):1099-1104.
268. Aluru N, Karchner SI, & Hahn ME (2011) Role of DNA methylation of AHR1 and AHR2 promoters in differential sensitivity to PCBs in Atlantic Killifish, Fundulus heteroclitus. *Aquat Toxicol* 101(1):288-294.
269. Li DL, C.; Yu, H.; Zeng, X.; Xing, X.; Chen, L. (2014) AhR is negatively regulated by miR-203 in response to TCDD or BaP treatment. *Toxicology Research* 3(2):142-151.
270. Covarrubias S*, et al.* (2017) CRISPR/Cas-based screening of long non-coding RNAs (lncRNAs) in macrophages with an NF-kappaB reporter. *J Biol Chem* 292(51):20911-20920.
271. Awji EG*, et al.* (2015) Wood smoke enhances cigarette smoke-induced inflammation by inducing the aryl hydrocarbon receptor repressor in airway epithelial cells. *Am J Respir Cell Mol Biol* 52(3):377-386.
272. Vogel CF*, et al.* (2016) Transgenic Overexpression of Aryl Hydrocarbon Receptor Repressor (AhRR) and AhR-Mediated Induction of CYP1A1, Cytokines, and Acute Toxicity. *Environ Health Perspect* 124(7):1071-1083.
273. Karchner SI*, et al.* (2009) The active form of human aryl hydrocarbon receptor (AHR) repressor lacks exon 8, and its Pro 185 and Ala 185 variants repress both AHR and hypoxia-inducible factor. *Mol Cell Biol* 29(13):3465-3477.
274. MacPherson L*, et al.* (2014) Aryl hydrocarbon receptor repressor and TiPARP (ARTD14) use similar, but also distinct mechanisms to repress aryl hydrocarbon receptor signaling. *Int J Mol Sci* 15(5):7939-7957.
275. Lin P*, et al.* (2003) Overexpression of aryl hydrocarbon receptor in human lung carcinomas. *Toxicol Pathol* 31(1):22-30.
276. Safe S, Lee SO, & Jin UH (2013) Role of the aryl hydrocarbon receptor in carcinogenesis and potential as a drug target. *Toxicol Sci* 135(1):1-16.
277. Monteleone I, MacDonald TT, Pallone F, & Monteleone G (2012) The aryl hydrocarbon receptor in inflammatory bowel disease: linking the environment to disease pathogenesis. *Curr Opin Gastroenterol* 28(4):310-313.
278. Wang C, Ye Z, Kijlstra A, Zhou Y, & Yang P (2014) Decreased expression of the aryl hydrocarbon receptor in ocular Behcet's disease. *Mediators Inflamm* 2014:195094.
279. Wei P*, et al.* (2014) Role of the aryl hydrocarbon receptor in the pathogenesis of chronic rhinosinusitis with nasal polyps. *Inflammation* 37(2):387-395.
280. Di Meglio P*, et al.* (2014) Activation of the aryl hydrocarbon receptor dampens the severity of inflammatory skin conditions. *Immunity* 40(6):989-1001.
281. Jeong KT, Hwang SJ, Oh GS, & Park JH (2012) FICZ, a tryptophan photoproduct, suppresses pulmonary eosinophilia and Th2-type cytokine production in a mouse model of ovalbumin-induced allergic asthma. *Int Immunopharmacol* 13(4):377-385.
282. Thatcher TH*, et al.* (2016) Endogenous ligands of the aryl hydrocarbon receptor regulate lung dendritic cell function. *Immunology* 147(1):41-54.
283. Monteleone I*, et al.* (2011) Aryl hydrocarbon receptor-induced signals up-regulate IL-22 production and inhibit inflammation in the gastrointestinal tract. *Gastroenterology* 141(1):237-248, 248 e231.

284. Ji T*, et al.* (2015) Aryl Hydrocarbon Receptor Activation Down-Regulates IL-7 and Reduces Inflammation in a Mouse Model of DSS-Induced Colitis. *Dig Dis Sci* 60(7):1958-1966.
285. Wei P*, et al.* (2014) Increased aryl hydrocarbon receptor expression in patients with allergic rhinitis. *QJM* 107(2):107-113.
286. Goettel JA*, et al.* (2016) AHR Activation Is Protective against Colitis Driven by T Cells in Humanized Mice. *Cell Rep* 17(5):1318-1329.
287. Sarill M*, et al.* (2015) The aryl hydrocarbon receptor suppresses cigarette-smoke-induced oxidative stress in association with dioxin response element (DRE)-independent regulation of sulfiredoxin 1. *Free Radic Biol Med* 89:342-357.
288. Kurmi OP, Semple S, Simkhada P, Smith WC, & Ayres JG (2010) COPD and chronic bronchitis risk of indoor air pollution from solid fuel: a systematic review and meta-analysis. *Thorax* 65(3):221-228.
289. Diette GB*, et al.* (2012) Obstructive Lung Disease and Exposure to Burning Biomass Fuel in the Indoor Environment. *Glob Heart* 7(3):265-270.
290. Wang D*, et al.* (2017) The Chemical Chaperone, PBA, Reduces ER Stress and Autophagy and Increases Collagen IV alpha5 Expression in Cultured Fibroblasts From Men With X-Linked Alport Syndrome and Missense Mutations. *Kidney Int Rep* 2(4):739-748.
291. Porter AG & Janicke RU (1999) Emerging roles of caspase-3 in apoptosis. *Cell Death Differ* 6(2):99-104.
292. Mimura J*, et al.* (1997) Loss of teratogenic response to 2,3,7,8-tetrachlorodibenzo-p-dioxin (TCDD) in mice lacking the Ah (dioxin) receptor. *Genes Cells* 2(10):645-654.
293. Bock KW (1994) Aryl hydrocarbon or dioxin receptor: biologic and toxic responses. *Rev Physiol Biochem Pharmacol* 125:1-42.
294. Furness SG, Lees MJ, & Whitelaw ML (2007) The dioxin (aryl hydrocarbon) receptor as a model for adaptive responses of bHLH/PAS transcription factors. *FEBS Lett* 581(19):3616-3625.
295. Evans BR*, et al.* (2008) Repression of aryl hydrocarbon receptor (AHR) signaling by AHR repressor: role of DNA binding and competition for AHR nuclear translocator. *Mol Pharmacol* 73(2):387-398.
296. Sekine H*, et al.* (2009) Hypersensitivity of aryl hydrocarbon receptor-deficient mice to lipopolysaccharide-induced septic shock. *Mol Cell Biol* 29(24):6391-6400.
297. Hecht E*, et al.* (2014) Aryl hydrocarbon receptor-dependent regulation of miR-196a expression controls lung fibroblast apoptosis but not proliferation. *Toxicol Appl Pharmacol*.
298. Sarill M*, et al.* (2015) The aryl Hydrocarbon receptor suppresses cigarette-smoke-induced oxidative stress in association with dioxin response element (DRE)-independent regulation of sulfiredoxin 1. *Free Radic Biol Med*.
299. Cauchi S*, et al.* (2001) Polymorphisms of human aryl hydrocarbon receptor (AhR) gene in a French population: relationship with CYP1A1 inducibility and lung cancer. *Carcinogenesis* 22(11):1819-1824.
300. Bojesen SE, Timpson N, Relton C, Davey Smith G, & Nordestgaard BG (2017) AHRR (cg05575921) hypomethylation marks smoking behaviour, morbidity and mortality. *Thorax*.

301. Thatcher TH*, et al.* (2007) Aryl hydrocarbon receptor-deficient mice develop heightened inflammatory responses to cigarette smoke and endotoxin associated with rapid loss of the nuclear factor-kappaB component RelB. *Am J Pathol* 170(3):855-864.
302. Butler R*, et al.* (2012) Uric acid stones in the urinary bladder of aryl hydrocarbon receptor (AhR) knockout mice. *Proc Natl Acad Sci U S A* 109(4):1122-1126.
303. Singh KP, Garrett RW, Casado FL, & Gasiewicz TA (2011) Aryl hydrocarbon receptor-null allele mice have hematopoietic stem/progenitor cells with abnormal characteristics and functions. *Stem Cells Dev* 20(5):769-784.
304. Harstad EB, Guite CA, Thomae TL, & Bradfield CA (2006) Liver deformation in Ahr-null mice: evidence for aberrant hepatic perfusion in early development. *Mol Pharmacol* 69(5):1534-1541.
305. Shimizu Y*, et al.* (2000) Benzo[a]pyrene carcinogenicity is lost in mice lacking the aryl hydrocarbon receptor. *Proc Natl Acad Sci U S A* 97(2):779-782.
306. Cavarra E*, et al.* (2001) Effects of cigarette smoke in mice with different levels of alpha(1)-proteinase inhibitor and sensitivity to oxidants. *Am J Respir Crit Care Med* 164(5):886-890.
307. Kawakami M, Paul JL, & Thurlbeck WM (1984) The effect of age on lung structure in male BALB/cNNia inbred mice. *Am J Anat* 170(1):1-21.
308. McGovern TK, Robichaud A, Fereydoonzad L, Schuessler TF, & Martin JG (2013) Evaluation of respiratory system mechanics in mice using the forced oscillation technique. *J Vis Exp* (75):e50172.
309. Robichaud A*, et al.* (2017) Automated Full-Range Pressure-Volume Curves in Mice and Rats. *J Appl Physiol (1985)*:jap 00856 02016.
310. Lamontagne M*, et al.* (2013) Refining susceptibility loci of chronic obstructive pulmonary disease with lung eqtls. *PLoS One* 8(7):e70220.
311. Bourbeau J*, et al.* (2014) Canadian Cohort Obstructive Lung Disease (CanCOLD): Fulfilling the need for longitudinal observational studies in COPD. *COPD* 11(2):125-132.
312. Sheridan JA*, et al.* (2015) Decreased expression of the NF-kappaB family member RelB in lung fibroblasts from Smokers with and without COPD potentiates cigarette smoke-induced COX-2 expression. *Respir Res* 16:54.
313. Taylor SC, Carbonneau J, Shelton DN, & Boivin G (2015) Optimization of Droplet Digital PCR from RNA and DNA extracts with direct comparison to RT-qPCR: Clinical implications for quantification of Oseltamivir-resistant subpopulations. *J Virol Methods* 224:58-66.
314. Papandrinopoulou D, Tzouda V, & Tsoukalas G (2012) Lung compliance and chronic obstructive pulmonary disease. *Pulm Med* 2012:542769.
315. Boschetto P*, et al.* (2006) Association between markers of emphysema and more severe chronic obstructive pulmonary disease. *Thorax* 61(12):1037-1042.
316. Li Y*, et al.* (2016) Relationships of MMP-9 and TIMP-1 proteins with chronic obstructive pulmonary disease risk: A systematic review and meta-analysis. *J Res Med Sci* 21:12.
317. Kim JH*, et al.* (2007) Aryl hydrocarbon receptor gene polymorphisms affect lung cancer risk. *Lung Cancer* 56(1):9-15.
318. Tsuchiya M*, et al.* (2005) Analysis of the AhR, ARNT, and AhRR gene polymorphisms: genetic contribution to endometriosis susceptibility and severity. *Fertil Steril* 84(2):454-458.

319. Kim SH, *et al.* (2007) Association between susceptibility to advanced stage endometriosis and the genetic polymorphisms of aryl hydrocarbon receptor repressor and glutathione-S-transferase T1 genes. *Hum Reprod* 22(7):1866-1870.
320. Brokken LJ, *et al.* (2013) Association between polymorphisms in the aryl hydrocarbon receptor repressor gene and disseminated testicular germ cell cancer. *Front Endocrinol (Lausanne)* 4:4.
321. Guerassimov A, *et al.* (2004) The development of emphysema in cigarette smoke-exposed mice is strain dependent. *Am J Respir Crit Care Med* 170(9):974-980.
322. O'Donnell MD, *et al.* (1999) Ultrastructure of lung elastin and collagen in mouse models of spontaneous emphysema. *Matrix Biol* 18(4):357-360.
323. Wert S, Jones T, Korfhagen T, Fisher J, & Whitsett J (2000) Spontaneous emphysema in surfactant protein D gene-targeted mice. *Chest* 117(5):248s-248s.
324. Bonniaud P, *et al.* (2004) Smad3 null mice develop airspace enlargement and are resistant to TGF-beta-mediated pulmonary fibrosis. *J Immunol* 173(3):2099-2108.
325. Celli BR, Decramer M, Lystig T, Kesten S, & Tashkin DP (2012) Longitudinal inspiratory capacity changes in chronic obstructive pulmonary disease. *Respir Res* 13:66.
326. Zaman M, Mahmood S, & Altayeh A (2010) Low inspiratory capacity to total lung capacity ratio is a risk factor for chronic obstructive pulmonary disease exacerbation. *Am J Med Sci* 339(5):411-414.
327. Casanova C, *et al.* (2005) Inspiratory-to-total lung capacity ratio predicts mortality in patients with chronic obstructive pulmonary disease. *Am J Respir Crit Care Med* 171(6):591-597.
328. Domagala-Kulawik J (2008) Effects of cigarette smoke on the lung and systemic immunity. *J Physiol Pharmacol* 59 Suppl 6:19-34.
329. Holt PG (1987) Immune and inflammatory function in cigarette smokers. *Thorax* 42(4):241-249.
330. Boorsma M, *et al.* (2008) Long-term effects of budesonide on inflammatory status in COPD. *COPD* 5(2):97-104.
331. Ludwig PW, Schwartz BA, Hoidal JR, & Niewoehner DE (1985) Cigarette smoking causes accumulation of polymorphonuclear leukocytes in alveolar septum. *Am Rev Respir Dis* 131(6):828-830.
332. Ruparelia P, *et al.* (2011) Quantification of neutrophil migration into the lungs of patients with chronic obstructive pulmonary disease. *Eur J Nucl Med Mol Imaging* 38(5):911-919.
333. Milde R, *et al.* (2015) Multinucleated Giant Cells Are Specialized for Complement-Mediated Phagocytosis and Large Target Destruction. *Cell Rep* 13(9):1937-1948.
334. McNally AK & Anderson JM (2011) Macrophage fusion and multinucleated giant cells of inflammation. *Adv Exp Med Biol* 713:97-111.
335. Schoolmeester JK & Smyrk TC (2013) Multinucleated epithelial giant cells in the duodenum. *Int J Surg Pathol* 21(2):202-204.
336. Chuang HC, *et al.* (2018) Effects of physical characteristics of carbon black on metabolic regulation in mice. *Environ Pollut* 232:494-504.
337. Martin RR (1973) Altered morphology and increased acid hydrolase content of pulmonary macrophages from cigarette smokers. *Am Rev Respir Dis* 107(4):596-601.
338. Quinn MT & Schepetkin IA (2009) Role of NADPH oxidase in formation and function of multinucleated giant cells. *J Innate Immun* 1(6):509-526.

339. Zhu XW, Price NM, Gilman RH, Recarvarren S, & Friedland JS (2007) Multinucleate giant cells release functionally unopposed matrix metalloproteinase-9 in vitro and in vivo. *J Infect Dis* 196(7):1076-1079.
340. Fan D*, et al.* (2016) MicroRNA-183 functions as the tumor suppressor via inhibiting cellular invasion and metastasis by targeting MMP-9 in cervical cancer. *Gynecol Oncol* 141(1):166-174.
341. Zhu W*, et al.* (2011) Overexpression of members of the microRNA-183 family is a risk factor for lung cancer: a case control study. *BMC Cancer* 11:393.
342. Nho RS, Im J, Ho YY, & Hergert P (2014) MicroRNA-96 inhibits FoxO3a function in IPF fibroblasts on type I collagen matrix. *Am J Physiol Lung Cell Mol Physiol* 307(8):L632-642.
343. Dang X*, et al.* (2017) Bioinformatic analysis of microRNA and mRNA Regulation in peripheral blood mononuclear cells of patients with chronic obstructive pulmonary disease. *Respir Res* 18(1):4.
344. Kara M, Kirkil G, & Kalemci S (2016) Differential Expression of MicroRNAs in Chronic Obstructive Pulmonary Disease. *Adv Clin Exp Med* 25(1):21-26.
345. Sato T*, et al.* (2010) Reduced MiR-146a Increases Prostaglandin E2 in Chronic Obstructive Pulmonary Disease Fibroblasts. *Am J Respir Crit Care Med*.
346. Martey CA, Baglole CJ, Gasiewicz TA, Sime PJ, & Phipps RP (2005) The aryl hydrocarbon receptor is a regulator of cigarette smoke induction of the cyclooxygenase and prostaglandin pathways in human lung fibroblasts. *Am J Physiol Lung Cell Mol Physiol* 289(3):L391-399.
347. Tigges J*, et al.* (2013) Aryl hydrocarbon receptor repressor (AhRR) function revisited: repression of CYP1 activity in human skin fibroblasts is not related to AhRR expression. *J Invest Dermatol* 133(1):87-96.
348. Wang WB*, et al.* (2012) Paraptosis accompanied by autophagy and apoptosis was induced by celastrol, a natural compound with influence on proteasome, ER stress and Hsp90. *J Cell Physiol* 227(5):2196-2206.
349. van den Bogaard EH*, et al.* (2013) Coal tar induces AHR-dependent skin barrier repair in atopic dermatitis. *J Clin Invest* 123(2):917-927.
350. Guo H*, et al.* (2017) Kaempferol induces hepatocellular carcinoma cell death via endoplasmic reticulum stress-CHOP-autophagy signaling pathway. *Oncotarget* 8(47):82207-82216.
351. Liu K*, et al.* (2014) CHOP mediates ASPP2-induced autophagic apoptosis in hepatoma cells by releasing Beclin-1 from Bcl-2 and inducing nuclear translocation of Bcl-2. *Cell Death Dis* 5:e1323.
352. Lee YK & Lee JA (2016) Role of the mammalian ATG8/LC3 family in autophagy: differential and compensatory roles in the spatiotemporal regulation of autophagy. *BMB Rep* 49(8):424-430.
353. Baglole CJ*, et al.* (2005) Isolation and phenotypic characterization of lung fibroblasts. *Methods Mol Med* 117:115-127.
354. Wikenheiser KA*, et al.* (1993) Production of immortalized distal respiratory epithelial cell lines from surfactant protein C/simian virus 40 large tumor antigen transgenic mice. *Proc Natl Acad Sci U S A* 90(23):11029-11033.
355. Ahmed S, Wang A, Celius T, & Matthews J (2014) Zinc finger nuclease-mediated knockout of AHR or ARNT in human breast cancer cells abolishes basal and ligand-

dependent regulation of CYP1B1 and differentially affects estrogen receptor alpha transactivation. *Toxicol Sci* 138(1):89-103.
356. Baglole CJ, Sime PJ, & Phipps RP (2008) Cigarette smoke-induced expression of heme oxygenase-1 in human lung fibroblasts is regulated by intracellular glutathione. *Am J Physiol Lung Cell Mol Physiol* 295(4):L624-636.
357. Carp H & Janoff A (1978) Possible mechanisms of emphysema in smokers. In vitro suppression of serum elastase-inhibitory capacity by fresh cigarette smoke and its prevention by antioxidants. *Am Rev Respir Dis* 118(3):617-621.
358. Hassler JR*, et al.* (2015) The IRE1alpha/XBP1s Pathway Is Essential for the Glucose Response and Protection of beta Cells. *PLoS Biol* 13(10):e1002277.
359. Bruhat A*, et al.* (1997) Amino acid limitation induces expression of CHOP, a CCAAT/enhancer binding protein-related gene, at both transcriptional and post-transcriptional levels. *J Biol Chem* 272(28):17588-17593.
360. Majumder M*, et al.* (2012) A novel feedback loop regulates the response to endoplasmic reticulum stress via the cooperation of cytoplasmic splicing and mRNA translation. *Mol Cell Biol* 32(5):992-1003.
361. Rutkowski DT*, et al.* (2006) Adaptation to ER stress is mediated by differential stabilities of pro-survival and pro-apoptotic mRNAs and proteins. *PLoS Biol* 4(11):e374.
362. Yamamoto A*, et al.* (1998) Bafilomycin A1 prevents maturation of autophagic vacuoles by inhibiting fusion between autophagosomes and lysosomes in rat hepatoma cell line, H-4-II-E cells. *Cell Struct Funct* 23(1):33-42.
363. Mofarrahi M*, et al.* (2013) Autophagic flux and oxidative capacity of skeletal muscles during acute starvation. *Autophagy* 9(10):1604-1620.
364. Kovacs AL & Klionsky DJ (2013) A pioneer in the field of autophagy microscopy: Attila L Kovacs. *Autophagy* 9(12):1908-1921.
365. Patel RD, Murray IA, Flaveny CA, Kusnadi A, & Perdew GH (2009) Ah receptor represses acute-phase response gene expression without binding to its cognate response element. *Lab Invest* 89(6):695-707.
366. Yao Y*, et al.* (2017) A non-canonical pathway regulates ER stress signaling and blocks ER stress-induced apoptosis and heart failure. *Nat Commun* 8(1):133.
367. Arensdorf AM, Diedrichs D, & Rutkowski DT (2013) Regulation of the transcriptome by ER stress: non-canonical mechanisms and physiological consequences. *Front Genet* 4:256.
368. Seefeld MD, Corbett SW, Keesey RE, & Peterson RE (1984) Characterization of the wasting syndrome in rats treated with 2,3,7,8-tetrachlorodibenzo-p-dioxin. *Toxicol Appl Pharmacol* 73(2):311-322.
369. Benowitz NL (1996) Cotinine as a biomarker of environmental tobacco smoke exposure. *Epidemiol Rev* 18(2):188-204.
370. Ehrlich AK & Kerkvliet NI (2017) Is chronic AhR activation by rapidly metabolized ligands safe for the treatment of immune-mediated diseases? *Curr Opin Toxicol* 2:72-78.
371. Henry EC & Gasiewicz TA (2003) Agonist but not antagonist ligands induce conformational change in the mouse aryl hydrocarbon receptor as detected by partial proteolysis. *Mol Pharmacol* 63(2):392-400.
372. Walisser JA, Bunger MK, Glover E, & Bradfield CA (2004) Gestational exposure of Ahr and Arnt hypomorphs to dioxin rescues vascular development. *Proc Natl Acad Sci U S A* 101(47):16677-16682.

373. Vogel CF & Matsumura F (2009) A new cross-talk between the aryl hydrocarbon receptor and RelB, a member of the NF-kappaB family. *Biochem Pharmacol* 77(4):734-745.
374. Vogel CF*, et al.* (2007) RelB, a new partner of aryl hydrocarbon receptor-mediated transcription. *Mol Endocrinol* 21(12):2941-2955.
375. Akool el S*, et al.* (2003) Nitric oxide increases the decay of matrix metalloproteinase 9 mRNA by inhibiting the expression of mRNA-stabilizing factor HuR. *Mol Cell Biol* 23(14):4901-4916.
376. Huwiler A*, et al.* (2003) ATP potentiates interleukin-1 beta-induced MMP-9 expression in mesangial cells via recruitment of the ELAV protein HuR. *J Biol Chem* 278(51):51758-51769.
377. Yeager RL, Reisman SA, Aleksunes LM, & Klaassen CD (2009) Introducing the "TCDD-inducible AhR-Nrf2 gene battery". *Toxicol Sci* 111(2):238-246.
378. Hassan T*, et al.* (2014) miR-199a-5p silencing regulates the unfolded protein response in chronic obstructive pulmonary disease and alpha1-antitrypsin deficiency. *Am J Respir Crit Care Med* 189(3):263-273.
379. Shivanna B*, et al.* (2016) Gene Expression Profiling Identifies Cell Proliferation and Inflammation as the Predominant Pathways Regulated by Aryl Hydrocarbon Receptor in Primary Human Fetal Lung Cells Exposed to Hyperoxia. *Toxicol Sci* 152(1):155-168.
380. Moyer BJ*, et al.* (2016) Inhibition of the aryl hydrocarbon receptor prevents Western diet-induced obesity. Model for AHR activation by kynurenine via oxidized-LDL, TLR2/4, TGFbeta, and IDO1. *Toxicol Appl Pharmacol* 300:13-24.
381. Xu CX*, et al.* (2015) Aryl hydrocarbon receptor deficiency protects mice from diet-induced adiposity and metabolic disorders through increased energy expenditure. *Int J Obes (Lond)* 39(8):1300-1309.
382. Cao C*, et al.* (2012) Body mass index and mortality in chronic obstructive pulmonary disease: a meta-analysis. *PLoS One* 7(8):e43892.
383. Strimbu K & Tavel JA (2010) What are biomarkers? *Curr Opin HIV AIDS* 5(6):463-466.
384. Mannino DM (2015) Biomarkers in COPD: the search continues! *Eur Respir J* 45(4):872-874.
385. Sin DD & Vestbo J (2009) Biomarkers in chronic obstructive pulmonary disease. *Proc Am Thorac Soc* 6(6):543-545.
386. Hu W, Sorrentino C, Denison MS, Kolaja K, & Fielden MR (2007) Induction of cyp1a1 is a nonspecific biomarker of aryl hydrocarbon receptor activation: results of large scale screening of pharmaceuticals and toxicants in vivo and in vitro. *Mol Pharmacol* 71(6):1475-1486.
387. Nugent LF*, et al.* (2013) ITE, a novel endogenous nontoxic aryl hydrocarbon receptor ligand, efficiently suppresses EAU and T-cell-mediated immunity. *Invest Ophthalmol Vis Sci* 54(12):7463-7469.
388. Quintana FJ*, et al.* (2008) Control of T(reg) and T(H)17 cell differentiation by the aryl hydrocarbon receptor. *Nature* 453(7191):65-71.
389. Uppstad H, Ovrebo S, Haugen A, & Mollerup S (2010) Importance of CYP1A1 and CYP1B1 in bioactivation of benzo[a]pyrene in human lung cell lines. *Toxicol Lett* 192(2):221-228.
390. Arlt VM*, et al.* (2008) Metabolic activation of benzo[a]pyrene in vitro by hepatic cytochrome P450 contrasts with detoxification in vivo: experiments with hepatic cytochrome P450 reductase null mice. *Carcinogenesis* 29(3):656-665.

391. Arlt VM*, et al.* (2015) Pulmonary Inflammation Impacts on CYP1A1-Mediated Respiratory Tract DNA Damage Induced by the Carcinogenic Air Pollutant Benzo[a]pyrene. *Toxicol Sci* 146(2):213-225.
392. Uno S*, et al.* (2004) Oral exposure to benzo[a]pyrene in the mouse: detoxication by inducible cytochrome P450 is more important than metabolic activation. *Mol Pharmacol* 65(5):1225-1237.
393. Carney SA, Prasch AL, Heideman W, & Peterson RE (2006) Understanding dioxin developmental toxicity using the zebrafish model. *Birth Defects Res A Clin Mol Teratol* 76(1):7-18.
394. Narayanan GA, Murray IA, Krishnegowda G, Amin S, & Perdew GH (2012) Selective aryl hydrocarbon receptor modulator-mediated repression of CD55 expression induced by cytokine exposure. *J Pharmacol Exp Ther* 342(2):345-355.
395. Jin UH, Lee SO, & Safe S (2012) Aryl hydrocarbon receptor (AHR)-active pharmaceuticals are selective AHR modulators in MDA-MB-468 and BT474 breast cancer cells. *J Pharmacol Exp Ther* 343(2):333-341.
396. Yin XF, Chen J, Mao W, Wang YH, & Chen MH (2012) A selective aryl hydrocarbon receptor modulator 3,3'-Diindolylmethane inhibits gastric cancer cell growth. *J Exp Clin Cancer Res* 31:46.
397. Safe S (2017) Carbidopa: a selective Ah receptor modulator (SAhRM). *Biochem J* 474(22):3763-3765.
398. Fritz WA, Lin TM, Safe S, Moore RW, & Peterson RE (2009) The selective aryl hydrocarbon receptor modulator 6-methyl-1,3,8-trichlorodibenzofuran inhibits prostate tumor metastasis in TRAMP mice. *Biochem Pharmacol* 77(7):1151-1160.
399. Murray IA*, et al.* (2010) Development of a selective modulator of aryl hydrocarbon (Ah) receptor activity that exhibits anti-inflammatory properties. *Chem Res Toxicol* 23(5):955-966.
400. Sulzer D (2007) Multiple hit hypotheses for dopamine neuron loss in Parkinson's disease. *Trends Neurosci* 30(5):244-250.
401. Tuder RM, Janciauskiene SM, & Petrache I (2010) Lung disease associated with alpha1-antitrypsin deficiency. *Proc Am Thorac Soc* 7(6):381-386.